# Radar backscatter from three

## agricultural crops:

## beet, potatoes and peas

*B.A.M. Bouman*

CABO-Verslag nr. 71
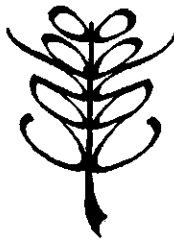
**Centre for Agrobiological Research (CABO) 1987**

INDEX

Index

ABSTRACT

Microwave backscatter from the crops beet, peas and potatoes was
analysed in relation to crop growth, changes in canopy morphology and
geometry, and meteorological data, at two areas.
The Cloud model for vegetation was used as a means of curve fitting to
the original data set. The results for 1979 were used to predict the
backscatter in 1980 in another area. The general trend in microwave
backscatter was reasonably well predicted by the model. However many
fluctuations in the measured microwave backscatter were unpredictable,
supposedly because of temporary changes in canopy geometry caused by
the action of wind and rain.
The microwave soil cover of the crop obtained through the Cloud model,
is compared with the optical soil cover. An almost linear relationship
is observed for the crops during the vegetative part of the growing
season. Such a relationship might be useful for integrating remote
sensing data with growth models for crops.

# I INTRODUCTION

## I.1 The ROVE Programme

During the years 1975-1981, the ROVE team (Radar Observation of VEgetation) collected an extensive series of measurements on the radar backscatter of agricultural crops during the growing season. These ground-based measurements were performed on bare soils and on crops at different research farms in the Netherlands. The objective of this research was to assess the potentials of radar for classification, monitoring and yield prediction of agricultural crops (Ref.7,8).

## I.2 Instruments and measurements

Radar backscatter was measured with a FM-CW scatterometer mounted on a trailer. The median frequency of this scatterometer was 9.5 GHz ( with a corresponding wavelength of 3.0 cm) with a frequency sweep of about 0.4 GHz. The scatterometer was calibrated by directing the radar beam on a corner reflector of known radar cross-section. The radar backscatter parameter obtained was $\gamma$ : radar cross-section of the target per unit projected area of the cross-section of the radar beam (m2/m2).
Measurements were performed at different angles of incidence ranging from $10°$ to $80°$ grazing angle and at the polarization states HH, VV, HV and VH. Furthermore, the scatterometer was mounted in such a way that the distance along the axis of the beam to the target could remain 10 m at all angles of incidence. The irradiated ground area was about 0.6 m2 with a beam of power level 3 dB and of $4°$ width. For more information on the configuration, see Ref.4 and 7.

Simultaneously with the radar measurements, visual observations and quantitative measurements were made of the soil surface and of the crops.
Quantitative measurements were made of the following variables: soil moisture content of 5 cm topsoil (percentage by weight), fresh and dry weight of the above ground biomass (kg/m2), vegetation height (m), vegetation cover (%) and for some crops the dimensions and numbers of leaves per plant.
Visual observations consisted of descriptions of crops and soil surfaces: structure, morphology, phenological stage, cover percentage, slaking, etc.
In addition, some meteorological data were collected during the period of growth: direction and speed of wind, rainfall, temperature and solar irradiation.

## I.3 Measuring accuracy of the radar backscatter

Measurement inaccuracies can be divided into two categories: a) inaccuracies of the radarsystem and b) inaccuracies due to averaging of the backscatter.

ad a)
The inaccuracy of the scatterometer is $\pm$ 1.5 db, of the calibration $\pm$ 1.0 db and of the data processing $\pm$ 0.5 db (Ref.4). Thus, the absolute inaccuracy is $\pm$ 1.7 db at a 90%-confidence interval. However this system inaccuracy is a worst case guess and in practice it can can be reduced to values of $\pm$ 0.6 db (Ref.4).

ad b)

A (microwave-)irradiated surface can be considered as a collection of
uncorrelated scatter elements (Ref.6). If the number of these elements
is sufficiently large, the radar cross-section of such a surface
displays a probability density which can be described by a Raleigh
distribution function. Within a vegetation cover, we are dealing with
compound reflectors (stems, leaves, fruits, etc) which are constantly
moving in the wind. Consequently, the radar backscatter will come from
continually varying combinations of elements and will be of varying
strength. To obtain an accurate value for the radar cross-section of a
vegetation surface, averaging over a large number of independent
observations is needed. The number of independent observations with a
radar system depends on field size and angle of incidence. For the
measurement configuration used by the ROVE-team, the number of
independent samples ranged from ca 15 at $80^\circ$ to ca 35 at $15^\circ$ grazing
angle. Using the probability density of real average power intensity
given by Wallace (Ref.4), these values correspond with a
90%-confidence interval of -1.3 and +2.1 db.

Total inaccuracy (a + b) thus is $\pm$ 2.5 db

I.4 Study objective

The main objective of this study is to arrive at a synthesis of
microwave remote sensing with crop growth models. Therefore, a
detailed analysis of the radar backscatter from three different
agricultural crops in relation to growth and changes in morphology is
made. The purpose of this report is to evaluate the sensitivity of
X-band radar (around 10 GHz) to changes in crop morphology and
geometry. It also aims to develope some insight into the usefulness of
a vegetation model for the prediction of radar backscatter.

The radar backscatter of some crops are extensively studied in
relation with ground truth in the years 1979 and 1980. In 1979,
measurements were carried out at the experimental farm 'De Bouwing'
(alluvial clay soil) and in 1980 at 'De Schreef' (marine clay soil).
For both years, the measurement series comprise the period from before
emergence until after harvest for most crops. The Cloud model for
vegetation (Ref.1) is used as a procedure for curve fitting in both
years, while the results from 1979 are used to predict the radar
backscatter in 1980. Furthermore, relations are searched for between
fluctuations in radar backscatter and changes in plant geometry (which
are deduced from field observations), meteorological data and changes
in soil moisture. Finally, some comparison is made between the radar
backscatter from vegetation at two states of polarization.

From the many crops on which backscatter measurements have been
performed, a selection is made here for sugarbeet, potatoes and peas.
This selection is based on their relative uniform canopy architecture
throughout the growing season (beet and potatoes), the form and
dimensions of their leaves, and on the fitting results obtained with
the Cloud model (Ref.2).
From the various measurement series, a further selection is made for
the polarization state VV, while the number of incidence angles is
reduced to $20^\circ$, $40^\circ$ and $80^\circ$ grazing angle. This combination of state
of polarization with angle of incidence is termed VV20, VV40 and VV80
respectively.

## II MICROWAVE THEORY

### II.1 The radar system

A radar system generally comprises two subsystems: a transmitter in which microwaves of the desired frequency are generated and an antenna system for spatial distribution of the generated radiation. Microwaves which are reflected by an object are first received by an antenna and then detected at the radar receiver. Generally, the same antenna is used for transmission as well as for reception of radiation.
The Radar equation relates for any point-target the received microwave power Pr (Watt) to the transmitted microwave power Pt (Ref.11):

$$Pr = [G^2 \lambda^2 Pt/(4Pi)^3 d^4] \cdot \sigma \qquad (1)$$

in which: G = antenna gain (no dimension)
$\lambda$ = wavelength (m)
d = distance between radar and target (m)
$\sigma$ = radar cross-section of target (m2)

The radar backscatter of an object is expressed by its radar cross-section $\sigma$ : the microwave reflective power in the direction of the source. This $\sigma$ of an object can readily be determined by measuring Pr if the system parameters $\lambda$ , G and Pt as well as the distance d are known. The system parameters can be eliminated by calibration while distance d to an object can directly be calculated from the radar measurements itself. For extended surfaces such as land or vegetation covers, $\sigma$ is normalised to irradiated area A or to unit area Ai of the cross-section of the radar beam:

$$\sigma^0 = \sigma/A \quad (m2/m2) \qquad (2)$$
$$\gamma = \sigma/Ai \quad (m2/m2) \qquad (3)$$

Furthermore, radar measurements are usually expressed in decibels dB:

$$\gamma(dB) = 10 \cdot \log(\gamma) \qquad (4)$$

### II.2 Radar backscatter from vegetation

From the standpoint of wave propagation, a vegetation canopy is a dielectric mixture consisting of discrete dielectric inclusions (leaves, stalks, fruit, etc.) distributed in a host or background material of air. These inclusions have various sizes, shapes and orientations and their dimensions are comparable to or larger than the wavelength in the microwave region. This means that the canopy is an inhomogeneous anisotropic medium for microwaves. Wave propagation through such a medium is governed by processes of scattering and absorption, taken together by the term extinction. Models describing the backscatter from vegetation canopies are often developed in terms of the volume absorption, scattering and extinction coefficients of the canopy Ka, Ks and Ku respectively:

$$Ku = Ka + Ks \qquad (5)$$

Extinction of microwaves in a vegetation canopy can be described by a Loss factor L. This factor is defined as the total attenuation of radiation through vegetation at a specific angle of incidence $\theta$ (grazing angle):

$$L(\theta) = \exp(\int_0^{h/\cos\theta} Ku(\theta,z)dz) \qquad (6)$$

in which: $Ku(\theta,z)$ = coefficient of extinction at depth z at angle of incidence $\theta$

        h = height of vegetation (m)

If the transmitted power is Po, then the power Pz at depth z of the vegetation becomes:

$$Pz = Po.\exp(-\int_0^{z/\cos\theta} Ku(\theta,z)dz)$$

$$= Po.1/L(\theta) \qquad (watt) \qquad (7)$$

Both the coefficient of absorption and the coefficient of scattering depend on the state of polarization and the angle of incidence of the incident radiation. They are governed by the dielectric constant, the volume fraction and the geometry (size, shape and orientation relative to the wave's electric field) of the various types of vegetation material present. The dielectric constant of the vegetation material is strongly influenced by its water content and the tension, temperature and salt content of this water. No specific models are currently available that can successfully relate Ka and Ks to measurable physical properties of the plants.

The coefficient of absorption of a vegetation canopy can be estimated from its dielectric constant (Ref.12):

$$Ka = (2Pi.e")/(\lambda_o\sqrt{e'}) \qquad (8)$$

in which: $\lambda_o$ = wavelength in vacuum (m)

     e = e'-e" = dielectric constant of the vegetation canopy

     e' = permitivity of the vegetation canopy

        = real part of the dielectric constant

     e" = imaginary part of the dielectric constant

For the calculation of e, various dielectric mixing models can be used (Ref.14,15). These mixing models calculate e from the dielectric constants and volume fractions of the various materials in the vegetation canopy (air, leaves, stems, etc.). As yet, however, this method has only occasionnaly lead to acceptable results.

For the calculation of the coefficient of scattering from vegetation parameters and geometry, no theoretical solutions have yet been developed. However suggestions have been made that scattering only plays a minor role in the process of extinction in vegetation canopies (Ref.12).

Because of the complexity of the problem, semi-empirical models with a high degree of simplification have been developed.

II.3 The Cloud model

The Cloud model departs from the assumption that a vegetation canopy can be modelled as a cloud of water droplets. This assumption is based

on the fact that the microwave dielectric constant of dry vegetation material is much smaller than that of water and that a vegetation canopy is usually composed for more than 99% air by volume. The model is furthermore developed under the following simplifications and assumptions:
1) The vegetation cloud contains identical water droplets which are randomly distributed in space
2) Only single scattering need be considered
3) For a specific crop, the amount of droplets in the cloud is proportional to the amount of water by volume in the vegetation canopy.

The contribution of the radar backscatter of the underlying soil surface is also included in the model. The total radar backscatter is then given as a function of the water content of the vegetation canopy and of the moisture content of the underlying soil surface (Ref.1,2):

$$\gamma = C[1-\exp(-DW/\sin(\theta))] + G.\exp(Km-DW/\sin(\theta)) \quad (m2/m2) \qquad (9)$$

in which: $W$ = plant water per unit soil surface (kg/m2)
$m$ = soil moisture content (percentage by volume)
$C,G$ = model parameters, angle-dependent (m2/m2)
$D,K$ = model parameters, angle-independent (no dimension)
$\theta$ = grazing angle
$\gamma$ = radar cross-section of target (m2/m2)

N.b: the amount of plant water is defined as the fresh weight minus the dry weight of all above ground plant material.

In this formula, the first term gives the radar backscatter from the vegetation canopy and the second term gives the contribution from the soil surface. The backscatter from the vegetation is modelled as volume scattering, while the backscatter from the soil is modelled as surface reflection which is attenuated by the vegetation canopy. The model parameter C gives the maximum vegetation backscatter from a full grown crop which covers the soil completeley and D is the increase of vegetation backscatter with vegetation water W. Also, D is an attenuation factor for the extinction of microwaves in vegetation. The model parameter G gives the backscatter from the soil in dry condition while K gives the increase in backscatter with soil moisture content. From theoretical and empirical considerations, K ~ 0.051, while the other parameters have to be determined empirically for each different crop and soil surface separately (Ref.2,3).
Whith no vegetation present, W = 0 kg/m2, the left term in the model remains zero and the right term is reduced to the unattenuated backscatter from the soil surface: $\gamma = G.\exp(Km)$. During the growing season, the amount of vegetation water W increases. The backscatter from the vegetation increases hereby with a (1-exp.)-function and the backscatter from the soil reduces with the same factor. In the case of complete soil cover, the vegetation backscatter reaches its maximum level C and the backscatter from the soil is fully attenuated. The contribution from the soil surface will then depend on the value of the attenuation factor D.

The driving force in the Cloud model is the amount of water divided into vegetation water and soil moisture. Distribution effects arising from the roughness of the soil surface and the vegetation canopy are

not taken into consideration. These effects are included in the model
parameters C and G which are taken to be constant during the whole
growing season. If one considers the changes in soil surface roughness
and canopy architecture during the growing season, it will be clear
that these factors are time dependent. However the assumption is that
these parameters are constant over a fairly wide range of spatial and
temporal conditions.
The attenuation of microwaves in vegetation depends on its geometry
and on the ·state of polarization and angle of incidence of the
incoming radiation. The attenuation factor D, however, is simplified
to be independent of the angle of incidence. Since crop geometry
changes during the growing season, it seems clear that D, in reality,
is also time dependent.

The above described Cloud model has been extended into two-layer
models to better accommodate the radar backscatter from wheat
canopies. In these models, the canopy is subdivided into two more or
less homogeneous layers: one of stems and leaves and one of ears. Each
layer is characterized by its specific model parameters C and D, thus
introducing time variance (Ref.2,3,13).

III SUGARBEET

III.1 Crop development

In 1979 and 1980 the same sugarbeet variety Monohil was sown. The
direction of the radar beam was parallel to the direction of sowing.
Emergence took place around May-23 in both years and crop growth and
development was nearly identical, Figs. 3.1 and 3.2. In these figures
soil cover of the crop and the amount of plant water (fresh weight
minus dry weight of all above-ground plant material per unit of soil
surface, kg/m2) is plotted against time.
In 1979, a stable cover of 93% is reached after 55 days after
emergence while the amount of plant water reaches its maximum of 6.3
kg/m2 at 80 days after emergence. In 1980, stable cover of 99% is
reached after 65 days and a maximum amount of plant water of 5.9 kg/m2
at 79 days after emergence. For both years, an S-shaped growth curve
is distinguished for soil cover as well as for the amount of plant
water.
Some differences, however, are observed in the density of plant water
(the amount of plant water per unit enveloping plant volume) during
the growing season. In 1979, this density increased from 5 mg/cm3 at
the beginning to 10 mg/cm3 at the end of the growing season. In 1980,
the density was more stable and increased only from 7.5 to 9.5 mg/cm3.
During the exponential growth stage, the density of plant water was
about 1.5 times larger in 1980 than it was in 1979.
Furthermore, emergence of the crop was somewhat worse in 1980 than it
was in 1979. This caused additional planting to be done at 15 days
after emergence to ensure normal crop development and complete soil
cover. As a result, the crop canopy remained somewhat irregular in
plant size and plant shape throughout the growing season. This had no
effect on crop development and growth of biomass.

In Figs. 1 and 2 the soil moisture content (upper 5 cm topsoil, by
percentage of weight) is plotted against time for soils under the
crops beet, potatoes and peas. 1979 is characterized by large peaks in
the beginning of the growing season, followed by a period of drought
and again two well defined moisture peaks. On the other hand, 1980
begins with a period of drought after which a long period of
intermitting dips and peaks follows. In general, the soil moisture
content follows the same trend under all crops which makes
extrapolation to other fields within the same area feasible. Only with
potatoes as soil cover, some significant discrepancies are observed.
These can be attributed to the specific cultivation on ridges which
renders the determination of a field average dubious.

III.2 Backscatter curves

The radar backscatter of beet is plotted against time for the three
angles of incidence VV20, VV40 and VV8, Figs. 3.3 and 3.4.
The curves of 1979 are smoother in appearance than the curves of 1980;
the peaks and dips are less pronounced and smaller in amplitude. For
both years, the curves of VV20 and VV40 are similar in shape while the
curves of VV80 show a deviating pattern. The backscatter at VV20 and
VV40 steadily increases to a level of saturation after which it
remains fluctuating around this level. The backscatter at VV80 also
increases to a level of saturation but the fluctuations around this
level do not coincide with those at the other angles of incidence. For

both years, the level of saturation is highest at VV80 and lowest at VV20. Finally, the radar backscatter is higher in 1980 than it was in 1979 at all angles of incidence.

For 1979 the following additional remarks can be made:
The radar backscatter correlates fairly well with soil moisture content in the period of growth before 60% soil cover. Fluctuations at the radar saturation level do not show any correlation with fluctuations in soil moisture content. The coefficient of correlation r between radar backscatter and soil moisture content for that period is 0.16 for VV20, -0.10 for VV40 and -0.17 for VV80.
For 1980 the following additional remarks can be made:
During the early growth stage, the radar backscatter curves do not exhibit any large fluctuations. This agrees well with the pattern of soil moisture which is continually low in this period. Simultaneously with the sudden rise in soil moisture content, the radar backscatter sharply increases to a local maximum, after which it decreases to its level of saturation. This pattern is especially pronounced at VV80. At the level of saturation, the radar backscatter appears more correlated to soil moisture than it did in 1979: r VV20 = 0.45, r VV40 = 0.60, r VV75 = 0.54 and r VV80 = 0.48. These relative high coefficients of correlation cannot be readily explained by existing theory. In 1980, the same amount of plant water was present while soil cover and density of plant water were somewhat higher. Thus, the blocking of the soil for microwaves should be the same or even greater in 1980 than in 1979.

Figure 3.5 depicts the radar backscatter at 40° grazing angle for both states of polarization VV and HH.
In 1979, the backscatter at the state of HH polarization is continuously higher than at the state of VV polarization. The overall shape of the backscatter curves is the same and only a few larger deviations occur.
In 1980, the backscatter is nearly identical for both states of polarization and no structural differences are observed. Both curves cross each other frequently and the deviation between the backscatter is 10-15% in some single instances only.

From these observations, two main conclusions can be drawn. First, since the measurements in the different states of polarization were not carried out simultaneously, the similarities in the curves indicate that the fluctuations observed in the backscatter curves are not due to statistical dispersion in the determination of the field average. Hence, the inaccuracy of the measurements appears in practice to be much smaller than was expected from theoretical considerations. Secondly, the difference in backscatter between the states of polarization in the two years imply some difference in crop geometry (Ref.12). However no difference could be deduced from field observations and descriptions on the canopy geometry during the years of measurement.

III.3 Cloud fitting

For 1979 and 1980, Hoekman (Ref. 2) and van Kasteren (personal communication) determined the parameters of the Cloud model for vertical like polarization VV:

1979:

D = 0.76

| θ | 15 | 20 | 30 | 40 | 50 | 60 | 70 | 75 | 80 (°) |
|---|---|---|---|---|---|---|---|---|---|
| C | 0.634 | 0.717 | 0.804 | 0.876 | 0.929 | 0.959 | 0.933 | 0.933 | 0.919 |
| G | 0.015 | 0.021 | 0.032 | 0.043 | 0.061 | 0.090 | 0.166 | 0.284 | 0.479 |

Coefficient of correlation r = 0.97
Standard error of estimate SEE = 21%

1980:

D = 0.46

| θ | 15 | 20 | 30 | 40 | 50 | 60 | 70 | 75 | 80 (°) |
|---|---|---|---|---|---|---|---|---|---|
| C | 0.930 | 0.980 | 1.150 | 1.170 | 1.150 | 1.200 | 1.190 | 1.210 | 1.060 |
| G | 0.042 | 0.055 | 0.065 | 0.076 | 0.095 | 0.120 | 0.174 | 0.269 | 0.525 |

Coefficient of correlation r = 0.97
Standard error of estimate SEE = 26%

Comparing the results for the two years, one notices first the difference in attenuation factor D: this factor is larger in 1979 than in 1980. A smaller value for D means that the attenuation of microwaves is smaller and that the backscatter increases less with plant water. This result compares favorably with the above stated remark that the influence of soil moisture seems to be greater in 1980 than in 1979. However this latter remark applied to the period of backscatter saturation in which the model does not predict any influence of soil moisture on the radar backscatter.
Secondly, one notices the differences in saturation factor C: this factor appears to be larger in 1980 than in 1979. At small grazing angles, the difference is about a factor 1.40, and at large grazing angles 1.27. This agrees with the fact that the radar backscatter at saturation level is indeed higher in 1980 than in 1979. However the saturation factor C might be somewhat overestimated in 1980 due to a local maximum occurring before the saturation level is reached (fig. 3.4).
An explanation for these differences cannot be readily found. No differences existed in plant variety, direction of sowing, crop growth or development. Field descriptions and measurements on crop morphology (e.g. dimensions and number of leaves per plant) also offer no solution. The only difference encountered so far is the difference in

plant water density.


The Figs. 3.3 and 3.4 also give the curves of the calculated
backscatter using the model parameters obtained by curve fitting. In
1979, a good fit between calculated and measured backscatter is
observed, especially for the incidence angles VV20 and VV40. In 1980,
the results are less favourable, although the general trend in radar
backscatter is fairly well described. The model does not describe the
local maximum in backscatter around the beginning of July for VV20 and
VV40, while this local maximum is described, but underestimated, at
VV80. For both years it is obvious that the model is completely unable
to describe any fluctuation occurring at the saturation level of the
radar backscatter. In 1979, saturation of the backscatter occurs for
VV20 at an amount of plant water W of 1.94 kg/m2, for VV40 at W = 3.6
kg/m2 and for VV80 at W = 4.95 kg/m2. In 1980, these values are
respectively 3.28, 5.18 and 5.42 kg/m2. These figures suggest that
high grazing angles (steep incidence) are more suitable for monitoring
the amount of plant water than low grazing angles.
The results of the fitting procedure can also be evaluated by the
slope h of the graph between measured and calculated values. Good
agreement between these values should result in slopes close to the
value 1. Table 3.1 summarizes the the coefficients of correlation and
the slopes h for each angle of incidence in both years separately.

Table 3.1: coefficient of correlation r and slope h

| year | | 1979 | | | 1980 | | |
| --- | --- | --- | --- | --- | --- | --- | --- |
| grazing angle | | VV20 | VV40 | VV80 | VV20 | VV40 | VV80 |
| coeff. of corr. | r | 0.97 | 0.95 | 0.92 | 0.88 | 0.85 | 0.86 |
| slope | h | 0.85 | 0.98 | 0.85 | 0.82 | 0.86 | 0.37 |

Since these coefficients of correlation are calculated for each angle
of incidence separately instead of for all angles together, these
values are lower than those calculated by Hoekman and v. Kasteren.
Furthermore, the results appear less favourable in 1980 than in 1979,
which is in agreement with the visual interpretation. The low value
for h at VV80 1980 is caused by the large local maximum observed at
this angle of incidence.

III.4 The Cloud model for prediction

The crop parameters of the Cloud model determined for 1979 were used
to predict the radar backscatter from beet in 1980. Because in 1980
the experiments were conducted at a different test site, the soil
parameter G determined for 1980 itself was used to calculate the soil
contribution. The results of this prediction are also depicted in Fig.
3.4. As expected, the predicted curve closely follows the measured
backscatter in the early stage of growth and is too low at the level
of saturation. Table 3.2 summarizes the coefficients of correlation
and the slopes h for each angle of incidence.

Table 3.2: coefficient of correlation r and slope h

| grazing angle | | VV20 | VV40 | VV80 |
|---|---|---|---|---|
| coeff. of corr. | r | 0.89 | 0.89 | 0.86 |
| slope | h | 0.57 | 0.64 | 0.29 |

Although the predicted values are below the observed values, the coefficients of correlation are practically the same as for the fitted values. The better performance of the fitting procedure can, however, be inferred from the slope h which is greater than for the predicted case, Table 3.1.


III.5 Relation between radar backscatter and soil cover

The Cloud model (Eq.9) can also be written as:

$$\gamma = C.f + G.\exp(K\theta).(1-f) \qquad (10)$$

in which: $f = (1-\exp(-DWh/\sin\theta))$ (11)

The factor f can be considered as the definition for the microwave soil cover of the crop in the direction of incidence of the radar beam. When no cover is present, f is zero and the backscatter is reduced to the unattenuated backscatter from the soilsurface. During the growing season, the amount of plant water increases and f reaches its maximum value of 1. The backscatter from the crop canopy then equals C and the backscatter from the soil surface is maximal attenuated.
Figure 3.6 depicts a graph of the microwave soil cover versus the optical soil cover for both years. The optical cover was estimated in the field and the microwave cover is calculated from the amount of plant water W, the attenuation factor D and the grazing angle $\theta$, Eq. 11.
Up to 60% optical cover, the relationship is quite linear for VV20, while for VV40 and VV80 the relationship is more of an S-shaped form. The scatter around the curves is not very large and the relations might be useful in estimating the (optical) soil cover as an input into crop growth models.


III.6 Relation between radar backscatter and crop morphology

The crop canopy of beet does not exhibit great phenological changes during the growing season. No flowering or fruit setting takes place and no period of ripening occurs. Beet can thus be characterized by a relative simple development and growth of the canopy. The curve of the radar backscatter exhibits an accordingly simple pattern: the backscatter increases steadily to a level of saturation. Fluctuations occurring at that level of saturation cannot be explained by changes in plant water or in soil moisture content. They can also not result from statistical dispersion in the averages of the radar backscatter from the fields. However they could be the result of changes in plant geometry caused by wind or rain.
In the following sections, these fluctuations are studied in relation

to changes in canopy geometry which are derived from field
descriptions and meteorological data.

III.6.1 Beet in 1979

Table 3.3 summarizes pronounced peaks and dips that are present in the
backscatter curves at the three angles of incidence. All peaks and
dips are relative to neighbouring values. Only peaks and dips
occurring after the beginning of July are included to eliminate the
effect of soil moisture as much as possible. Also included in Table
3.3 are some data on wind speed and wind direction as an average over
the period of measurement.

Table 3.3: Peaks and dips in the backscatter from beet, and some data
           on wind direction and wind speed, 1979

| Date   | Incidence angle | | | Wind direction in classes of speed | | |
|--------|------|------|------|-----------|-----------|-----------|
|        | VV20 | VV40 | VV80 | <3 m/s | >3 m/s | >5 m/s |
| Jul-02 | -    | -    | -    | 7 |   |   |
| Jul-04 | -    | D    | -    | 1 |   |   |
| Jul-06 | -    | -    | P    | 8 |   |   |
| Jul-10 | d    | -    | -    | 8 |   |   |
| Jul-13 | -    | -    | D    | 2 |   |   |
| Jul-17 | P    | P    | -    | 7 |   |   |
| Jul-20 | D    | -    | -    |   | 7 |   |
| Jul-24 | P    | -    | -    | 7 |   |   |
| Jul-27 | -    | -    | D    | 1 |   |   |
| Jul-31 | D    | -    | D    |   |   | 6 |
| Aug-03 | -    | D    | P    |   | 7 |   |
| Aug-07 | P    | -    | -    | 6 |   |   |
| Aug-10 | D    | -    | -    | 8 |   |   |
| Aug-16 | P    | -    | P    | 7 |   |   |
| Aug-17 | D    | -    | -    |   | 8 |   |
| Aug-21 | P    | P    | -    |   | 6 |   |
| Aug-24 | -    | -    | P    |   | 6 |   |
| Aug-28 | D    | -    | D    |   | 6 |   |
| Aug-31 | -    | -    | -    | 8 |   |   |

N.B: D=dip; P=peak; Wind direction: N=1; NE=2; E=3; SE=4; S=5; SW=6;
W=7; NW=8

Wind direction and wind speed:
Little variation occurred in wind direction and wind speed, Table 3.3.
The predominant wind direction was from south to west and the average
wind speed varied between 2.5 and 3.5 m/s. Because of this uniformity,
no relationship is discerned with peaks and dips in the backscatter
curves. It can only be remarked that the uniformity in wind variables
is reflected in a relative smooth appearance of the backscatter curve.

Rainfall:
Rain has fallen during the days of measurement on the following dates:
Jun-11,-13,-15,-29; Jul-17,-31 and Aug-10,-17,-21.
Until June 29th, rainfall coincided with peaks in soil moisture

content and the resulting peaks in radar backscatter can be
contributed to the latter. After June 29th, the vegetation canopy is
quite effective in blocking the soil for microwaves. Any changes in
crop geometry due to the impact of rain could therefore cause
considerable deviations in radar backscatter which are not caused by
variations in soil moisture (Ref.5,10):
Jun-29: no specific features
Jul-17: peak VV20 and VV40; high backscatter VV80
Jul-31: small dip VV20 and·VV40; no specific feature VV80
Aug-10: small dip VV20; no specific features VV40 and VV80
Aug-17: small dip VV20; no specific features VV40 and VV80
Aug-21: small peak VV20 and VV40; no specific feature VV80

Rainfall has no outstanding effect on the radar backscatter. In three
out of five cases the backscatter at VV20 displays a minor dip while
in the other two cases it displays a minor peak. Also, the large
fluctuations occurring in the backscatter curves do not coincide with
days of rainfall.

Remarkable field observations:
Jun-08: plants have been thinned out and the field has been hoed: no
        specific features discernable
Jul-10: erect leaves: small dip VV20
Jul-13: nice green crop: no specific features discernable
Jul-17: erect leaves: small peak VV20 and VV40, high backscatter VV80
        that remains high
Jul-24: drooping leaves caused by the heat: small peak VV20, high
        backscatter VV80
Jul-27: all leaves erect: no specific features discernable
Jul-31: from here on, the crop is irregular in plantheight and
        plantshape
Aug-07: erect, vertical leaves: small peak VV20

Except for July-24, the canopy is always described as being lush green
with nice erect leaves. On this one day, no remarkable deviations in
radar backscatter are observed. Nor do fluctuations in radar
backscatter coincide with any remarkable field observation. Thus, the
fluctuations in radar backscatter are not matched by the field
observations on changes in canopy geometry.

## III.6.2 Beet in 1980

Table 3.4 summarizes pronounced peaks and dips from the backscatter curves at the three angles of incidence. Only peaks and dips occurring after the midst of July are included. Also included are some data on wind speed and wind direction as an average over the period of measurement.

Table 3.4: Peaks and dips in the backscatter from beet, and some data on wind direction and wind speed, 1980

| Date | Incidence angle | | | Wind direction in classes of speed | | |
|------|------|------|------|------|------|------|
| | VV20 | VV40 | VV80 | <3 m/s | >3 m/s | >5 m/s |
| Jul-15 | D | d | – | | 8 | |
| Jul-18 | P | p | – | | 7 | |
| Jul-22 | D | D | – | 6 | | |
| Jul-25 | P | P | – | | 3 | |
| Jul-29 | h | d | D | | | 2 |
| Aug-01 | h | P | P | 4 | | |
| Aug-05 | D | D | – | | | 7 |
| Aug-08 | P | P | – | 4 | | |
| Aug-12 | D | D | P | | | 7 |
| Aug-15 | P | P | D | 4 | | |
| Aug-19 | – | 1 | – | 8 | | |
| Aug-21 | D | D | – | | | 8 |
| Aug-26 | P | h | – | 4 | | |
| Aug-290 | – | P | – | 5 | | |
| Sep-09 | D | D | – | 7 | | |

N.B: D=dip; P=peak; h= high backscatter; l=low backscatter
     Wind direction: N=1; NE=2; E=3; SE=4; S=5; SW=6; W=7; NW=8

Wind direction and wind speed:
Contrary to 1979, this year was characterized by a large variation in wind direction and wind speed. Also, the average wind speed was higher, around 4.5 m/s.
The following relation seems to exist with the radar backscatter at VV20 and VV40: wind from the west (directed towards the radar) coincides with dips in the backscatter and wind from the south-east ( directed from the radar) coincides with peaks in the backscatter. This effect could be enhanced by the high speed (>5 m/s) with which the winds blew from the south-east. Furthermore, large variations in wind direction and wind speed coincide with relative large fluctuations of the radar backscatter (as compared to 1979).

Rainfall:
Rain has fallen during the days of measurement on the following dates:
Jun-16,-20,-23,-27 and Aug-12,-19,-21,-26
These days are characterized by the following features in the radar backscatter:
Jun-16: no specific features
Jun-20: increased backscatter at VV80 (this can also be explained by the increase in soil moisture content)
Jun-23: very small peak VV20, no specific features

Jun-27: very small peak VV40, no specific features
Aug-12: dip VV20 and VV40; small peak VV80
Aug-19: no specific features
Aug-21: dip VV20 and VV40; high backscatter VV80
Aug-26: high backscatter all incidence angles

No relation is established between radar backscatter and rainfall during the day of measurement.

Remarkable field observations:
May-30: fields have been hoed: no specific features on radar backscatter
Jul-01: at some locations pools of rainwater remains in tracks: small peak VV40, high backscatter VV20, low backscatter VV80
Jul-29: weeding has been carried out: dip VV40 and VV80
        from here on a lush, green crop canopy
Aug-01: leaves are drooping because of the heat, topsoil is wet: peak VV40 and VV80

Except for the drooping of the leaves on August-01, the crop canopy is uniformly lush and green throughout the growing season. The drooping of the leaves on that specific day could enhance the effect of the wind and explain for the peak at VV80. In 1979, the drooping of the leaves did, however, show no influence on the radar backscatter. Furthermore, no fluctuations in the radar backscatter coincide with any remarkable field observation or vice versa.

Summarizing for both years, the fluctuations of the radar backscatter at the saturation level seem to be related to wind speed and direction. Little variation in the wind in 1979 coincides with relative smooth curves of the radar backscatter, while large variations in 1980 coincide with curves characterized by large fluctuations. In 1980, a relation is distinguished between direction and speed of wind and the radar backscatter.
Most, if not all of the fluctuations in radar backscatter could not be explained from the field observations. Thus, no relationships are established between the radar backscatter and visually observed changes in canopy geometry.

IV POTATOES

IV.1 Crop development

In both years the same variety Bintje was used and the direction of
the radar beam was parallel to the direction of planting. It is seen
in Figs. 4.1 and 4.2 that crop growth and development were quite
similar in both years. Soil cover reached a maximum of about 93% at 40
days after emergence and remained at this level for about 25 days.
Hereafter, cover declined due to yellowing and dying of the crop and
reduced to about 30% in 1979 and to 50% in 1980. These latter figures,
are only indicative because of the difficulty in estimating soil cover
at the end of the growing season. In Fig. 4.2, some discrepancies in
the growth of plant water (fresh weight minus dry weight of all
above-ground plant material per unit soil surface) is observed. In
1979, plant water increased following a S-shaped curve to a maximum of
1.9 kg/m2 at 50 days after emergence, whereafter it decreased
immediately to a value of 0.6 kg/m2 at 95 days after emergence. In
1980, plant water increased following a linear curve to a maximum of
2.0 kg/m2 at 60 days after emergence and than slowly declined to 1.4
kg/m2 at 105 days after emergence. So, in 1979, yellowing and dying of
the canopy proceeded more rapidly than in 1980. This fact can also be
deduced from the field observations on the crop: in 1979, lodging and
yellowing of the canopy started already at 76 days after emergence,
while in 1980 this did not take place until 100 days after emergence.
The density of plant water (amount of plant water per unit enveloping
volume) was nearly identical in both years. In 1979, the density
decreased from 5.6 mg/cm3 at the beginning of the growing season to
3.2 mg/cm3 at the end. In 1980, these figures were 5.2 and 3.2 mg/cm3
respectively.


IV.2 Backscatter curves

The radar backscatter of potatoes during the growing season for the
grazing angles VV20, VV40 and VV80 is presented in Figs. 4.3 and 4.4.
As in the case of beet, the curves of 1979 are smoother in appearance
than the curves of 1980; the peaks and dips are less pronounced and
smaller in amplitude.
In both years, the backscatter increases to a level of saturation at
all angles of incidence. The level of saturation is highest at VV80
and lowest at VV20. Large fluctuations around these levels of
saturation occur which don't show any correlation at the various
angles of incidence in 1979, while some correlation between VV20 and
VV40 exists in 1980. In this same year, a remarkable feature is
observed in the month of July: at VV80, the radar backscatter displays
a broad peak between July-04 and July-22. This peak does not occur in
1979 and it can not be explained by any changes in crop morphology,
plant growth or soil moisture.

The coefficients of correlation between the backscatter at the level
of saturation and the soil moisture content are as follows:
1979: VV20: r = -0.16; VV40: r = 0.30; VV80: r = 0.69
1980: VV20: r = -0.47; VV40: r = 0.14; VV80: r = 0.59
One can notice a relative high coefficient of correlation at VV80.
This suggests that the crop is less effective in attenuating
microwaves at large grazing angles than at small grazing angles.

Furthermore, a negative coefficient of correlation is observed at the grazing angle VV20. The relatively high negative value for VV20 in 1980 is caused by the steady increase in backscatter from 70 days after emergence onwards, while at the same time the soil moisture content decreases. Considering the deviating behaviour of the backscatter at VV20, this high correlation is probably incidental.

Furthermore, a phenomenon of 'backscatter-inversion' is observed. Especially in 1979, a peak in the backscatter at some angle of incidence frequently coincides with a dip at another angle, and vice versa. This phenomenon also occurs in 1980, although to a lesser extent. Fig. 4.5 illustrates this effect for some instances in 1979. This Figure should be read as a polair diagram: the angle between the vector to a point with the horizontal corresponds with the grazing angle while the length of this vector indicates the value of the radar backscatter. On July-24 and 31 the backscatter is relatively small at grazing angles larger than $45^{\circ}$, and relatively large at grazing angles smaller than $45^{\circ}$. On July-27 and August-03, exactly the opposite effect is observed. In this particular example, a relatively high soil moisture content was measured on July-24 and 31 which could possibly have had some effect on this phenomenon. The other examples, however, show that the 'backscatter-inversion' also takes place under conditions of a constant soil moisture regime.

Fig. 4.6 depicts the radar backscatter at $40^{\circ}$ grazing angle for both states of polarization VV and HH. In both years, the level of backscatter is the same in both states of polarization, while especially in 1979 the curves of the different polarization states cross each other frequently. The differences in backscatter are in general below 10%. The cause for these differences and for the crossing of the curves (statistical dispersion in the observations, varying canopy architecture ?) could not be determined. In 1980, a remarkable feature is observed in July: the backscatter in the state of HH polarization remains well below that in the state of VV polarization. This same phenomenon is observed at $20^{\circ}$ grazing angle and coincides with the already observed strange behaviour in this period of the backscatter at $80^{\circ}$ grazing angle. This suggests a structural cause in the architecture of the canopy, although no significant observations were made in the field. Except for this difference in backscatter, the fluctuations in the curves of HH and VV polarization coincide better in 1980 than in 1979.

## IV.3 Cloud fitting

For 1979 and 1980, the parameters of the Cloud model are determined by Hoekman (Ref.2) and v. Kasteren (personal communication) for vertical like polarization VV:

### 1979:

D = 0.25

| θ | 15 | 20 | 30 | 40 | 50 | 60 | 70 | 75 | 80 (°) |
|---|-----|-----|-----|-----|-----|-----|-----|-----|-----|
| C | 0.284 | 0.368 | 0.546 | 0.726 | 0.994 | 1.260 | 1.547 | 1.606 | 1.725 |
| G | 0.023 | 0.034 | 0.049 | 0.067 | 0.079 | 0.092 | 0.115 | 0.132 | 0.180 |

Coefficient of correlation r = 0.94
Standard error of estimation SEE = 24%

### 1980:

D = 1.02

| θ | 15 | 20 | 30 | 40 | 50 | 60 | 70 | 75 | 80 (°) |
|---|-----|-----|-----|-----|-----|-----|-----|-----|-----|
| C | 0.300 | 0.320 | 0.440 | 0.490 | 0.560 | 0.630 | 0.710 | 0.790 | 0.870 |
| G | 0.071 | 0.093 | 0.117 | 0.135 | 0.151 | 0.170 | 0.195 | 0.209 | 0.214 |

Coefficient of correlation r = 0.86
Standard error of estimation SEE = 38%

Comparing these results for the two years, one first notices that the attenuation factor D for 1980 is 4 times the factor for 1979. This implies that in 1980 the radar backscatter increased at a faster rate to its saturation level and that the attenuation of microwaves in the canopy was much higher. In a comparative study, de Loor (Ref. 9) concluded that the value of 0.25 in 1979 is extremely low when compared to values in other years. Secondly, the saturation factors C are also different. At 15° grazing angle, values for C are about 0.30 in both years, and increase to 1.70 at 80° grazing angle in 1979 and to 0.87 in 1980. Both differences in values for C and D are opposite to the differences observed for beet. This means that the differences are not due to errors in measurement or calibration. Causes for the deviations should be searched for in differences in canopy architecture or in the curve fitting procedure itself.

Figs. 4.3 and 4.4 give the fitted curves of the Cloud model together with the measured curves. In 1979, the measured and fitted values are in good agreement, especially at the large grazing angle. However, many of the measured peaks and dips are not described by the Cloud model. Complete saturation of the radar backscatter does not seem to be reached. The small value for D allows the soil to contribute significantly to the calculated backscatter at full development of the

crop. Also, the maximum backscatter C from the vegetation is never reached at the large grazing angle of VV80.
In 1980, the results of the Cloud fitting are disappointingly bad. After an initial fast increase, the calculated backscatter attains a level of saturation without any fluctuation al all. Even at the large grazing angle VV80, no fluctuations due to varying soil moisture conditions are present in the radar backscatter.

Table 4.1 summarizes the coefficients of correlation and the slopes h for each angle of incidence:

Table 4.1: coefficient of correlation r and slope h

| year | | 1979 | | | 1980 | | |
|---|---|---|---|---|---|---|---|
| grazing angle | | VV20 | VV40 | VV80 | VV20 | VV40 | VV80 |
| coeff. of corr. | r | 0.62 | 0.82 | 0.62 | 0.42 | 0.55 | 0.69 |
| slope | h | 0.52 | 0.79 | 0.56 | 0.04 | 0.31 | 0.25 |

This Table clearly illustrates the poor results obtained for 1980, while the figures for 1979 are also not very good. The values of the calculated model parameters in 1980 thus seem doubtful.

As a first tentative to improvement for the data of 1980, the curve fitting procedure was applied to the early period of exponential growth only. The value thus obtained for D, however, is even much larger and values for C much smaller than before:

D = 1.95

| θ | 15 | 20 | 30 | 40 | 50 | 60 | 70 | 75 | 80 (°) |
|---|---|---|---|---|---|---|---|---|---|
| C | 0.190 | 0.210 | 0.290 | 0.320 | 0.320 | 0.340 | 0.310 | 0.300 | 0.360 |

Coefficient of correlation r = 0.75
Standard error of estimation SEE = 40%

This large value for D would imply the radar backscatter to increase at an even faster rate to its (lower) level of saturation. Also, attenuaton of microwaves within the crop canopy would be much larger, thus allowing hardly any contribution from the underlying soil. This result is in contradiction with the measured curves in which contribution from the soil surface is evident during the the early stages of growth. The division in the growing season of potatoes into a stage of exponential growth and a stage of complete soil cover does not lead to better results.

It is concluded that the results of the Cloud model are encouraging in 1979, but rather disappointing in 1980.

IV.4 The Cloud model for prediction

The crop parameters of the Cloud model determined for 1979 were used
to predict the radar backscatter from the potatoes in 1980 (The soil
parameters for 1980 served as an input for the soil contribution).
Fig. 4.7 depicts the predicted curves along with the measured curves
of 1980. Due to the lower value of D in 1979, the contribution from
the soil background is considerably larger in the predicted curves
than in the fitted curves (Fig.4.4). Consequently, more peaks and dips
appear in the predicted curves which correspond with fluctuations in
the measured curves. Though the radar backscatter is overestimated
during the early stage of growth, the similarity in shape is better
than for the fitted curves itself.
Table 4.2 summarizes the coefficients of correlation r and the slopes
h:

Table 4.2: coefficient of correlation r and slope h

| grazing angle | | VV20 | VV40 | VV80 |
|---|---|---|---|---|
| coeff. of corr. | r | 0.05 | 0.55 | 0.77 |
| slope | h | 0.02 | 0.75 | 0.59 |

This Table testifies to the better performance of the predicted curves
at grazing angle VV40 and VV80. The poor results for VV20 can again be
attributed to the strange pattern of backscatter at this grazing
angle.

In another attempt to improve the model, the soil parameters K and G
are determined for the potato field separately. This was done by
linear regression on the backscatter measurements from the potato
field before emergence. The values of K and G were determined for each
angle of incidence separately:

| grazing angle | VV20 | VV40 | VV80 |
|---|---|---|---|
| K | 0.025 | 0.025 | 0.035 |
| G | 0.131 | 0.193 | 0.284 |
| coeff. of corr. | 0.63 | 0.54 | 0.72 |

Using these values as an input for the soil contribution, the radar
backscatter in 1980 was again predicted from the 1979 crop parameters.
The predicted and the measured backscatter are now in good agreement,
Fig. 4.8. Table 4.3 summarizes the coefficients of correlation and the
slopes h, and also testify that predicted and observed radar
backscatter agree fairly well:

Table 4.3: coefficient of correlation r and slope h

| grazing angle | | VV20 | VV40 | VV80 |
|---|---|---|---|---|
| coeff. of corr. | r | 0.73 | 0.92 | 0.89 |
| slope | h | 1.26 | 1.00 | 1.07 |

The crop parameters derived for 1979 can successfully be used in conjunction with on-site derived soil parameters to describe the measured radar backscatter in 1980. The improvement over the fitted curve for 1980 itself lies in the determination of the soil parameters K and G for each angle of incidence separately. The results also imply that either the microwave attenuation of a potato canopy is quite low, or that soil moisture somehow has an iderect effect on the radar backscatter from the canopy. In both ways, a better agreement is reached between calculated and measured backscatter using a low value ` for D (0.25) than using a high value (1.0-2.0).

IV.5 Relation between radar backscatter and soil cover

Figure 4.9 depicts a graph of the microwave soil cover versus the optical soil cover for both years. The optical cover was estimated in the field and the microwave cover is calculated from the amount of plant water W, the attenuation factor D and the grazing angle $\theta$, Eq. 11. For this purpose, the parameters from the best fitting Cloud curves were used, e.g. for 1979, the fitted Cloud parameters and for 1980, the values obtained with the 1979-crop parameters and the separately determined soil parameters.
Linear relationships up to 100% optical soil cover are found for VV80 and VV40, while for VV20 the relationship is slightly curved. The scatter around the lines is quite low.

IV.6 Relation between radar backscatter and crop morphology

During the growing season, the morphology of a potato crop is affected by phenological events. After emergence, the crop enters a stage of exponential growth in which the leaves change in size and shape. At full soil cover, a period of flowering occurs and after that the crop remains fairly constant of architecture for a considerable time. At the end of the growing season, the individual plants start lodging and the crop canopy collapses completely.
In this section, these structural as well as temporal changes in crop morphology are compared with the radar backscatter.

IV.6.1 Potatoes in 1979

The following crop developments are identified during the growing season:

may-23: emergence of the plants
Jun-29: the canopy covers the furrows for about 80%
Jul-02: appearance of flowers
Jul-24: first lodging of the canopy
Aug-16: first dying of the leaves
Aug-28: the crop is sprayed to death

No influence from flowering or lodging of the canopy can be discerned on the radar backscatter. From Aug-16 onwards, the influence of the soil background becomes more pronounced at VV40 and VV80, fig 4.3.

Table 4.4 summarizes pronounced peaks and dips in the backscatter curves at the three angles of incidence. Only peaks and dips occurring

after the end of June are included to eliminate the effect of soil moisture as much as possible. Also included in the Table are some data on wind speed and wind direction as an average over the period of measurement.

Table 4.4: Peaks and dips in the backscatter from potatoes, and some data on wind direction and wind speed, 1979

| Date | Incidence angle | | | Wind direction in classes of speed | | |
|------|------|------|------|------|------|------|
| | VV20 | VV40 | VV80 | <3 m/s | >3 m/s | >5 m/s |
| Jun-29 | 1 | - | P | 7 | | |
| Jul-02 | L | D | - | 7 | | |
| Jul-04 | D | - | - | 1 | | |
| Jul-06 | h | - | D | 8 | | |
| Jul-10 | h | - | - | 8 | | |
| Jul-13 | 1 | - | - | 2 | | |
| Jul-17 | D | - | - | 7 | | |
| Jul-20 | P | P | P | | 7 | |
| Jul-24 | D | - | - | 7 | | |
| Jul-27 | P | - | D | 1 | | |
| Jul-31 | D | D | P | | | 6 |
| Aug-03 | - | P | D | | 7 | |
| Aug-07 | - | - | D | 6 | | |
| Aug-10 | - | D | D | 8 | | |
| Aug-16 | - | P | P | 7 | | |
| Aug-17 | - | - | D | | 8 | |
| Aug-21 | P | - | P | | 6 | |
| Aug-24 | - | P | D | | 6 | |
| Aug-28 | - | - | P | | 6 | |
| Aug-31 | - | - | D | 8 | | |

N.B: D=dip; P=peak; h=high backsc.; l=low backsc.
     Wind direction: N=1; NE=2; E=3; SE=4; S=5; SW=6; W=7; NW=8

Except for the peak in backscatter on Jul-20 (which might be attributed to a peak in the soil moisture content), there appears to be no correlation between the dips and peaks at the various angles of incidence. The phenomenon of 'backscatter-inversion' occurs on Jul-27, Jul-31 and Aug-24.

Wind direction and wind speed:
Because of the relative uniformity in wind direction and wind speed, no relationships with the radar backscatter are detected. As for beet, this uniformity is reflected in a relative smooth appearance of the backscatter curves.

Rainfall:
Rain has fallen during the days of measurement on the following dates: Jun-11,-13,-15,-29; Jul-17,-31 and Aug-10,-17,-21.
No consistnet relation with the radar backscatter is observed, nor is rainfall during the day of measurement responsible for the observed 'backscatter-inversion'.

Remarkable field observations:
Jun-13: crop is blown down by the wind, lies across the furrow
Jun-15: erect crop
Jun-22: nice crop, the plants touch across the furrows
Jun-25: irregular canopy due to strong winds
Jun-27: nice, regular crop again, the furrows are now colmpletely
covered
Jul-04/Jul-17: nice regular crop, no specifics
Jul-24: first lodging of the crop, fairly strong winds
Jul-27: individually lodged plants
Aug-03: lodging of the crop
Aug-07: completely lodged crop, bare soil starts to appear in spots
Aug-16: first yellowing of leaves
Aug-17: considerable yellowing of leaves

A clear effect of a change in crop geometry on the radar backscatter
is observed on Jun-13. The wind has blown the crop across and down
into the furrows and this caused the backscatter to peak at
non-vertical incidence. The backscatter at vertical incidence, VV80,
lags behind the expected increase due to the growth in plant water.
No more clear relations are found between the observed changes in crop
geometry and responses in the radar backscatter. On Jun-25, the crop
is also blown by the wind but a pronounced dip only occurs at VV80.
From Jul-24 onward, various descriptions of lodging of the canopy
occur but no consistent responses in the radar backscatter are found.
No remarkable field description was made on Jul-03 to account for the
observed peaks and dips on that day. The minor peak in backscatter
that occurs at all angles of incidence on Jul-20 might be explained by
a peak in the soil moisture content. This explanation, however, is not
consistent with responses in the backscatter at other peaks and dips
in soil moisture.
The strange pattern of radar backscatter between Jul-04 and Jul-17
(fig.4.3) is not matched by any remarkable field observation during
that period, nor by a specific soil moisture regime. This pattern,
however, does occur at the onset of the flowering period. Due to a
lack in further descriptions on the flowering period, no conclusions
can be drawn for the existence of this relationship.


IV.6.2 Potatoes in 1980

The following descriptions on crop development have been made:

may-27: emergence of plants
Jun-23: the ridges are fully covered
Jul-04: flowering
Jul-15: the furrows are covered for about 92%
Jul-22: crop is on the brink of lodging
Aug-03: lodging of crop
Aug-29: plants start to die

Crop development can not be related to patterns in the radar
backscatter. At VV20, the period of lodging of the canopy coincides
with a steady increase in the backscatter which cannot be explained by
plant growth. At the other angles of incidence, however, no specific
reactions are observed during this period of lodging. In 1979, no
specific reactions on lodging of the canopy could either be observed.

Table 4.5 summarizes pronounced peaks and dips in the backscatter curves at the three angles of incidence. Only peaks and dips occurring after Jul-10 are included to eliminate the effect of soil moisture as much as possible. Also included in the Table are some data on wind speed and wind direction as an average over the period of measurement.

Table 4.5: Peaks and dips in the backscatter from potatoes, and some data on wind direction and wind speed, 1980

| Date | Incidence angle | | | Wind direction in classes of speed | | |
|------|------|------|------|------|------|------|
| | VV20 | VV40 | VV80 | <3 m/s | >3 m/s | >5 m/s |
| Jul-11 | - | - | P | | 8 | |
| Jul-15 | - | P | h | | 8 | |
| Jul-18 | - | D | h | | 7 | |
| Jul-22 | - | P | D | 6 | | |
| Jul-25 | - | - | - | | 3 | |
| Jul-29 | - | - | - | | | 2 |
| Aug-01 | D | - | P | | 4 | |
| Aug-05 | P | P | D | | | 7 |
| Aug-08 | D | D | - | | 4 | |
| Aug-12 | P | P | P | | | 7 |
| Aug-15 | - | D | D | | 4 | |
| Aug-19 | D | P | P | | 8 | |
| Aug-21 | P | P | D | | | 8 |
| Aug-26 | D | D | D | | 4 | |
| Aug-29 | P | P | P | | 5 | |
| Sep-097 | D | D | D | | | 7 |

N.B: D=dip; P=peak; h=high backsc.; l=low backsc.
Wind direction: N=1; NE=2; E=3; SE=4; S=5; SW=6; W=7; NW=8

Wind direction and wind speed:
Only a slight correlation is distinguished between radar backscatter and direction of wind at a wind speed exceeding 5 m/s. At VV20 and VV40, wind from the west (directed towards the radar) coincides with peaks in the radar backscatter, while wind from the south-east (blowing away from the radar) corresponds with the dips. Some of these peaks and dips, however, can also be described by the contributions from the underlying soil surface.
As for beet, the large variations in wind direction and wind speed coincide with relative large fluctuations of the radar backscatter (compared to 1979).

Rainfall:
Rain has fallen during the days of measurement on the following dates:
Jun-16,-20,-23,-27 and Aug-12,-19,-21,-26
No consistent relationship with the radar backscatter is observed.

Remarkable field observations:
Jun-16: the wind blows the leaves in the direction of the radar
Jun-23: the wind blows the leaves vertically aside from the radar
Jul-01: at some places the plants are lodged
Jul-04: some plants are flowering, ridges are completely covered by the crop

Jul-11: full flowering, the wind blows the leaves in the direction of
the radar
Jul-22: crop becomes irregular in height
Jul-25: the wind blows the leaves away from the radar
Aug-01: irregular canopy, the wind blows in the direction of the radar
Aug-12: the wind blows the leaves in the direction of the radar
Aug-15: many open spots appear in the canopy
Aug-21: the wind blows the leaves in the direction of the radar

Practically no consistent reaction of changes in crop geometry on the
radar backscatter is distinguished. The bending of the leaves towards
the radar on Aug-12 and Aug-21 coincides with peaks in the backscatter
at VV20 and VV40. This observation is consistent with the described
relation between radar backscatter and direction of the wind. However
no such reaction is distinguished on the other days of pronounced
winds.
Some of the large peaks and dips in the radar backscatter occur at
times when no specific field observations were made, e.g. Jul-04.
Notably the strange pattern in the backscatter between Jul-04 and
Jul-22 cannot be explained by any visual changes in the crop geometry.
As in 1979, this deviating pattern occurs at the period of flowering
but without any similarity to the pattern in that year.


Concluding for both years, only a minor relation between direction and
speed of wind and radar backscatter is distinguished. A relative
uniformity in wind variables is reflected in relative smooth
appearances of the radar backscatter curves. If the wind speed exceeds
5 m/s, some relation between the direction of the wind and the
backscatter seems to exist at low grazing angles.
Rainfall during the days of measurement has no specific effects on the
radar backscatter from vegetation. Furthermore, the radar does not
seem to be able to detect a period of flowering. At the end of the
growing season, yellowing and dying of the crop coincides with an
enhanced influence of the underlying soil background.
Finally, many peaks and dips in the radar backscatter cannot be
explained by any visual observation on the crop canopy or on the soil
background.

V PEAS

V.1 Crop development

In 1979 and 1980, two different varieties of peas were used: 'Rondo' in 1979 and 'Finale' in 1980. Beside this difference in variety, a large difference in growth and development of the crops occurred, figs. 5.1 and 5.2.

The crop in 1979 was characterized by a bad emergence and a near failure in growth and development. The soil cover increased within 45 days to a maximum of 72%, remained at this level for about 10 days and then declined again to 20% within 20 days. The amount of plant water (fresh weight minus dry weight of all above ground plant material per unit soil surface) increased at a slow rate to 1.0 kg/m2 at 45 days after emergence. Hereafter, no more measurements on plant water were performed but it seems likely that it only decreased again. Flowering and pod formation did hardly occur at all.
Beside this overall adverse growth and development, the field was characterized by a large heterogeneity. In the midst of the field, crop emergence was worst and the crop started yellowing at a very premature stage. At both ends of the field (from the standpoint of the radar), the emergence of the crop was slightly better, and some flowering and pod formation occurred.

The situation was completely different in 1980: soil cover rose within 40 days to 96%, remained so for some 40 days and thereafter declined to 60% within 25 days more. The amount of plant water sharply increased to 3.4 kg/m2 at 65 days after emergence, decreased slowly to 2.6 kg/m2 within 25 days and then rapidly fell back to 0.3 kg/m2 within 15 days time. The development of the crop could be divided in the phases of exponential growth, flowering, pod-formation and ripening.
The difference in crop growth in both years is also reflected in plant water density (the amount of plant water per unit enveloping volume, kg/m3): In 1979, the density declined from 5 mg/cm3 shortly after emergence to 3 mg/cm3 after 45 days; in 1980 the density varied from 14 mg/cm3 shortly after emergence through 5 mg/cm3 between 36 and 96 days after emergence to 18 mg/cm3 during the stage of ripening. The paradoxical increase in plant water density at the end of the growing season is caused by the decrease in soil cover that occured during ripening.

V.2 Backscatter curves

The radar backscatter curves of peas are given in Figs. 5.3 and 5.4 for 1979 and 1980 respectively. Despite the adverse growth of the crop in 1979, some similarity with the curves of 1980 is observed at the grazing angles VV20 and VV40.
In 1979, we notice at VV20 a steady increase in radar backscatter from the time of emergence to Jul-04. The radar backscatter then jumps to a higher level from Jul-13 to Jul-24. Hereafter, it quickly decreases again until Aug-17. At VV40, more or less the same pattern is observed, although less pronounced. The radar backscatter steadily increases til Jul-10, after which it sharply increases to a higher level of backscatter on Jul-20. On Jul-24, it declines again until Aug-17. The level of radar backscatter is lower at VV40 than it is at

VV20 and the backscatter displays a larger influence of the underlying soil surface. This could be explained by the fact that the radar beam at 40° grazing angle was directed to the midst of the field with the worst growth and development of the crop. At VV80, no growth or development of the crop is present in the backscatter curve at all. Nearly all peaks and dips can be attributed to variations in the soil moisture content, Figs. 1 and 2.

In 1980, the shape of the backscatter curves at VV20 and VV40 is similar to those in 1979. At VV20, the backscatter steadily increases til Jul-04, after which a sharp increase until Jul-15 is noticed. On Jul-29, it starts to decline again until Aug-26. At VV40, the backscatter steadily increases til Jul-18, then sharply jumps on Jul-22 and decreases again from Aug-01 onwards. The backscatter curve at VV80 is exceptional and displays no similarity at all with the curve of VV80, 1979. A well pronounced growth curve is only recognised between Jun-13 and Aug-01. Before and after this period, the underlying soil surface seems to be the dominant backscatter component. Finally, at all angles of incidence a broad dip is observed around Jun-18/20. This dip does not occur simultaneously at all angles of incidence but displays a slight displacement in time.

In both years, the backscatter curves are fairly smooth in appearance. No large peaks and dips (which were observed for beet and potatoes) are present in the curves of peas. The backscatter curves are also not smoother in appearance in one year than in the other. The observed smoothness could be due to the relative small dimensions of the scatter elements (e.g. leaves, flowers, pods) in the order of the size of the wavelength of X-band microwaves. This would make the radar backscatter from peas less sensitive to instantaneous changes in canopy geometry (caused by wind or rain) then that from beet and potatoes.

Fig 5.5 shows the radar backscatter at 40° grazing angle for both states of polarization VV and HH. In 1979, the backscatter is higher at horizontal polarization than at vertical polarization. The minor fluctuations that occur, coincide in time. In 1980, a different pattern is observed. To the midst of June, the backscatter is of equal magnitude for both states of polarization. Hereafter, the backscatter at vertical polarization steadily increases over that at horizontal polarization. Towards the midst of August, the backscatter curves cross each other and at the end, they reach the same value again. This pattern suggests that some structural changes in the canopy architecture took place during the growing season. Apparently, these changes did not take place, or to a lesser extent, in 1979.

## V.3 Cloud fitting

The above described shapes of the backscatter curves can only partially be described by the Cloud model. The sudden increase in backscatter around Jul-10 in 1979 and around Jul-11/22 in 1980 occurs at a time when plant water as a driving force has reached a stable level, Fig. 5.2. Nor can the sudden increase be attributed to a rise in the soil moisture content, Figs. 1 and 2. Therefore, it must be caused by some other mechanism. The decrease in backscatter after Jul-29, 1980, at VV20 and VV40 coincides with a decrease in plant water and can thus be explained by the theory of the Cloud model. In this period, a larger influence of the soil background is present at

VV75 and VV80.

The parameters of the Cloud model are determined by Hoekman (Ref.2) and v. Kasteren (personal communication) for vertical like polarization VV:

1979:

D = 0.41

| θ | 15 | 20 | 30 | 40 | 50 | 60 | 70 | 75 | 80 (°) |
|---|-----|-----|-----|-----|-----|-----|-----|-----|-----|
| C | 0.356 | 0.394 | 0.398 | 0.413 | 0.422 | 0.345 | 0.415 | 0.433 | 0.218 |
| G | 0.026 | 0.034 | 0.047 | 0.058 | 0.068 | 0.089 | 0.136 | 0.211 | 0.425 |

Coefficient of correlation r = 0.95
Standard error of estimate SEE = 21%

1980:

D = 0.94

| θ | 15 | 20 | 30 | 40 | 50 | 60 | 70 | 75 | 80 (°) |
|---|-----|-----|-----|-----|-----|-----|-----|-----|-----|
| C | 0.370 | 0.410 | 0.480 | 0.490 | 0.510 | 0.510 | 0.520 | 0.550 | 0.530 |
| G | 0.029 | 0.032 | 0.047 | 0.055 | 0.066 | 0.071 | 0.132 | 0.200 | 0.380 |

Coefficient of correlation r = 0.92
Standard error of estimate SEE = 26%

A comparison between these crop parameters can hardly be made. In 1979, the curve fitting was only applied to the firts 45 days after emergence because of the lack in data on plant water afterwards. In 1980, the procedure was applied to the whole growing season. This difference accounts for the relative high values for the C-parameters obtained in 1980. In this year, the high backscatter values after Jul-04 co-determined the value for C.

The difference in fitting procedure also has its effect on the accuracy with which the model can describe the measured backscatter curves, Figs. 3.3 and 3.4.
In 1979, a good agreement is reached between fitted and measured backscatter at all angles of incidence. At VV20 and VV40, the influence of soil moisture is somewhat overestimated but the growth in backscatter is fairly well described. In 1980, on the contrary, the agreement between fitted and measured backscatter is rather poor. Until Jul-01, the radar backscatter is overestimated at all angles of incidence, thereafter it becomes seriously underestimated. Only after Jul-29, as the amount of plant water starts to decline, the radar backscatter is fairly well described. This poor result is the consequence of the inability of the Cloud model to adequately describe the radar backscatter during the whole growing season of the peas. Table 5.1 summarizes the coefficients of correlation and the slopes h for each angle of incidence.

Table 5.1: coefficient of correlation r and slope h

| year | | 1979 | | | 1980 | | |
|------|---|------|------|------|------|------|------|
| grazing angle | | VV20 | VV40 | VV80 | VV20 | VV40 | VV80 |
| coeff. of corr. | r | 0.92 | 0.70 | 0.97 | 0.78 | 0.86 | 0.72 |
| slope | h | 0.73 | 0.71 | 0.86 | 0.74 | 0.58 | 0.42 |

This Table also illustrates the better results obtained in 1979 than in 1980.

V.4 The Cloud model for prediction

The crop parameters of the Cloud model determined for 1979 were used to predict the radar backscatter from the peas in 1980. Graphs of these predicted values are given in Fig. 5.6. For VV20 and VV40, good agreement is reached for the early period of growth for which the crop parameters were determined in 1979. The decrease in backscatter after Jul-29 is also fairly well described. At VV80, however, considerable deviations occur between the curves of the predicted and the measured backscatter. Peaks and dips are only fairly well described for the periods in which the backscatter from the soil background dominates, n.b. before Jun-13 and after Jul-29. The backscatter at large grazing angles is again exceptional.
Table 5.2 summarizes the coefficients of correlation and the slopes h for each angle of incidence:

Table 5.2: coefficient of correlation r and slope h

| grazing angle | | VV20 | VV40 | VV80 |
|------|---|------|------|------|
| coeff. of corr. | r | 0.92 | 0.80 | 0.58 |
| slope | h | 0.79 | 0.47 | 0.46 |

At VV20, these figures are better than for the fitted curve of 1980, Table 5.1. At VV40 an VV80, they are somewhat and much worse respectively.

When these coefficients are not determined for the complete growing cycle but only for the early period of growth for which the crop parameters were determined in 1979, n.b. before Jun-27, tese values become:

Table 5.3: coefficient of correlation r and slope h

| grazing angle | | VV20 | VV40 | VV80 |
|------|---|------|------|------|
| coeff. of corr. | r | 0.94 | 0.95 | 0.17 |
| slope | h | 1.07 | 1.11 | 0.17 |

High coefficients for VV20 and VV40 are evident, while the result for VV80 is poor.

As conclusion, it can be stated that a good prediction is made of the radar backscatter at VV20 and VV40 for the early period of growth. This good agreement is reached despite the large differences in crop growth and development in the two years. Furthermore, it is worthwhile to determine the crop parameter D separately for the high grazing angles VV70-VV80.

V.5 Relation between radar backscatter and soil cover

Figure 5.7 depicts a graph of the microwave soil cover versus the optical soil cover for both years. The optical cover was estimated in the field and the microwave cover is calculated from the amount of plant water W, the attenuation factor D and the grazing angle θ, Eq. 11.
In 1979, a fairly linear relationship exists up to 75% optical crop cover for VV20 and VV40. For VV80, the curve is of an S-shaped form. In 1980, the relationship is linear up to 50% optical cover. Thereafter, the microwave cover only increases slowly until 85% optical cover is reached. From there on, the microwave cover sharply increases to its maximum values of 70-95%.
In general, a linear relationship between the optical and microwave soil cover only exists during the vegetative period of growth. Because of the differences in development of the crop, different relationships are found in 1979 and 1980.

V.6 Relation between radar backscatter and crop morphology

Peas display changes in morphology which are related to the various stages of phenology. After emergence, exponential growth of the crop takes place until complete cover of the soil is reached. A period of flowering occurs and pod-formation takes place. These pods grow larger and thicker during the growing season and may, at the end, make up for most of the canopy. At this period of the growing season, the crop is extremely sensitive to lodging.

In 1979, almost no observations on these phenological stages were reported. The crop didn't have a normal development and at some places even failed to develop at all. Only some minor observations were made on the flowering of the crop but none on pod formation or pod development. From Jul-24 onwards, the canopy displayed bare spots in the field.

In 1980, the following field observations were been reported:

Jun-13: first flowering
Jun-16: flowering
Jun-18: flowering
Jun-20: first pods appear
Jun-23: flowering; pods are 7 cm large
Jun-25: flowering; pods are 8 cm large
Jun-27: flowering; pods are 9 cm large
Jul-01: still flowering at some places; pods 9 cm large
Jul-04: still flowering at some places; pods 9 cm large
Jul-11: flowering practically finished
Jul-18: crop is loaded with pods; crop is lodged at some places
Jul-22: crop is lodged until harvest

Aug-01: withering of leaves; pods are still green
Aug-05: few leaves are left; crop is dead for about 40%
Aug-19: crop is dead for 100%
Aug-21: harvest

In this year, a healthy crop is present which displays the different
stages of growth and phenology. The following relations with the radar
backscatter are distinguished:
-VV20: after the appearance of the first pods on Jun-20, the radar
backscatter increases sharply. From Jul-15 to Jul-29, the backscatter
is at its highest level while the crop is completely set with pods.
This period also coincides with the period of lodging of the crop. On
Jul-29, the backscatter decreases again which coincides with the onset
of withering and yellowing of the leaves.
-VV40: after the appearance of the first pods on Jun-20, the radar
backscatter increases sharply. From Jul-22 onwards, the crop is
heavily set with pods and the radar backscatter still increases. On
Jul-27, a sudden jump in the backscatter takes place at the onset of
lodging of the crop. Withering and yellowing of the leaves starts on
Aug-01 and the radar backscatter decreases.
-VV75: after the appearance of the first pods on Jun-20, the radar
backscatter steadily increases with a local minimum around Jul-18.
From this moment on, the crop is lodged and the radar backscatter
increases again until Aug-05. Hereafter, the crop withers and starts
to die while the backscatter displays the influence of the soil
background.
-VV80: after the appearance of the first pods on Jun-20, the radar
backscatter steadily increases until Jul-25. During withering and
dying of the crop, the backscatter displays the influence of the
underlying soil surface.

In comparing the measured radar backscatter to the predicted one (fig.
5.6), the Cloud model is unable to adequately describe the observed
backscatter from the moment the pods start to appear on Jun-20. It
seems that the appearance of the pods changes the canopy architecture
so that modification of the model is necessary. The pods are likely to
have a large effect on absorption and scatter characteristics of the
crop. This notice seems to be confirmed by the difference in observed
backscatter in the states of horizontal an vertical polarization, Fig.
5.5. At the onset of pod-formation, the backscatter at vertical
polarization clearly starts to exceed that at horizontal polarization.
This effect could be attributed to the vertical structure of the pods
which introduces a polarization dependent scatter component. Similar
effects are observed and discussed in literature for the vertical
heads of wheat plants, Ref. 11.
The effect of lodging on the radar backscatter is not unambiguously
determined. Some influence seems visible at VV40 and VV75, while no
effects are present at VV20 and VV80. It should be noted, however,
that the period of lodging occurs when the crop is fully set with
pods. This makes the discrimination between the effects due to the
different phenomena a difficult task.
The broad dip in radar backscatter around Jun-18/20 coincides with the
period of largest flowering. However the peak on Jun-16 might be
misleading for the interpretation of this dip since it could be the
result of rain that occurred on the day of measurement. It should also
be noted that this broad dip occurs not simulteneous at all angles of
incidence. So, at this stage, no specific conclusions can be drawn

with regard to the effect of flowering on the radar backscatter.

Finally, relations between the radar backscatter and remarkable field observations were searched for. As was the case with the previous crops, no consistent relationships can be established. Sporadically, the backscatter seemes to react on rain or on the presence of pools of water (respectively Jun-16 and Jul-01), but as many times an opposite reaction to the same phenomena was observed. Because of the poor results obtained for the previous crops, no effort was undertaken to relate the radar backscatter to wind and rainfall. Considering the smooth appearances of the backscatter curves, such relations are also not very likely.

As a concluding remark, it can be stated that the pattern of backscatter can be divided into three separate stages: a period of vegetative growth, a period of pod-formation, pod-growth and lodging, and thirdly a period of ripening of the crop. The first and the last period can be described by the Cloud model, while for the stage of pod-development (and lodging) the model needs to be further elaborated. This could be done by introducing a new set of crop parameters C and D for this stage separately.

VI SUMMARY AND CONCLUSIONS

VI.1 The radar backscatter curves

Beet display the highest radar backscatter while that from potatoes
and peas is mutually comparable. This could be related to the high
amount of plant water of beet, up to 6 kg/m2 compared with 3 kg/m2 and
2 kg/m2 for peas and potatoes. Other explanations could be the
relative large size of the beet leaves or the crop geometry in
general. The radar backscatter is highest at VV80 and lowest at VV20
for all three crops.
Beet also show the most distinct growth patterns in their backscatter
curves: increases up to a level of saturation around which
fluctuations occur. The backscatter from potatoes is similar in shape,
though much less pronounced. For both crops, the level of saturation
is reached at a later stage at steep incidence angles than at grazing
incidence angles. This observation suggests that a steep angle of
incidence is more suitable for crop growth monitoring than a grazing
angle of incidence. The backscatter curves from peas are characterized
by their relative smooth appearances. This could be due to the
relative small dimensions of the scatter elements (e.g. leaves,
flowers, pods) in the order of the size of the wavelength of X-band
microwaves. Furthermore, their shapes can be related to successive
phenological stages of the crop. After emergence, the radar
backscatter steadily increases until the stage of pod-formation is
reached. During this stage, the backscatter increases again and
remains relatively elevated until ripening. The shape and orientation
of the pods is suggested as a possible explanation for the extra
increase in radar backscatter. At the end of the growing season, the
backscatter rapidly declines until the level of the bare soil
backscatter is reached.
No consistent effect of lodging or flowering is demonstrated in the
radar backscatter curves. The radar does not seem to be able to detect
the flowering of potatoes, while the flowering of peas might induce a
decrease in the radar backscatter.

For beet and potatoes, a slight correlation was found between
direction and speed of wind and the radar backscatter. Little
variation in wind is reflected in relative smooth curves of the radar
backscatter, while large variations produce large fluctuations in the
backscatter curves. For potatoes, wind directed towards the radar
coincides with peaks in the backscatter at VV20 and VV40. Wind
directed away from the radar coincides with dips in the backscatter.
The opposite effect is observed for beet: peaks in the backscatter at
VV20 and VV40 coincide with wind directed away from the radar while
dips in the backscatter coincide with winds directed towards the
radar. This effect of direction of wind occurs when the speed of wind
exceeds 5 m/s.
There is no effect of wind on the radar backscatter from peas.

For none of the crops is any direct relationship established with
rainfall on the day of measurement. Furthermore, only a few visual
observations on the geometry of the crop were matched with
fluctuations in the radar backscatter. Most of these fluctuations,
however, could not be explained by any field observation or
meteorological data. These fluctuations also appeared to be crop
specific: the peaks and dips in radar backscatter from the three crops

did not coincide on the same days. This suggests that the fluctuations
in radar backscatter are due to specific changes in the crop, notably
in the crop geometry. Similar observations are made by Wu et al. (Ref.
16) who found that displacements of leaves and heads of corn and milo
plants by the wind caused large fluctuations in the radar backscatter.
In our study under uncontrolled field conditions, the number of
variables that influence crop geometry was too large to isolate
specific effects on the radar backscatter. The influence of crop
geometry on radar backscatter is too complicated to be derived in the
presented manner. Only visual observations on crop geometry are
insufficient to discriminate relationships with the radar backscatter.
For a better understanding of these relations, other experiments under
controlled 'ceteris paribus' conditions should be conducted. In these
experiments, fieldcrops can artificially be given various kinds of
geometry (like erect, lodged, bent towards different directions, etc)
while keeping the total biomass intact. From such experiments, the
indirect effect of soil moisture on the radar backscatter, through its
effect on the crop canopy, could also be identified (e.g.
drip-irrigation, under-ground irrigation).

The backscatter curves in the states of like polarization VV and HH
are of equal magnitude and similar in shape for beet and potatoes.
Furthermore, a high correlation is present for the occurrence of the
peaks and dips. Since the measurements in the different states of
polarization were not carried out simultaneously, this indicates that
the fluctuations in the backscatter curves are not due to statistical
dispersion in the determination of the field average. Hence, the
inaccuracy of the measurements appears in practice to be smaller than
was expected from theoretical considerations.


## VI.2 The Cloud model

The best results for curve fitting using the Cloud model were obtained
for beet. The coefficients of correlation between observed and
calculated radar backscatter were about 0.85 at the various angles of
incidence for the two years. Despite the large similarity in crop
development in the two years, values for C and D were found to deviate
by a factor of 1.5. These differences could not be explained.
The results for potatoes were less encouraging. The coefficients of
correlation varied in 1979 from 0.60 to 0.80, and in 1980 from 0.40 to
0.50. Especially in the latter year, the similarity between measured
and calculated radar backscatter was very poor. A division of the
growing season into a stage of exponential growth and a stage of
saturation of the backscatter did not improve the results.
The radar backscatter from peas could only be partially described by
the Cloud model. In 1979, the model was applied to the radar
backscatter for a limited period of 45 days. This yielded coefficients
of correlation between 0.70 and 0.95. In 1980, the whole growing
season was taken into account and the coefficients of correlation
decreased to values between 0.70 and 0.85. Only the period of
vegetative growth before pod-formation and the period of ripening
could adequately be described by the Cloud model.

Prediction of the radar backscatter for 1980, using the crop
parameters determined for 1979 (and the soil parameter G determined
for 1980) yielded the following results:

Beet: a fairly good result was reached, although the backscatter remained underestimated for the largest part of the growing season; r = 0.85-0.90.

Potatoes: the predicted backscatter was in better agreement with the observed backscatter than the fitted values itself; r = 0.55-0.77. Even better results were obtained when the soil parameter K was not taken to be 0.051 but determined for each angle of incidence separately: r = 0.70-0.90.

Peas: despite the large differences in crop development in the two years, good agreement was obtained for the period of growth before pod-formation and the period of ripening; r = 0.95. Only at the steep angle of incidence, the prediction of the Cloud model was very poor, r = 0.17.

These figures are similar to figures reported by Ulaby et al. (Ref.13). In an experiment on sorghum, wheat and corn, coefficients of correlation between predicted and measured radar backscatter varied between 0.6 and 0.8 only. These differences are due to the choice of crops in the two studies. In our study, the crops were carefully selected for applicability of the Cloud model. The radar backscatter from the crops used in the study of Ulaby could be better described by an extended multi-layer Cloud model.

The above results suggest the following attenuation coefficients D for the three crops:
Beet:      D = 0.46-0.76
Potatoes:  D = 0.25
Peas:      D = 0.40

These values are still the subject of discussion. De Loor (Ref.9) carried out extensive research to determine the general crop parameters from several years of measurements. He found a comparable value for beet, 0.58, but a much higher value for potatoes, 1.39. These values mean that the attenuation of microwaves in a potato canopy is larger than in a beet canopy. However, based on the values presented here, the attenuation of microwaves in a canopy of potatoes is less than that in a canopy of peas or beet. This is in agreement with the fact that some peaks and dips in the radar backscatter curves coincide with similar features in the graphs of the soil moisture content. However some relative large coefficients of correlation between radar backscatter and the soil moisture content were also observed for beet in 1980. This is in contradiction with the large coefficient of attenuation determined for this crop. In 1979, the coefficients of correlation for beet indicated no relationship with soil moisture contant at all. These paradoxical observations suggest that the direct or indirect influence of soil moisture on the radar backscatter needs further research.

VI.3 Radar for monitoring crop growth

If X-band radar were to be utilised for grop growth monitoring, the Cloud model could be used as a base for further development if the proper soil parameters K and G are known. Inversion of the model can lead to an estimation of the microwave soil cover which might be translated into an optical soil cover. Almost linear relationships between these two covers were observed for beet and potatoes for 1979 and 1980 taken together. The optical soil cover can serve as an input into models to estimate the rate of crop growth. Also, attempts could

be made to directly derive crop parameters like LAI or biomass from the radar backscatter data, Ref.12.

The curves of the radar backscatter from beet and peas show a relative large contrast between the backscatter from the full grown crop canopy and from the underlying soil surface. Therefore, possibilities for the monitoring of the growth of these crops seem realistic. The contrast between the backscatter from a potato canopy and the underlying soil surface is relative small. This implies little prospect for the monitoring of crop growth on the basis of X-band radar only. If radar remote sensing were to be utilised for the monitoring of crop growth and development, the Cloud model can serve as a basis for further elaboration. The use of X-band radar could, however, be seriously hampered by the fluctuations that occur in the curves of the radar backscatter. These fluctuations might be small from a technical point of view, in the order of 0.5 to 1.0 dB, they become large when the backscatter is used to derive crop parameters. This makes more insight into the effects of changes in crop geometry on the radar backscatter desirable. The curve of the backscatter from peas demonstrates that the fluctuations could be related to the size of the scatter elements in relation to the wavelength of incident radiation. This implies that microwaves of larger wavelengths could be less sensitive to changes in crop geometry of beet and potatoes.

## VII ACKNOWLEDGEMENTS

REFERENCES

1: Attema, E.P.W., F.T. Ulaby, 1978. Vegetation modeled as a water cloud, Radio Science 13, no. 2, (March/April) 357-364.

2: Hoekman, D.H., 1981. Modelvorming radarbackscatter voor gewassen (Dutch), Delft University of Technology, Department of Electrical Engineering, the Netherlands, Master's Thesis, Report 05-1-533-AV-90'81, August.

3: Hoekman, D.H., L. Krul, E.P.W. Attema, 1982. A multilayer model for radarbackscattering from vegetation canopies, Digest of the 2nd IEEE International Geoscience and Remote Sensing Symposium, Munich, West Germany, 1-4 June.

4: Kasteren, H.W.J. van, M.K. Smit, 1977. Measurements on the backscatter of X-band radiation of seven crops, throughout the growing season. Comparison of the return parameter Gamma with some properties of the crops and with the density on a SLAR-image, ROVE-report 1975, NIWARS publication 47.

5: Kasteren, H.W.J. van, 1981. Radar signature of crops. The effect of weather conditions and the possibilities of crop discrimination with radar. Signatures spectrales d'objets en teledetection, Avignon, 8-11 Sept. 1981.

6: Krul, L., 1984. Microwave remote sensing and vegetation; problems, progress and solutions, a review. Proceedings EARSeL Workshop 'Microwave remote sensing applied to vegetation', Amsterdam, 10-12 December, 1984.1

7: Loor, P. de., P. Hoogeboom, E.P.W. Attema, 1982. The Dutch ROVE Program, IEEE Transactions on Geoscience and Remote Sensing, GE-20, 1.

8: Loor, G.P. de, 1984. Variation of the radar backscatter of vegetation through the growing season. Proceedings EARSeL Workshop 'Microwave remote sensing applied to vegetation', Amsterdam, 10-12 December 1984.

9: Loor, G.P. de, 1985. Moisture determination in and under vegetation canopies. Physics and Electronics Laboratory TNO, the Hague, the Netherlands, report FEL 1985-52.

10: Ulaby, F.T., T.T. Bush, P.B. Betlivala, J. Cihlar, 1974. The effects of soil moisture and plant morphology on radar backscatter from vegetation. The University of Kansas, Remote Sensing Laboratory, RSL Technical Report 177-51.

11: Ulaby, F.T., R.K. Moore, A.K. Fung, 1982. Microwave remote sensing, active and passive. Volume II: Radar remote sensing and surface scattering and emission theory, Addison-Wesley publishing company.

12: Ulaby, F. T., C.T. Allen, 1984. Modelling the polarization dependence of the attenuation in vegetation canopies, Proceedings of IGARSS'84 Symposium, Strasbourg 27-30 August 1984.

13: Ulaby, F.T., C.T. Allen, G. Eger III, 1984. Relating the microwave backscattering coefficient to leaf area index. Remote Sensing of Environment 14;113-133.

14: Ulaby, F.T., R.P Jedlicka, 1984. Microwave dielectric properties of plant materials, IEEE Transactions on Geoscience and Remote Sensing, GE-22. 4, July.

15: Ulaby, F.T., E.A. Wilson, 1985. Microwave attenuation properties of vegetation canopies. IEEE Transactions on Geoscience and Remote Sensing, GE-23, 5, September.

16: Wu, L.K., R.K. Moore, R. Zoughi, A. Afifi, F.T. Ulaby, 1985. Preliminary results on the determination of the sources of scattering from vegetation canopies at 10 GHz, International Journal of Remote Sensing, 6, 299-313.
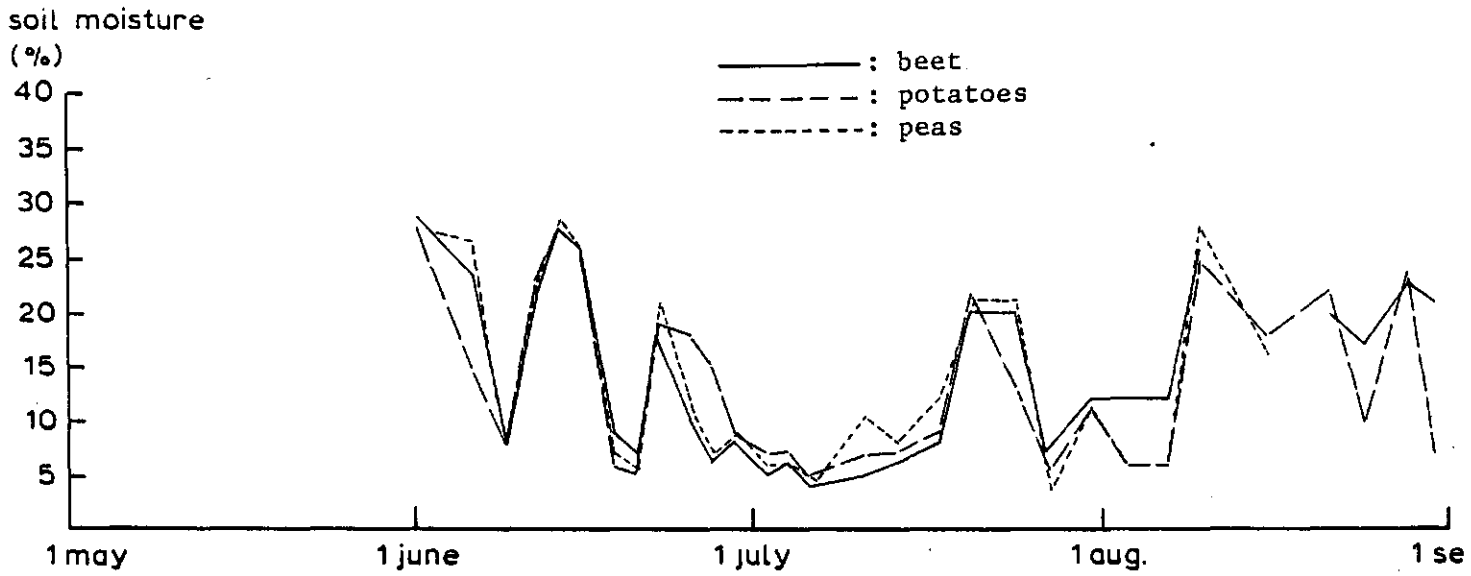
Figure 1: soil moisture by weight of the upper 5 cm topsoil with beet , potatoes
and peas as soil cover.    1979
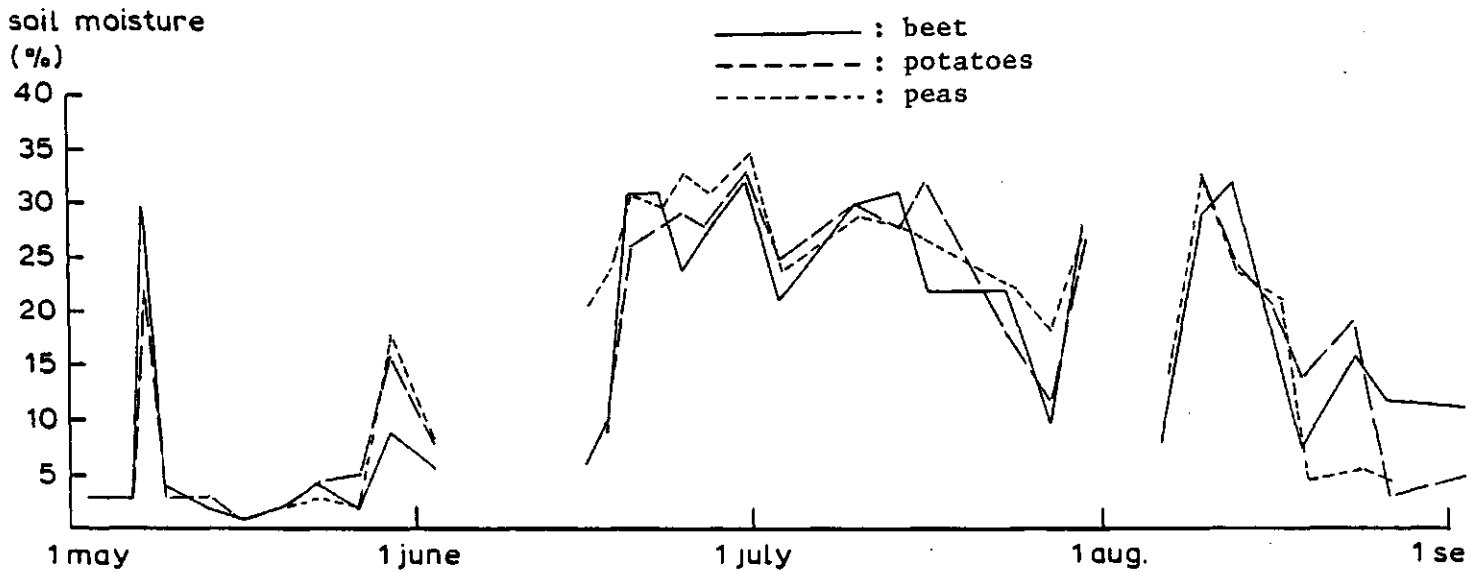


Figure 2: soil moisture by weight of the upper 5 cm topsoil with beet , potatoes
and peas as soil cover        1980
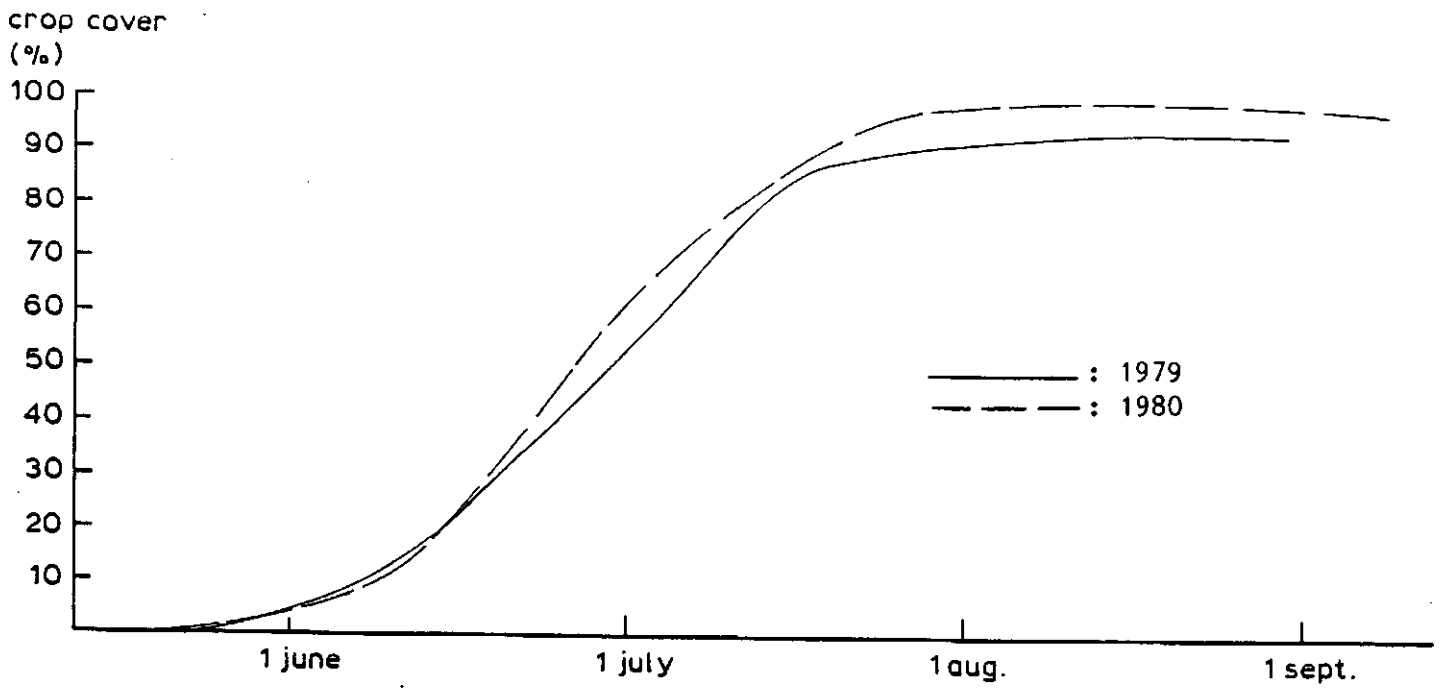
Figure 3.1: Sugarbeet ; crop cover during the growing season
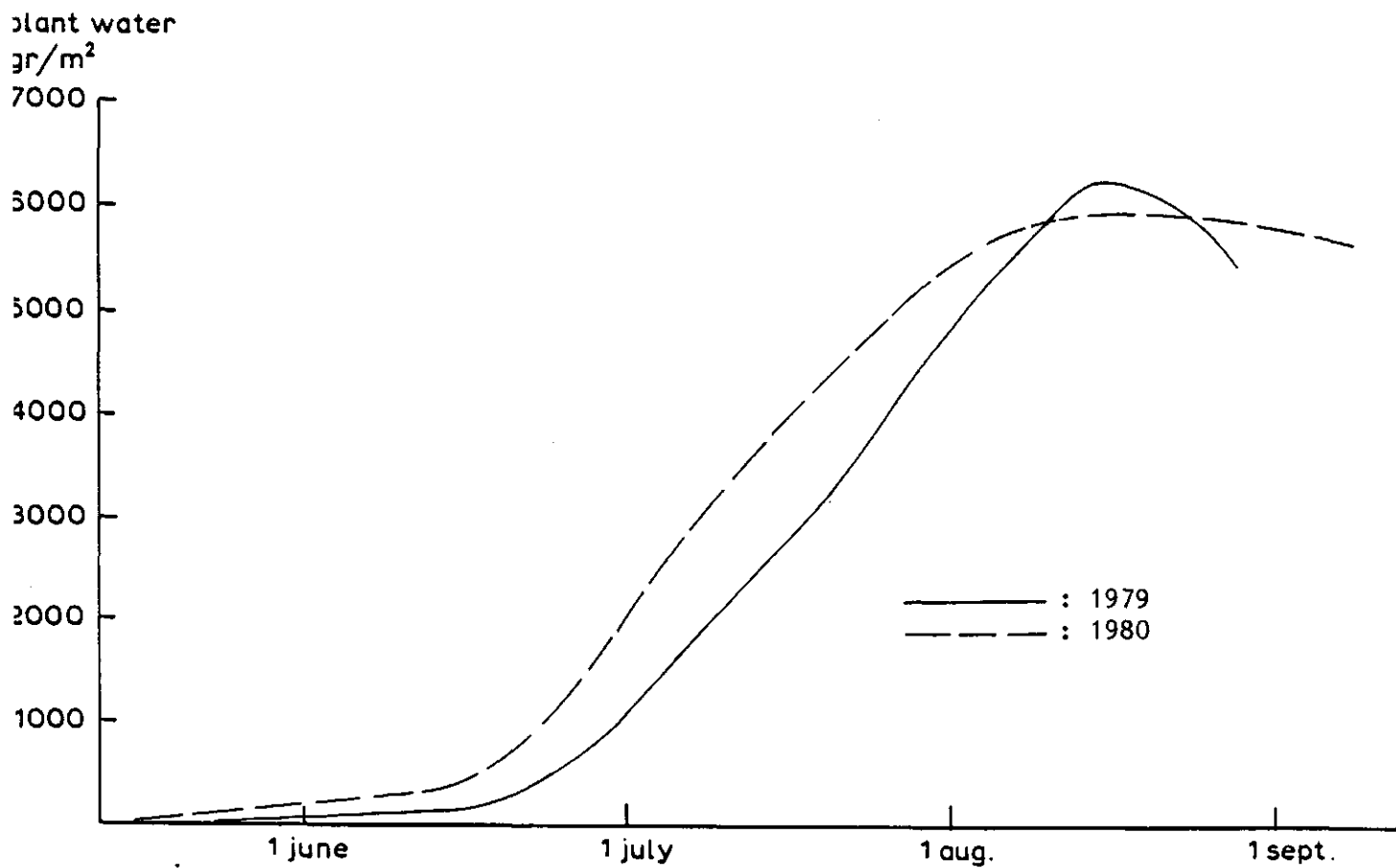


Figure 3.2: Sugarbeet ; amount of above-ground plantwater during the growing
season
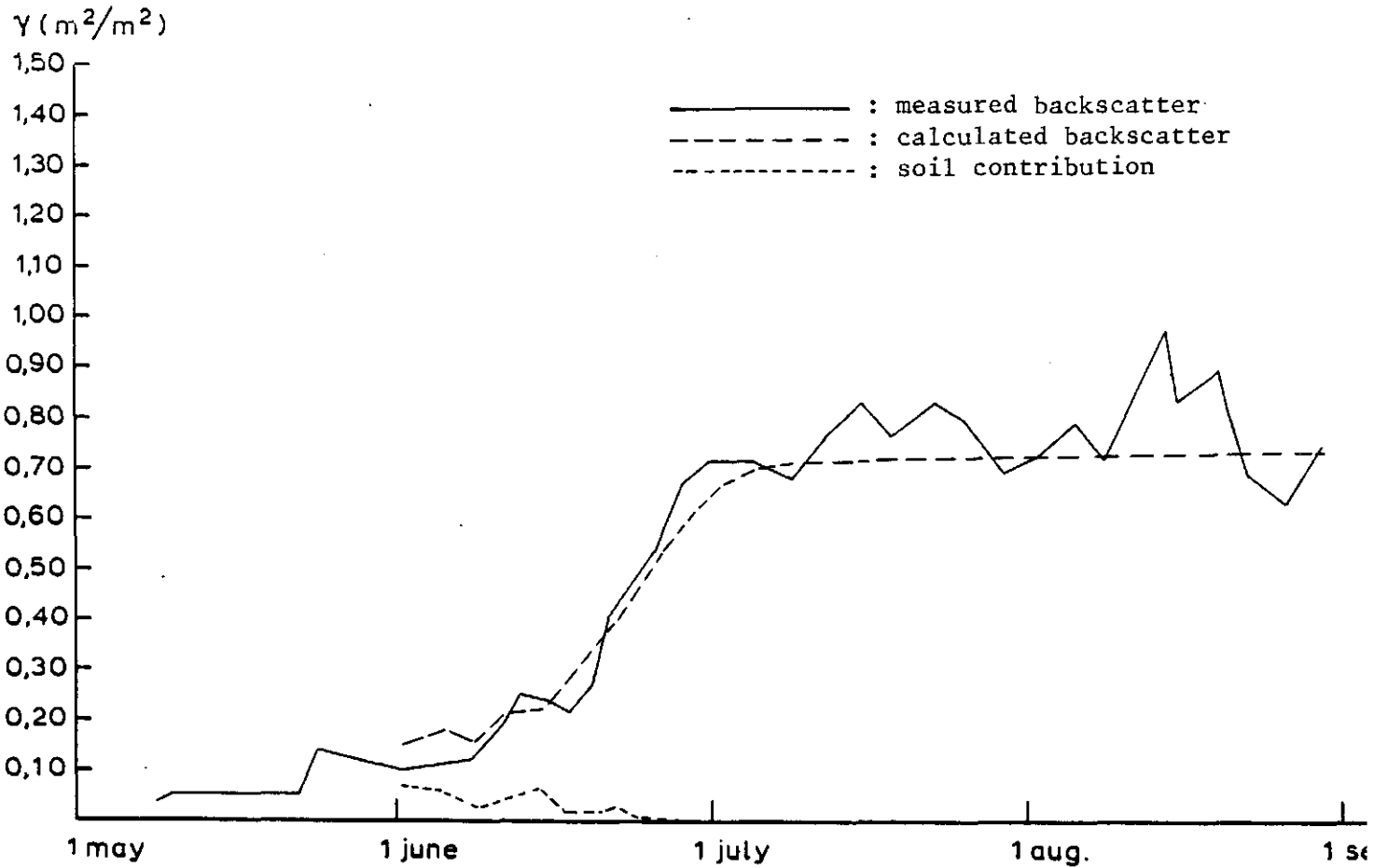
Figure 3.3a: Sugarbeet ; observed and calculated radar backscatter VV20, 1979
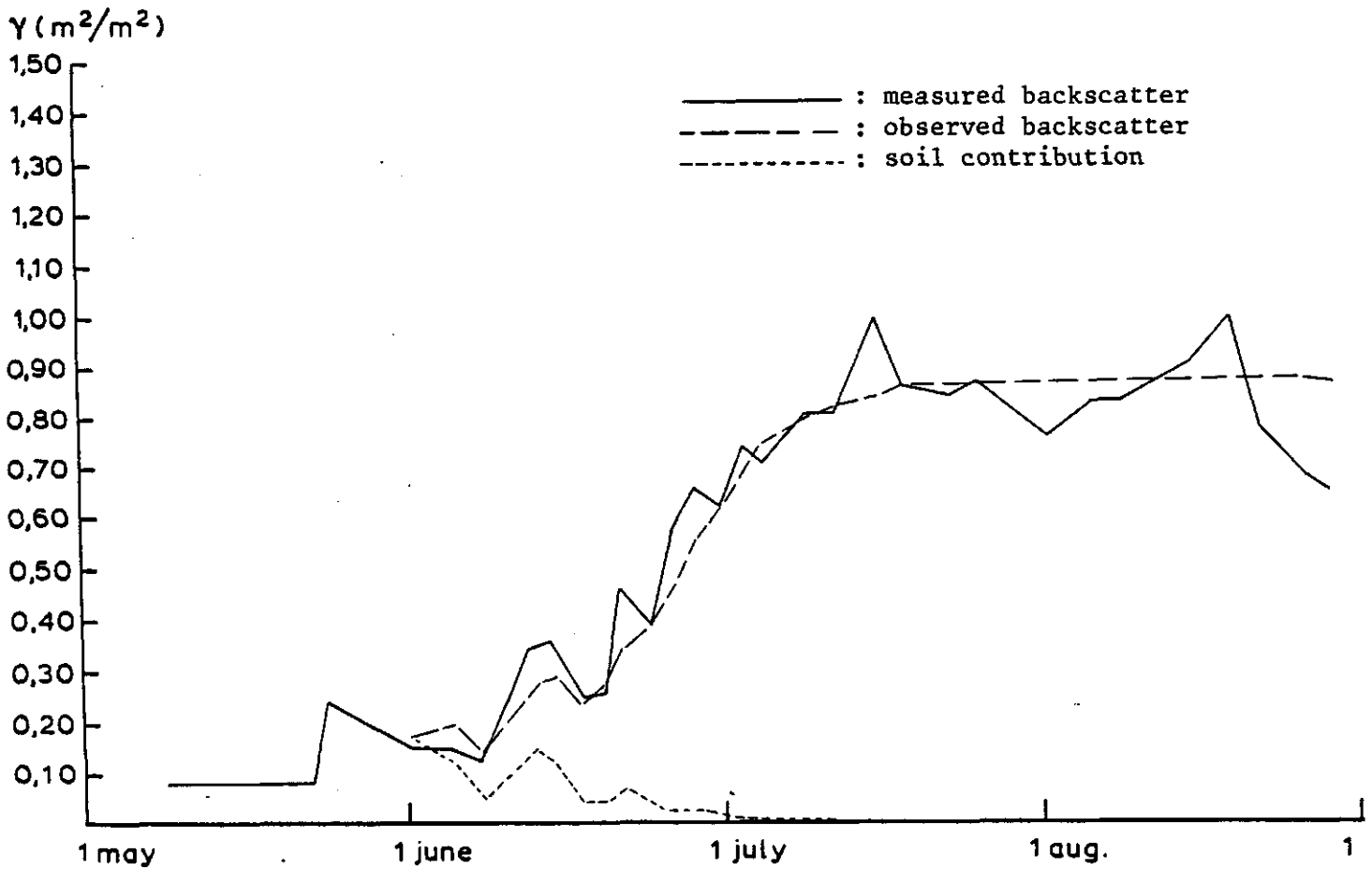


Figure 3.3b: Sugarbeet ; observed and calculated radar backscatter VV40, 1979
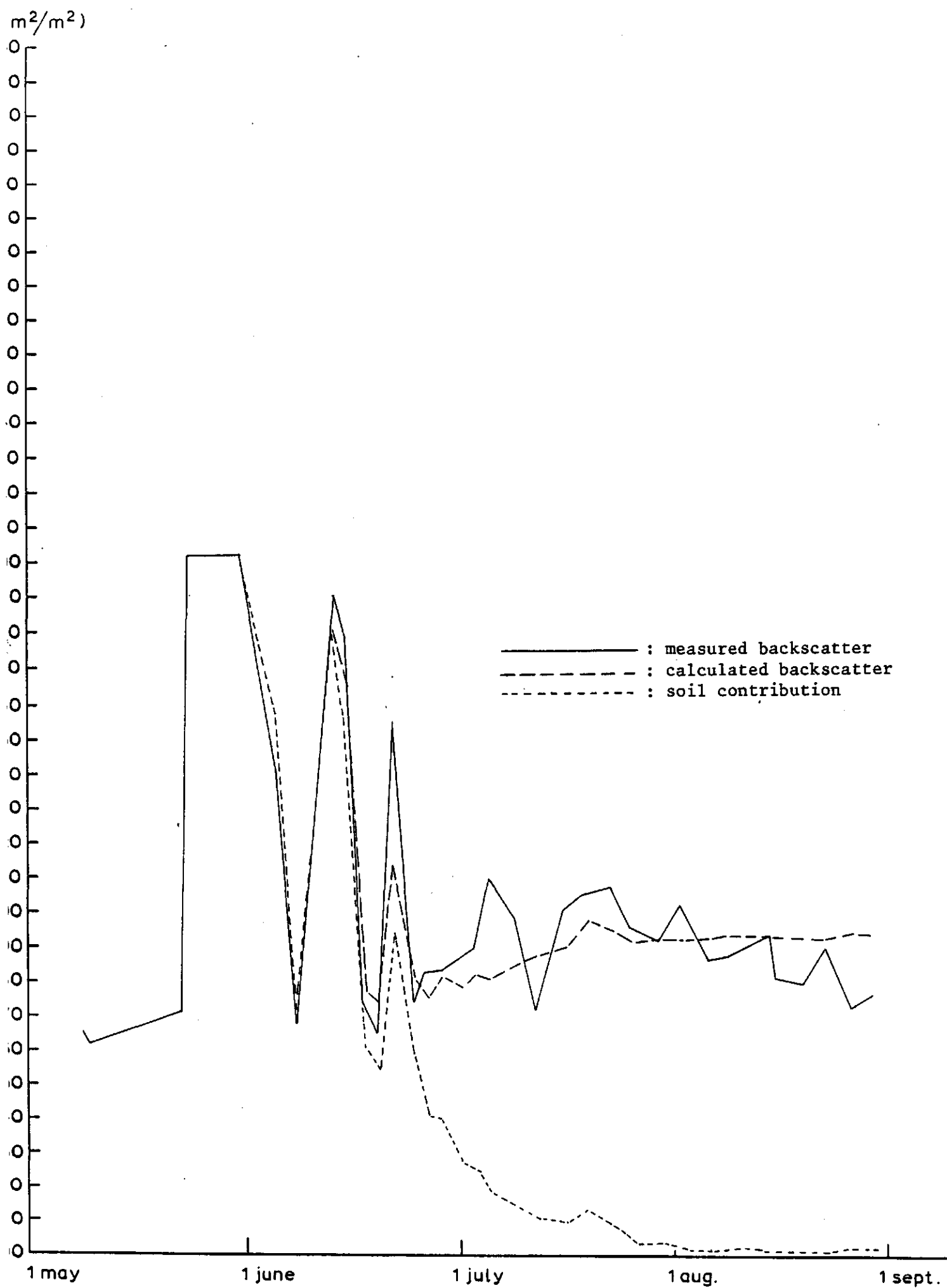
Figure 3.3c: Sugarbeet ; observed and calculated radar backscatter VV80, 1979
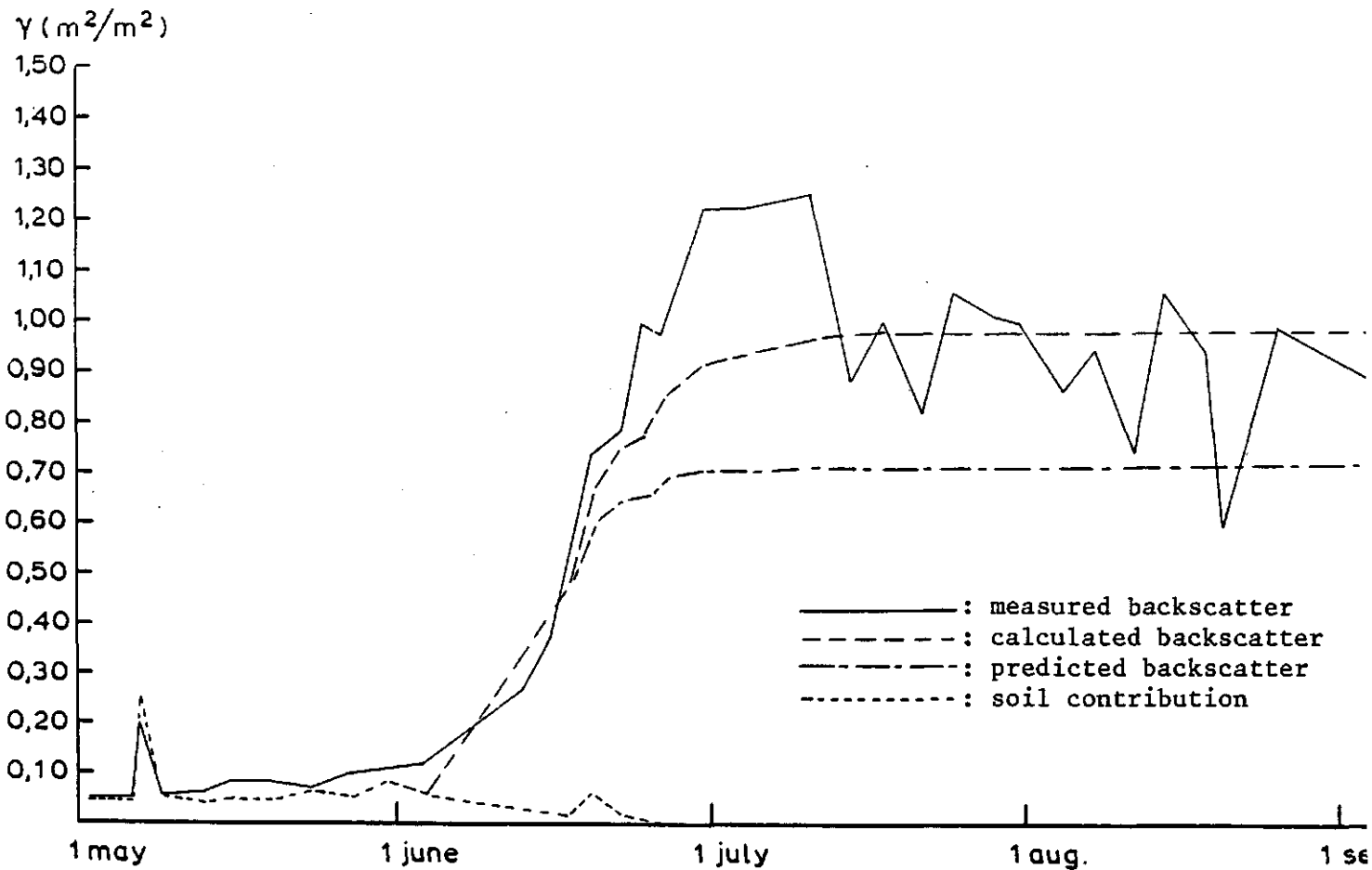
Figure 3.4a:  Sugarbeet ; observed, calculated and predicted radar backscatter
VV20, 1980
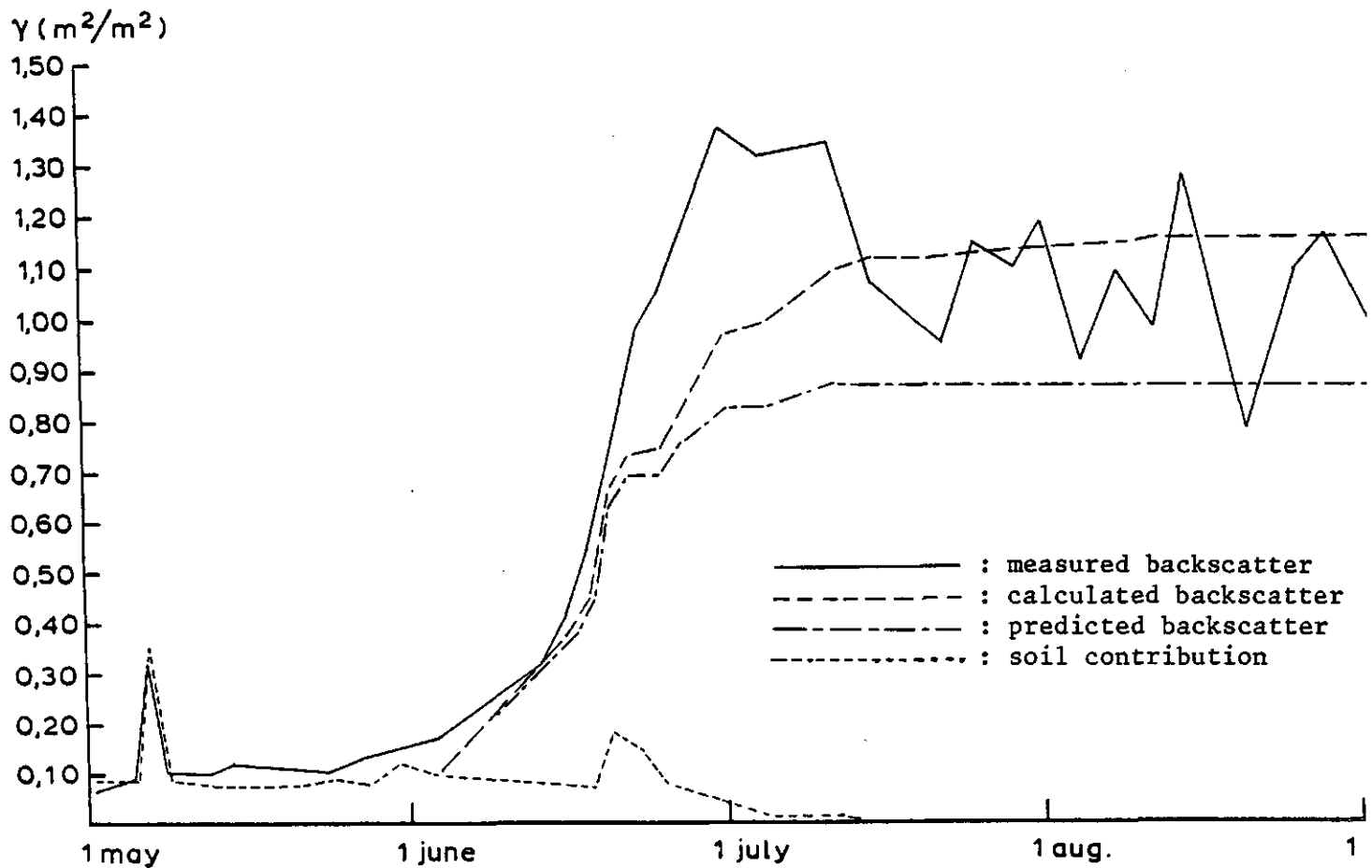


Figure 3.4b: Sugarbeet ; observed, calculated and predicted radar backscatter
VV40, 1980
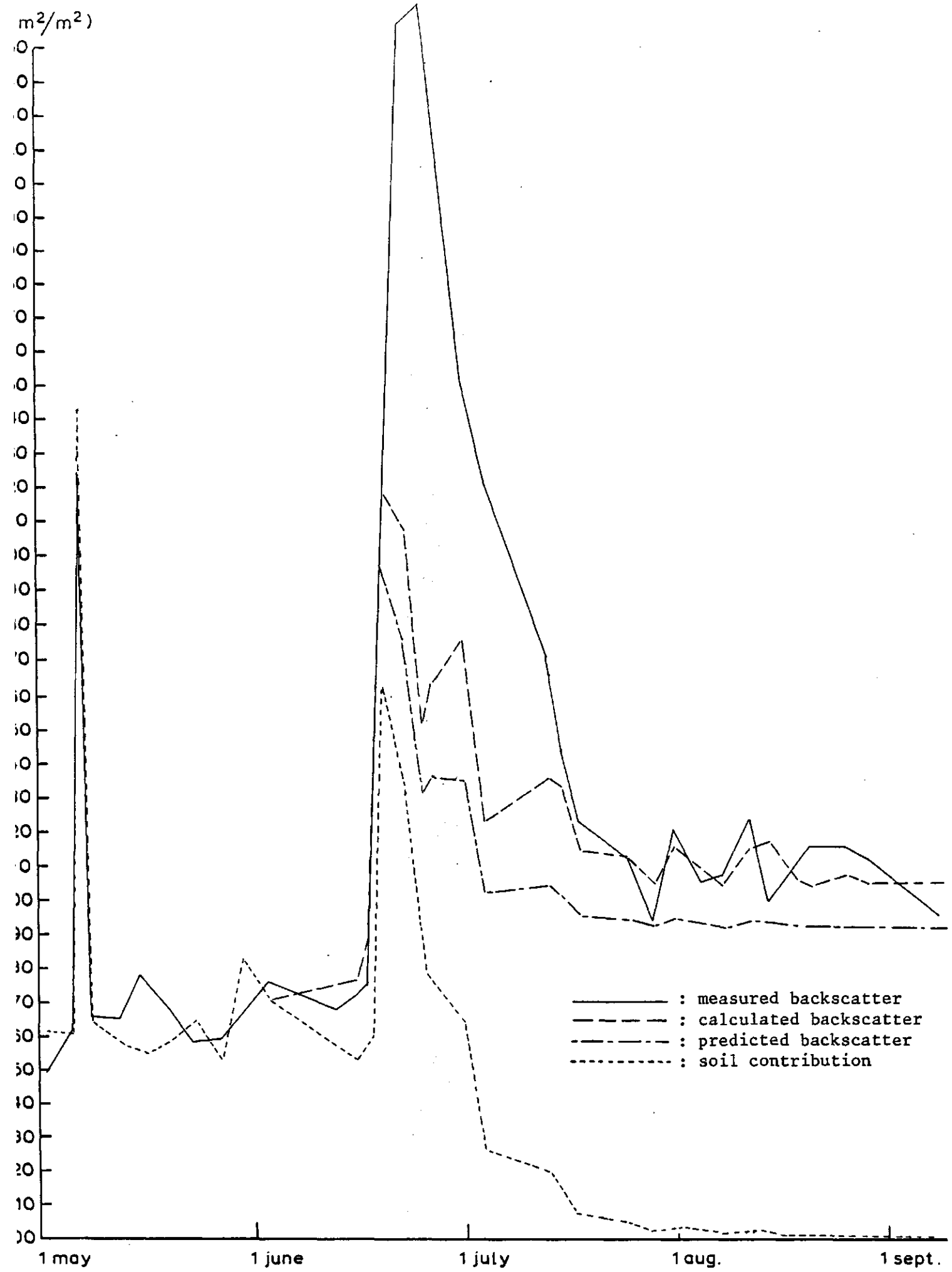
Figure 3.4c: Sugarbeet ; observed, calculated and predicted radar backscatter
VV80, 1980
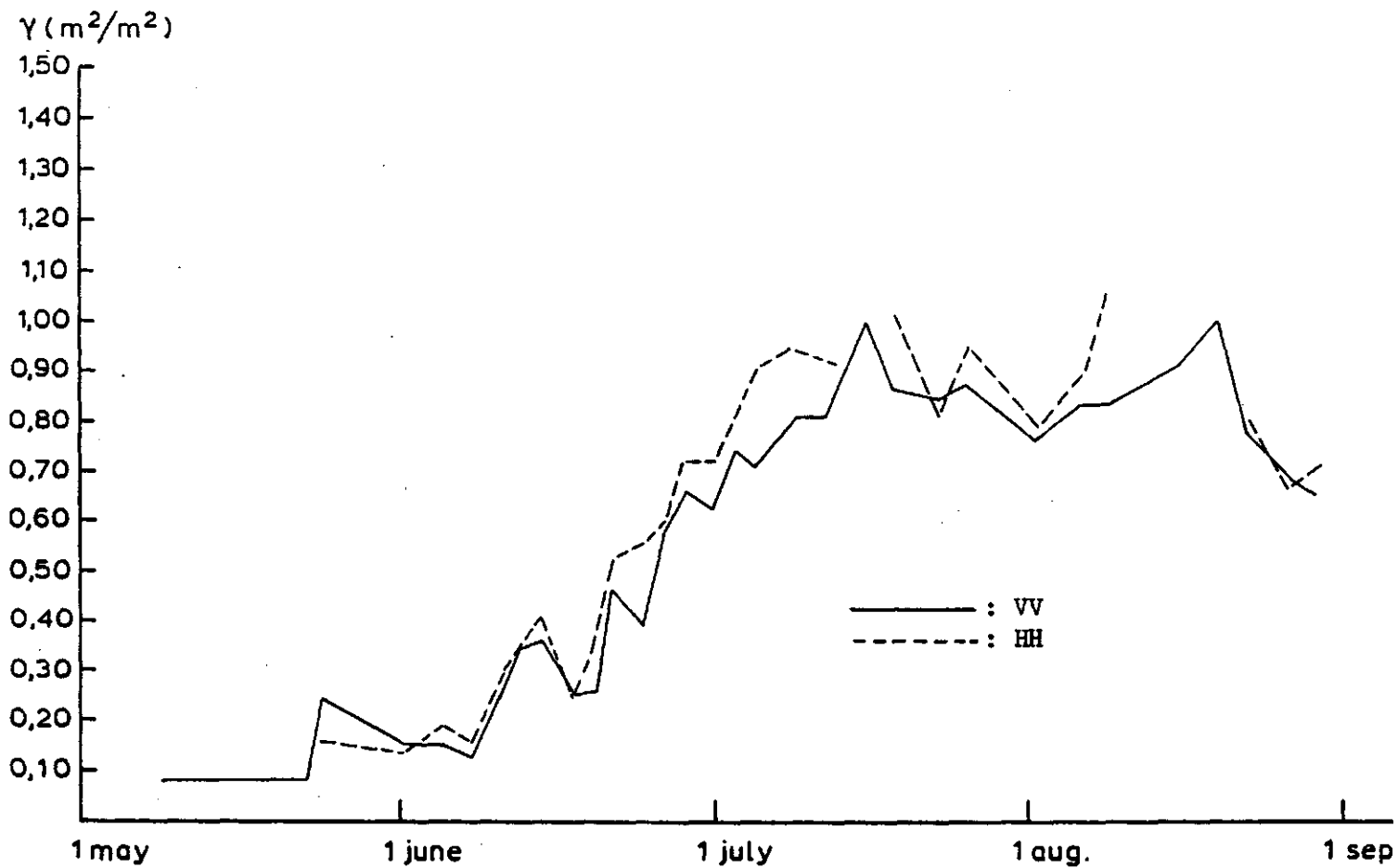
Figure 3.5a: Sugarbeet ; radar backscatter in VV and in HH polarisation 40° grazing angle, 1979
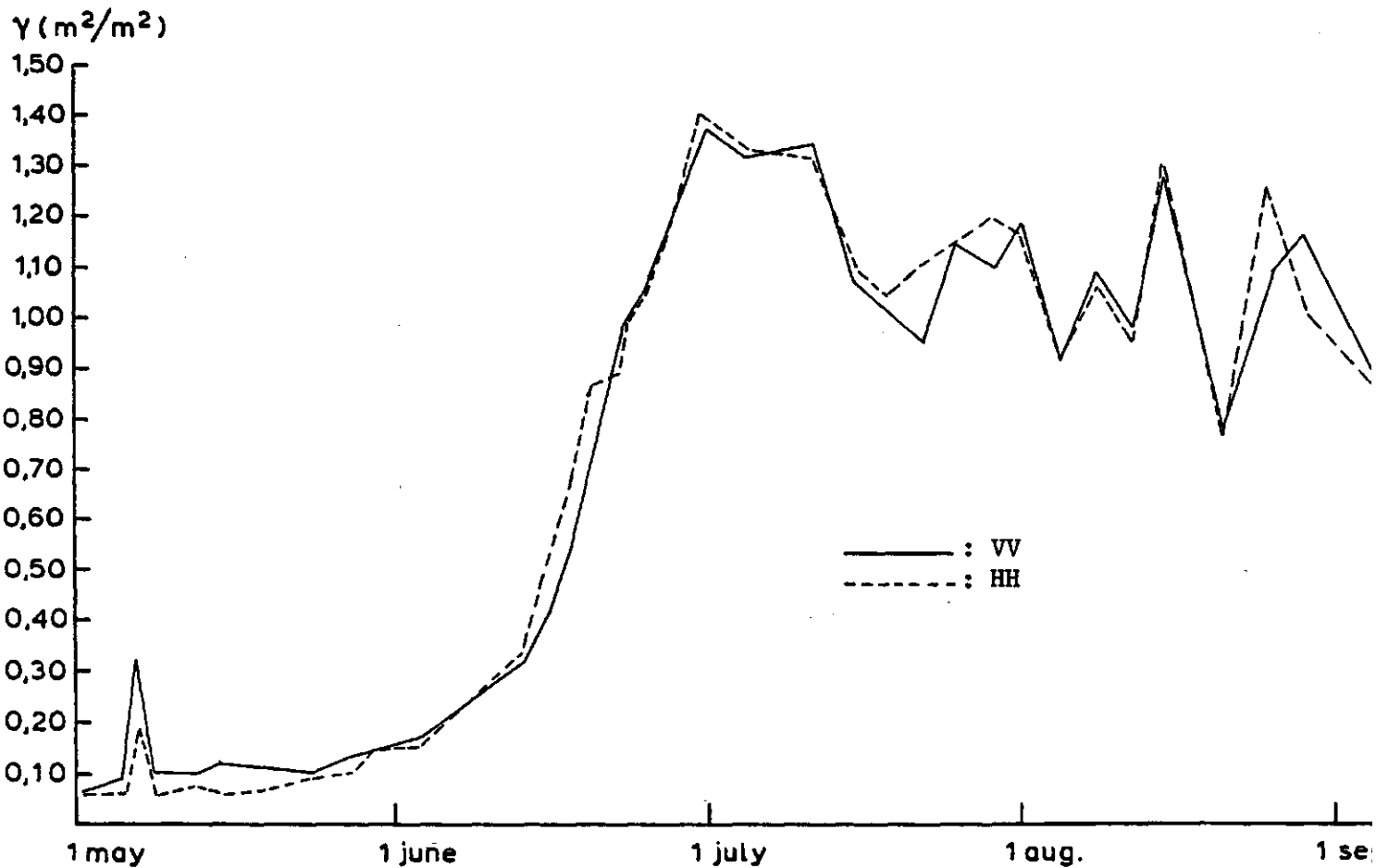


Figure 3.5b: Sugarbeet ; radar backscatter in VV and in HH polarisation 40° grazing angle, 1980
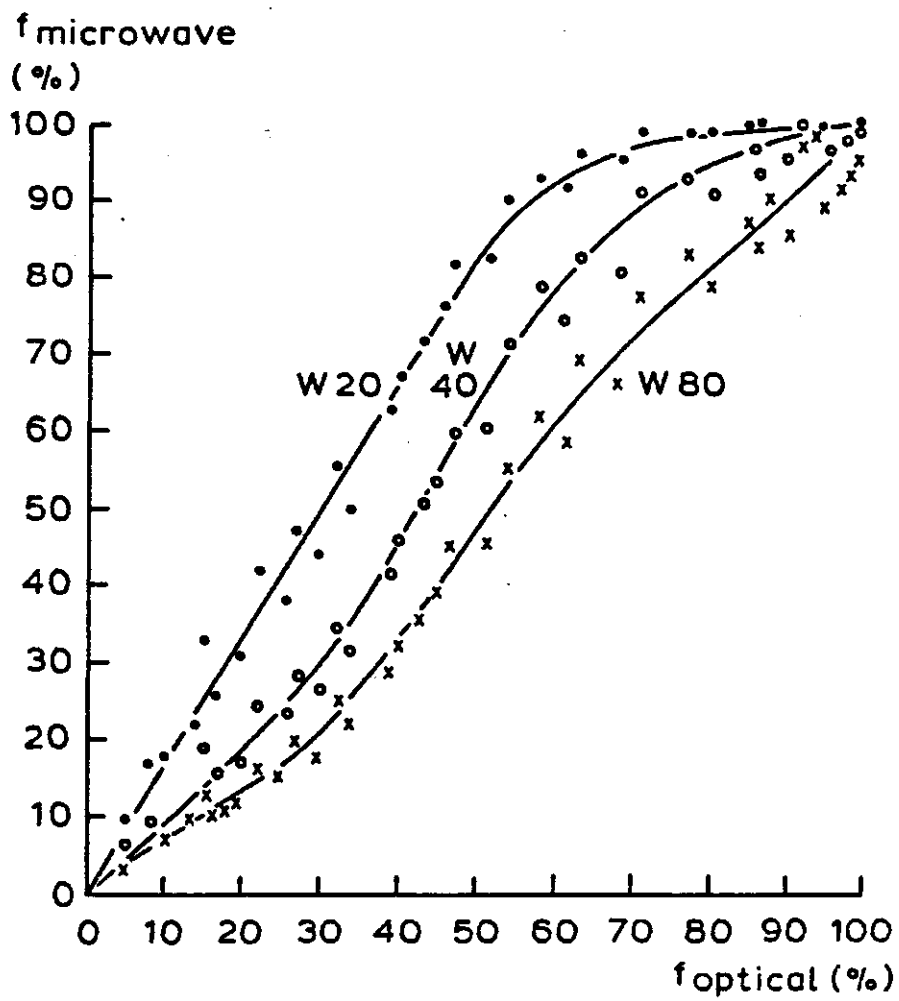
Figure 3.6: Sugarbeet ; optical crop cover versus microwave crop cover
1979 and 1980 combined
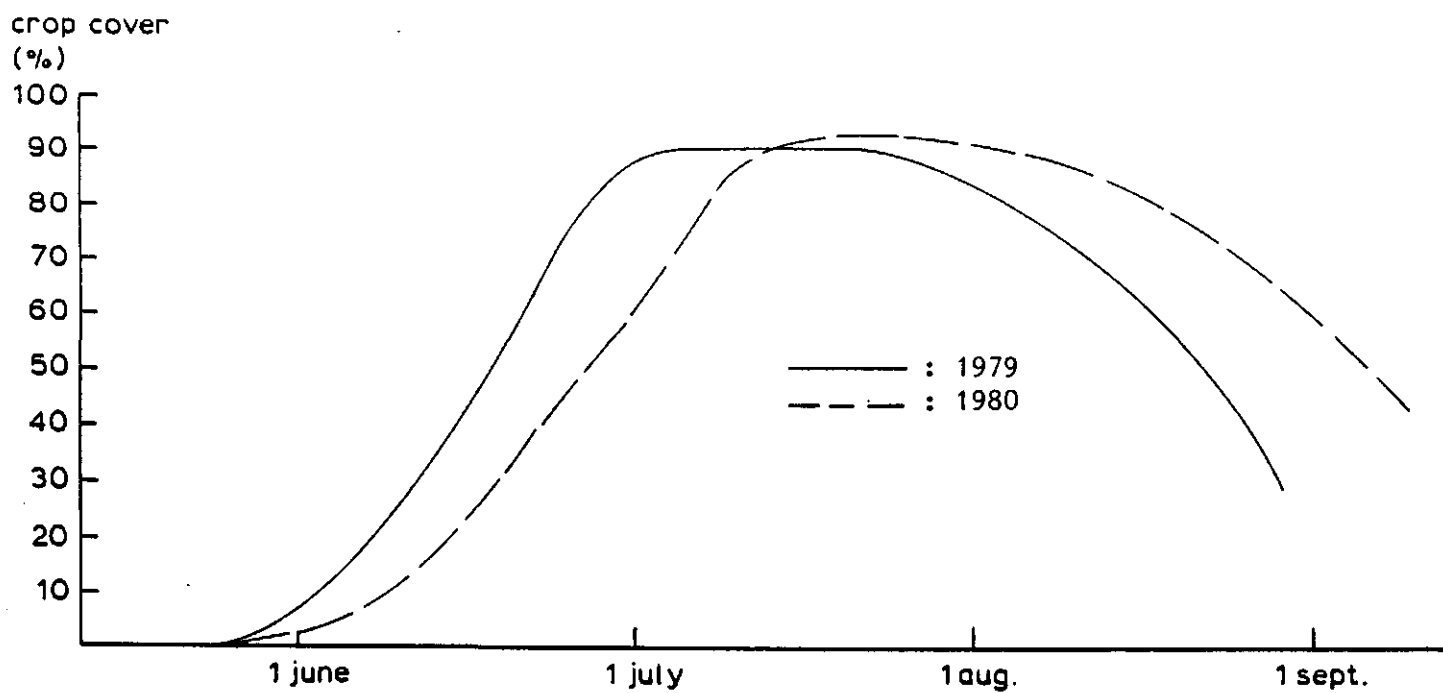
Figure 4.1: Potatoes; crop cover    during the growing season
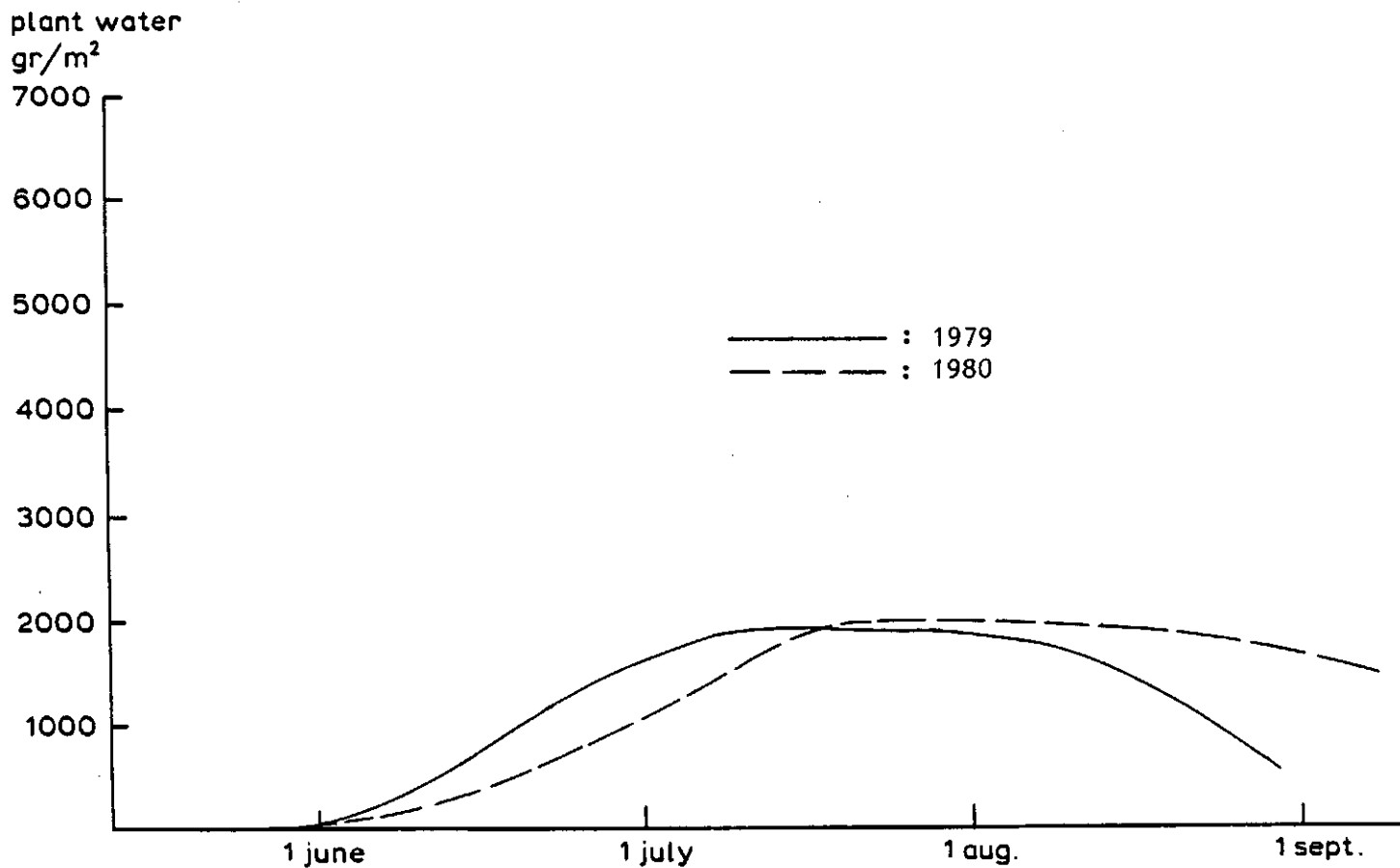


Figure 4.2: Potatoes; amount of above-ground plantwater during the growing season
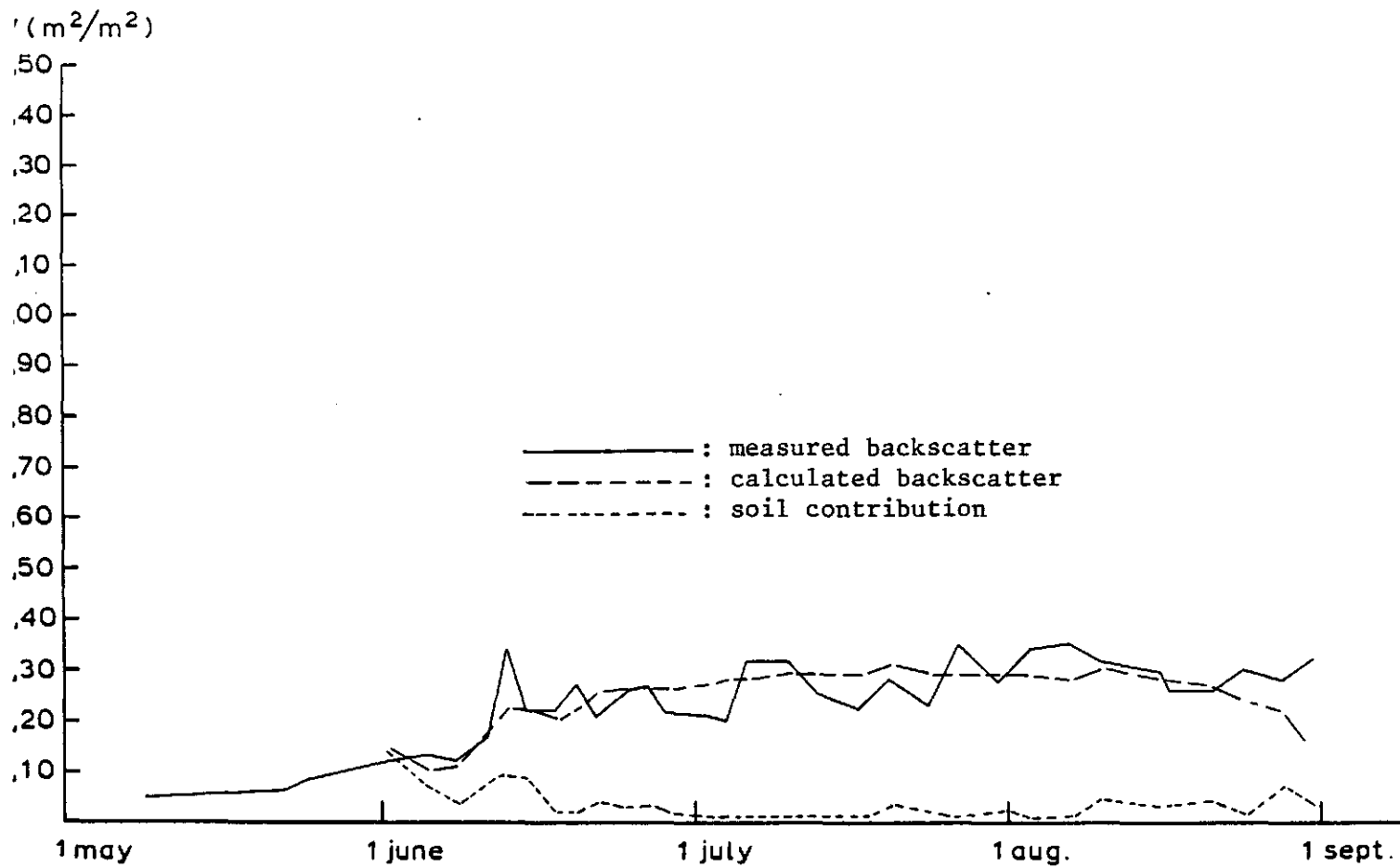
Figure 4.3a: Potatoes; observed and calculated radar backscatter VV20, 1979
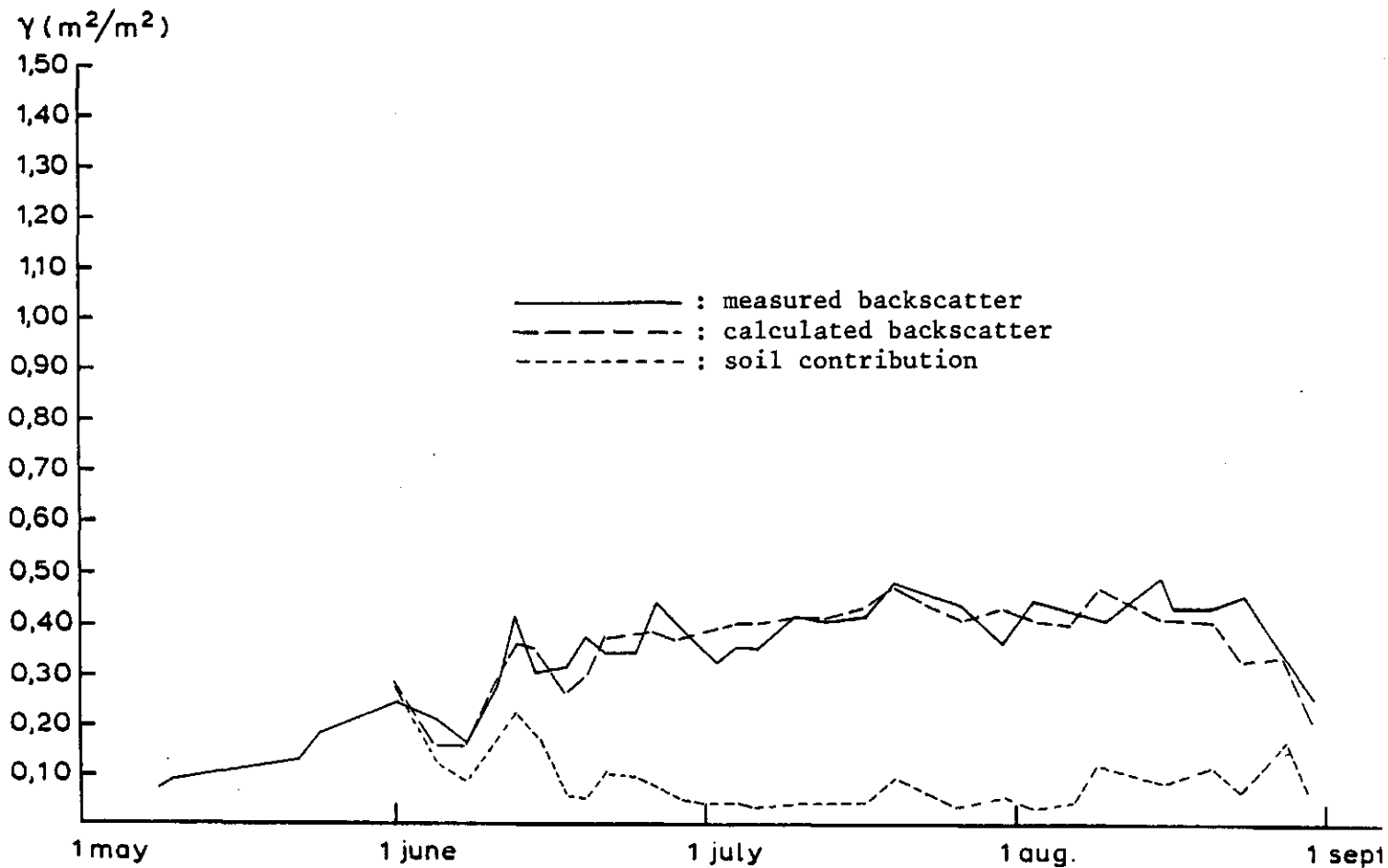


Figure 4.3b: Potatoes; observed and calculated radar backscatter VV40, 1979
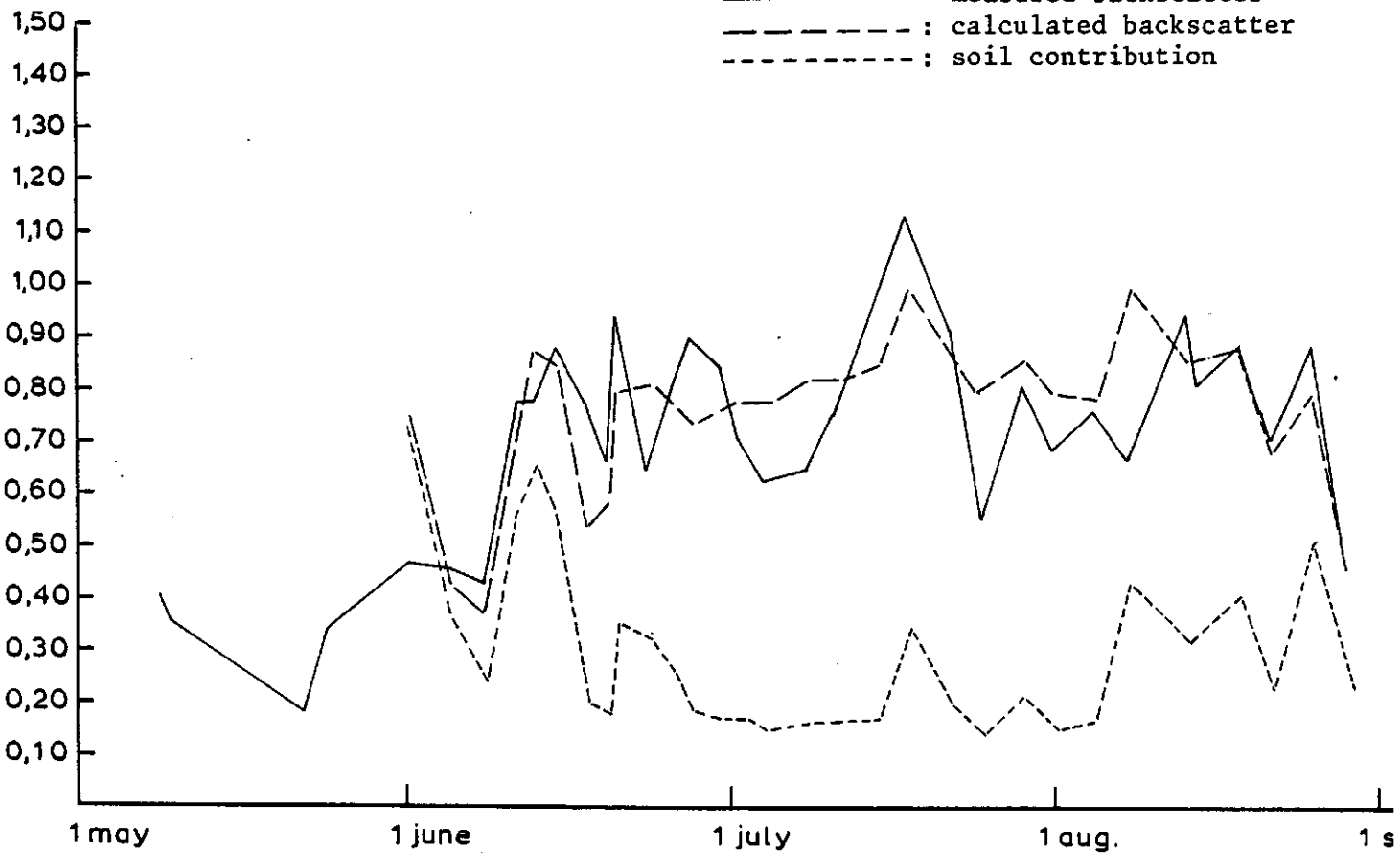
Figure 4.3c: Potatoes; observed and calculated radar backscatter VV80, 1979
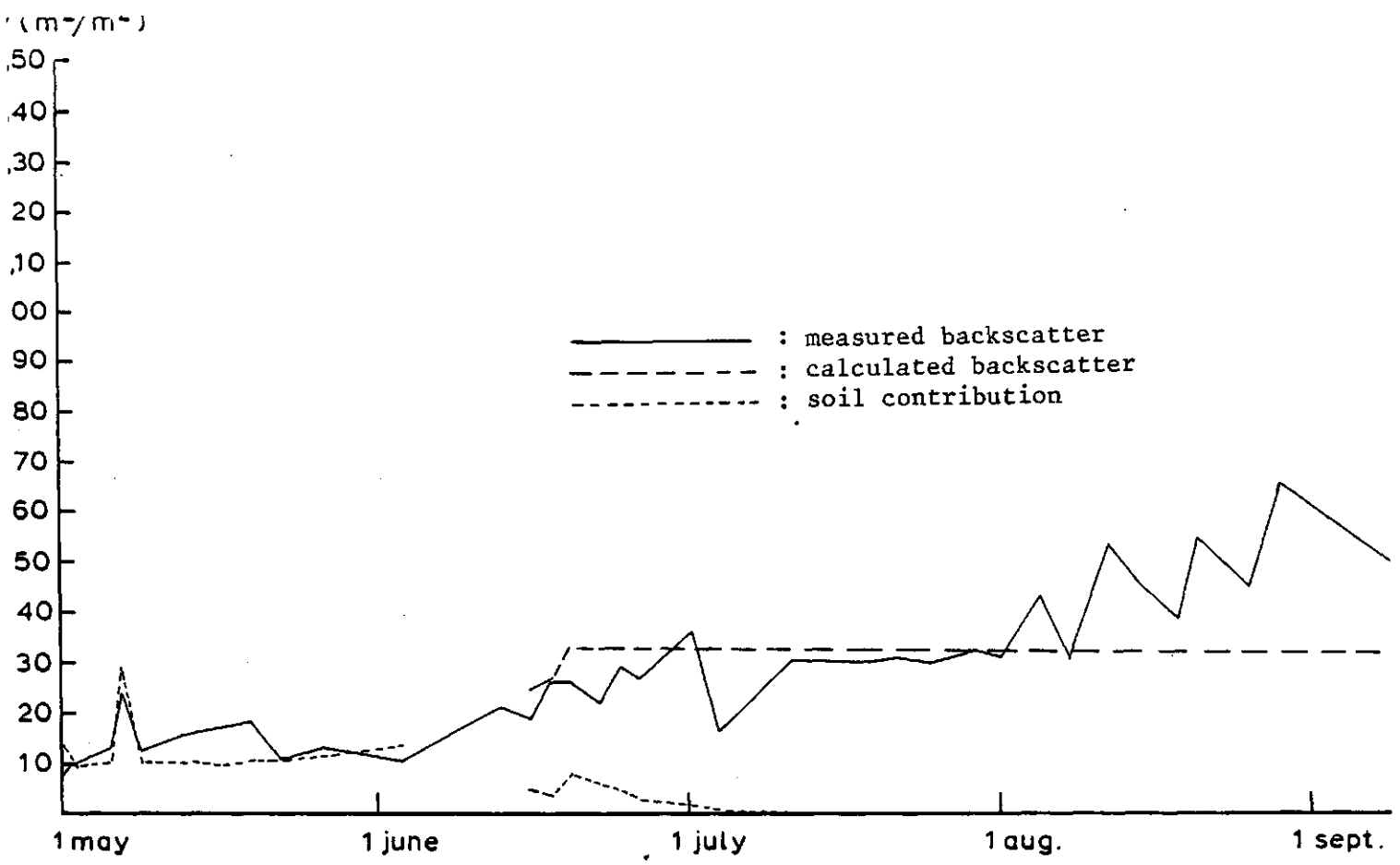
Figure 4.4a: Potatoes; observed and calculated radar backscatter VV20, 1980
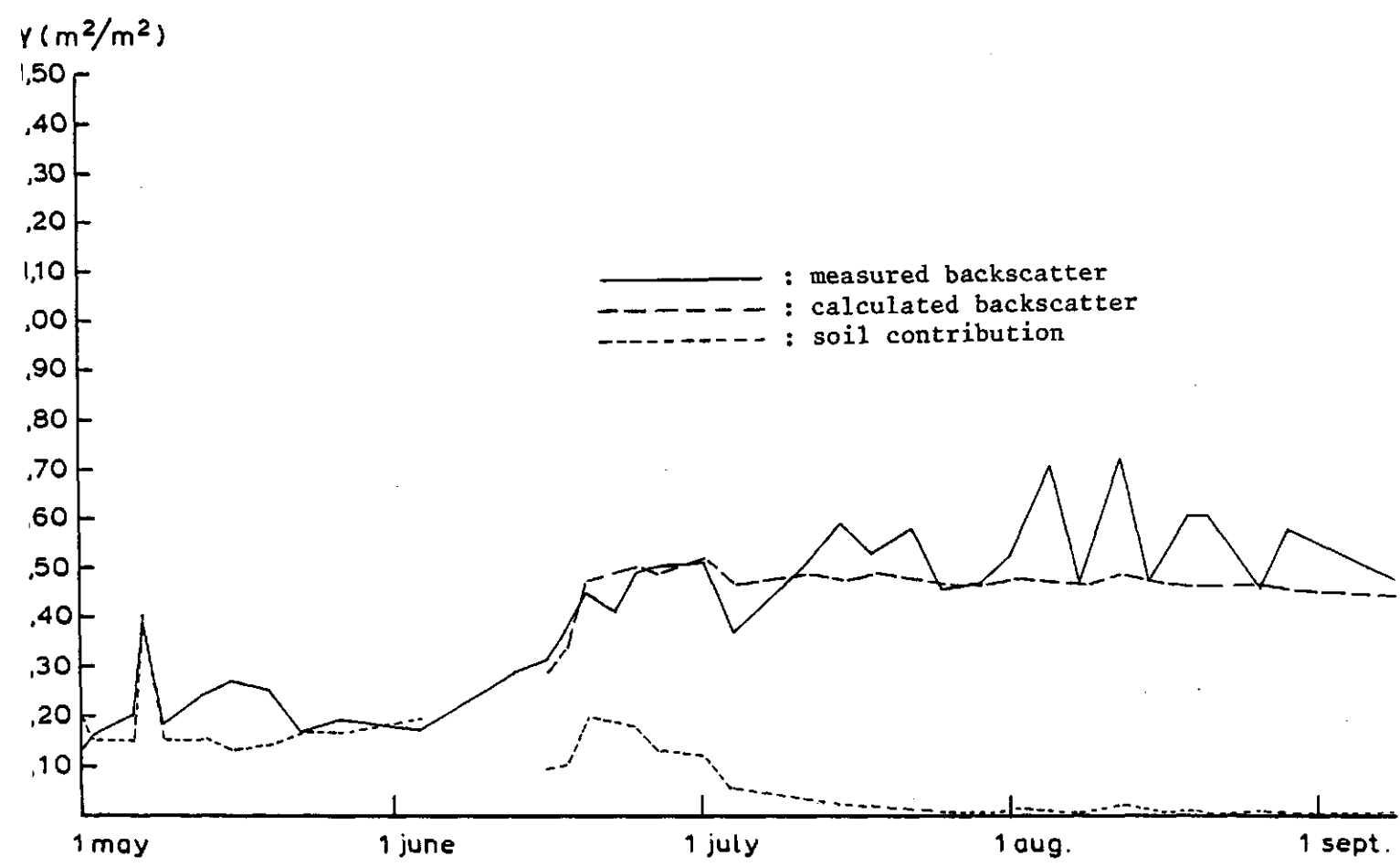


Figure 4.4b: Potatoes; observed and calculated radar backscatter VV40, 1980
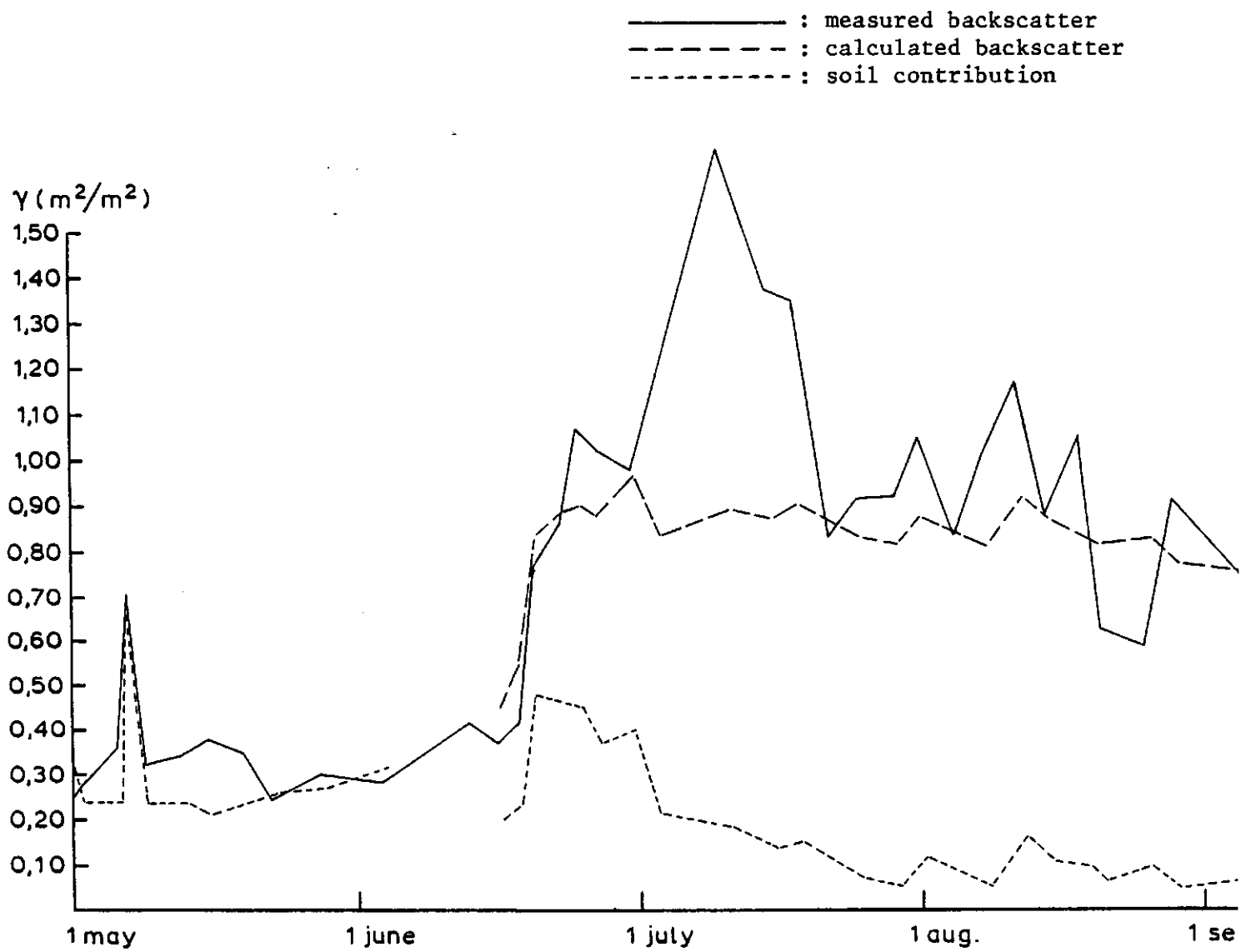
Figure 4.4c: Potatoes; observed and calculated radar backscatter VV80, 1480

| date | soil moistur. (%) | crop cover (%) | height (cm) | plant water (g7cm2) |
|---|---|---|---|---|
| ———— Jul-24 | 12 | 92 | 60 | 1915 |
| ——— Jul-27 | 5 | 91 | 55 | 1887 |
| —·—· Jul-31 | 12 | 88 | 50 | 1860 |
| ·········· Aug-03 | 6 | 85 | 50 | 1822 |

| date | soil moistur. (%) | crop cover (%) | height (cm) | plant water (g7cm2) |
|---|---|---|---|---|
| ———— Jul-04 | 7 | 90 | 57 | 1775 |
| ——— Jul-10 | 7 | 91 | 60 | 1885 |
| ·········· Jul-13 | 7 | 92 | 60 | 1915 |



| date | soil moisture (%) | crop cover (%) | height (cm) | plant water (g/cm2) |
|---|---|---|---|---|
| ———— Jun-20 | 5 | 54 | 40 | 1010 |
| ———— Jun-22 | 19 | 60 | 47 | 1150 |
| —— —— Jun-25 | 18 | 70 | 49 | 1300 |
| ············ Jun-27 | 15 | 77 | 52 | 1405 |
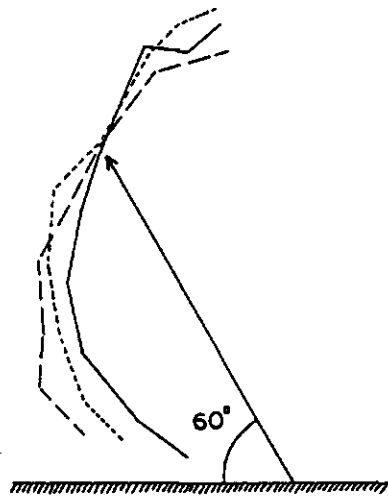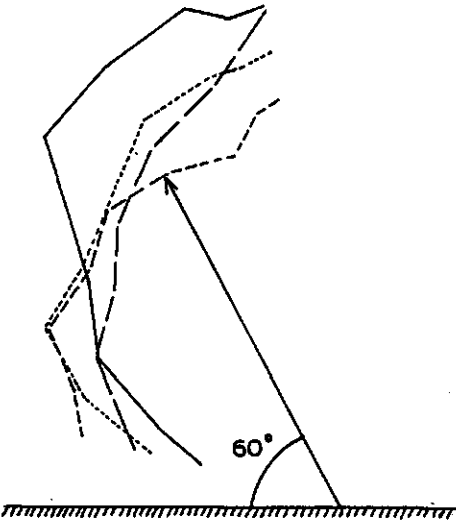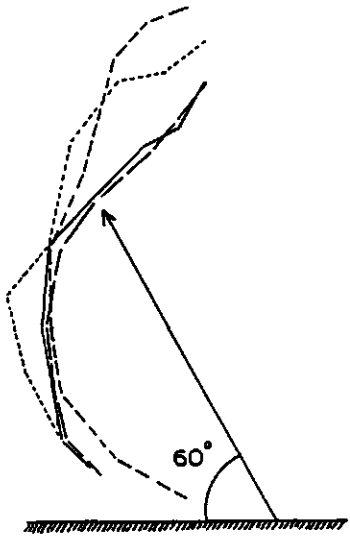


Figure 4.5: Potatoes ; polar diagram illustrating the phenomenon of backscatter-inversion. The angle between the vector and the horizontal corresponds with the grazing angle and the length of the vector indicates the relative value of the radar backscatter.
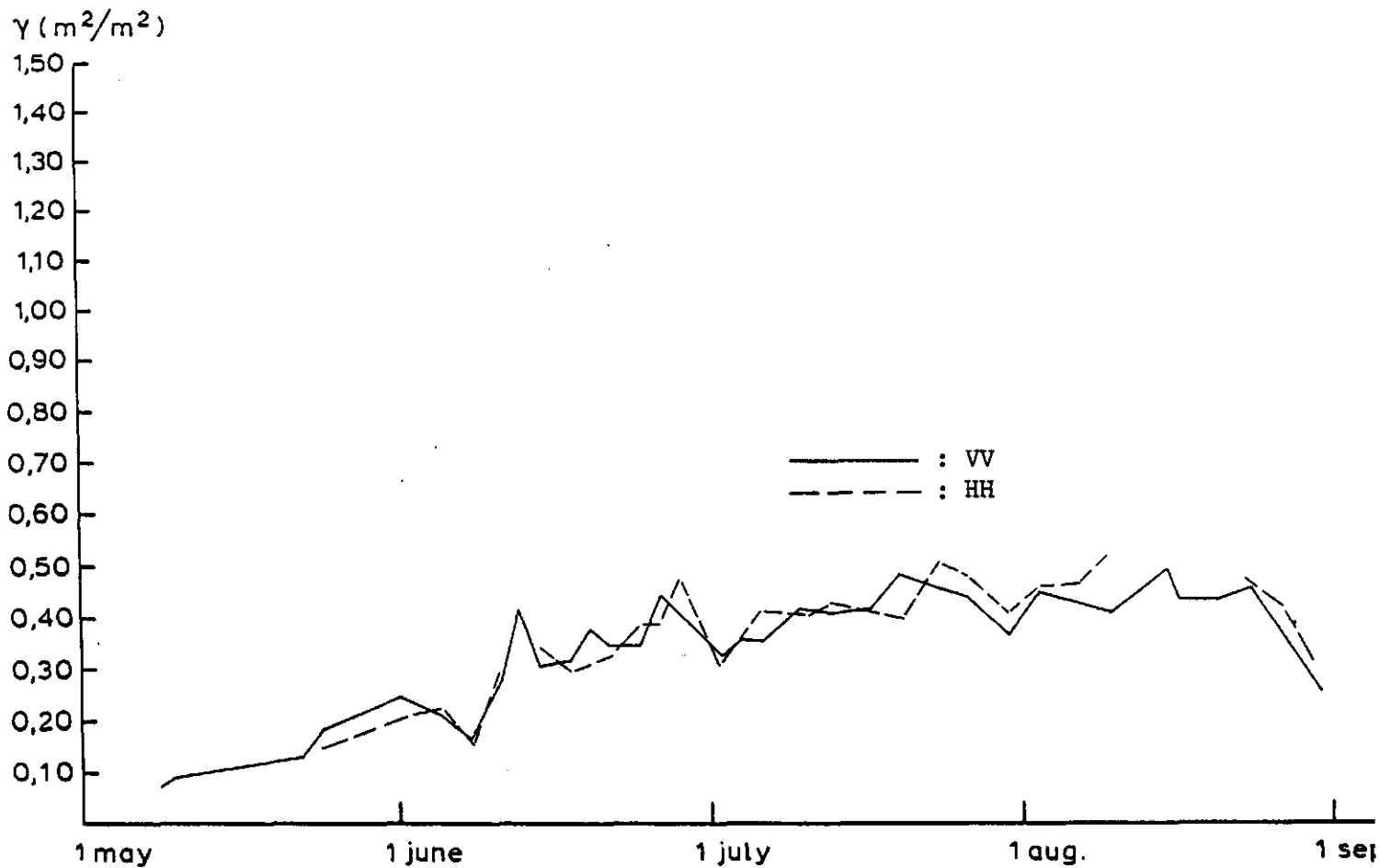
Figure 4.6a: Potatoes; radar backscatter in VV and in HH polarisation
40° grazing angle, 1979
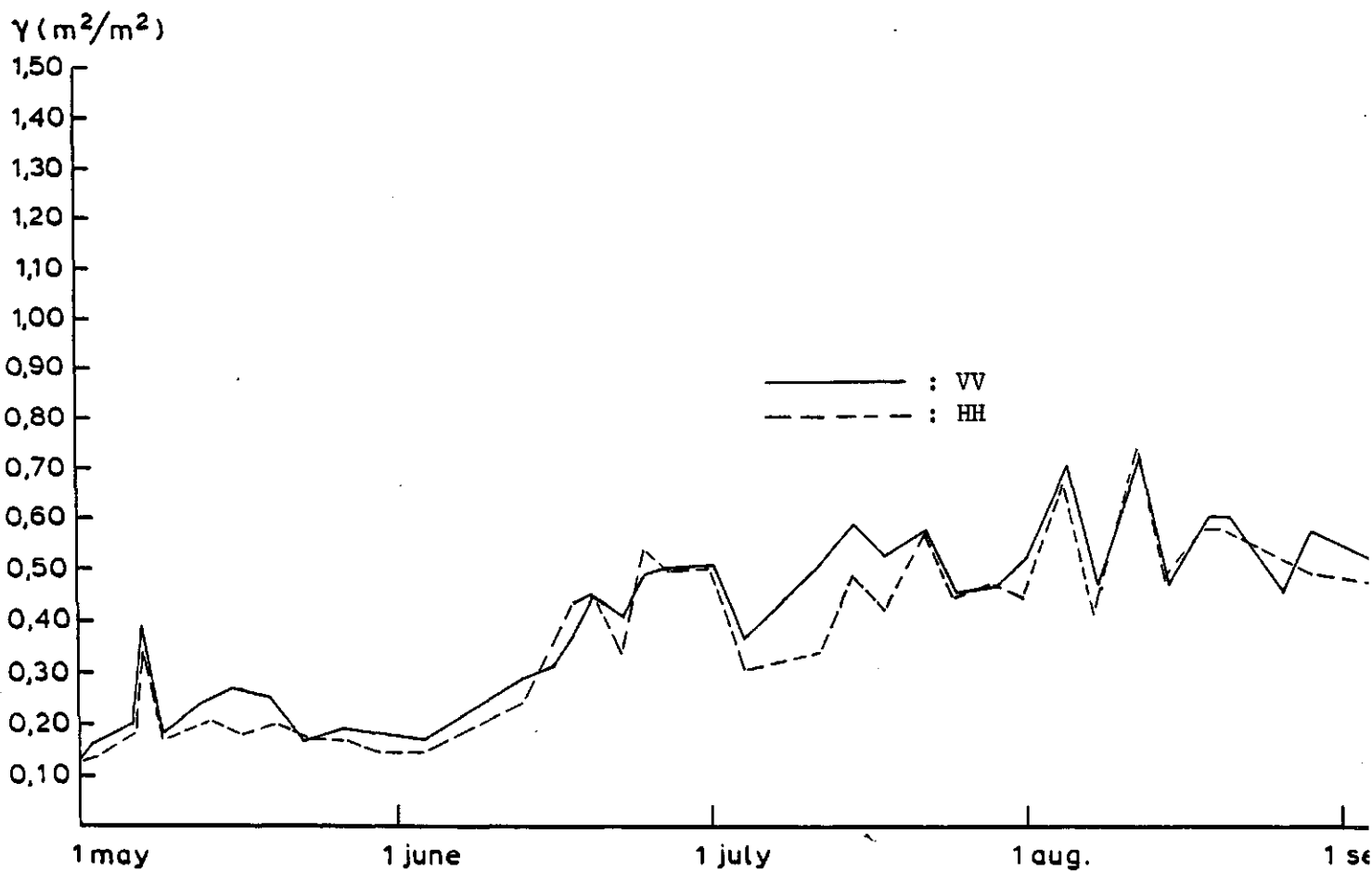


Figure 4.6b: Potatoes; radar backscatter in VV and in HH polarisation
40° grazing angle, 1980
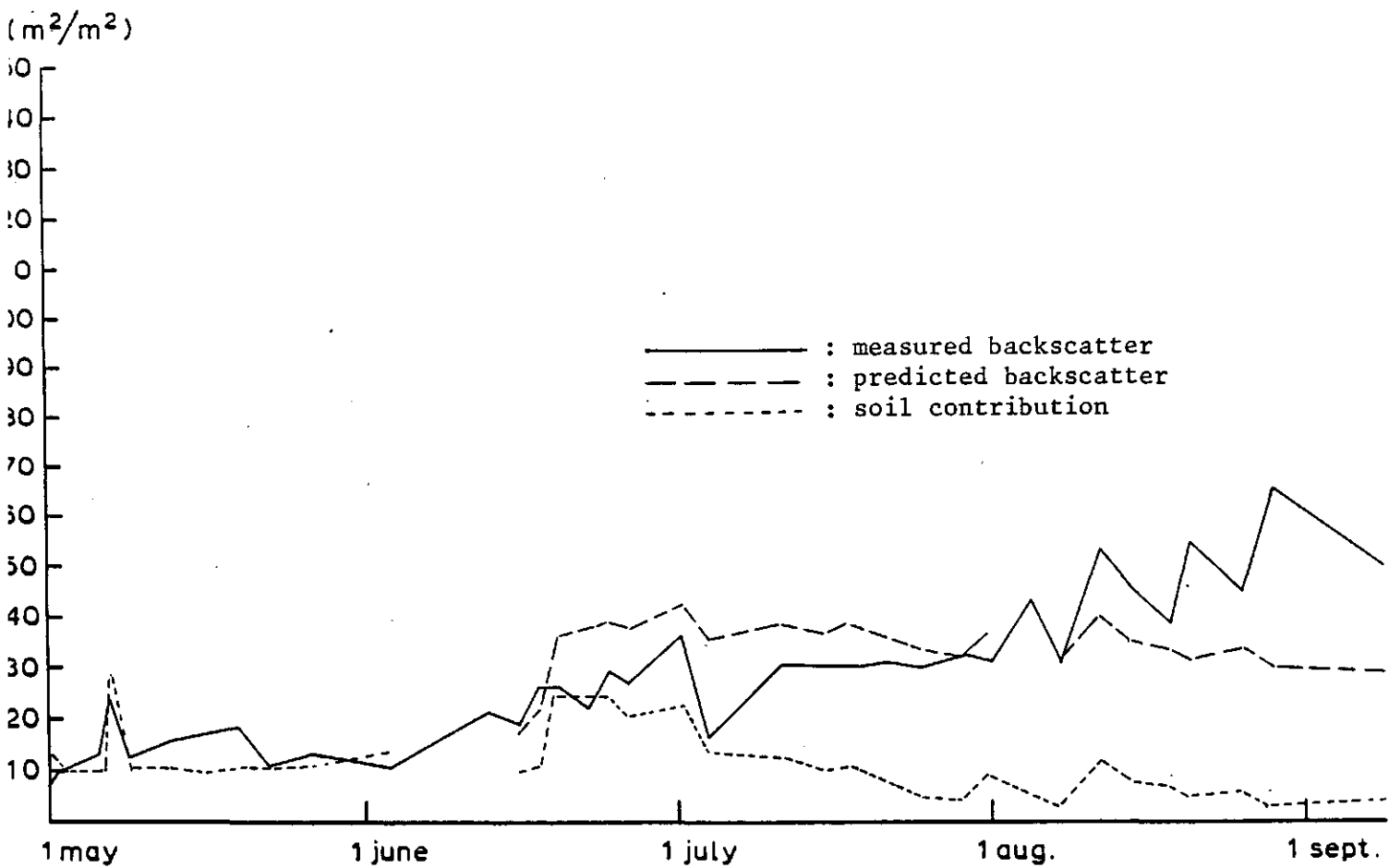
Figure 4.7a: Potatoes; observed and predicted radar backscatter VV20, 1980
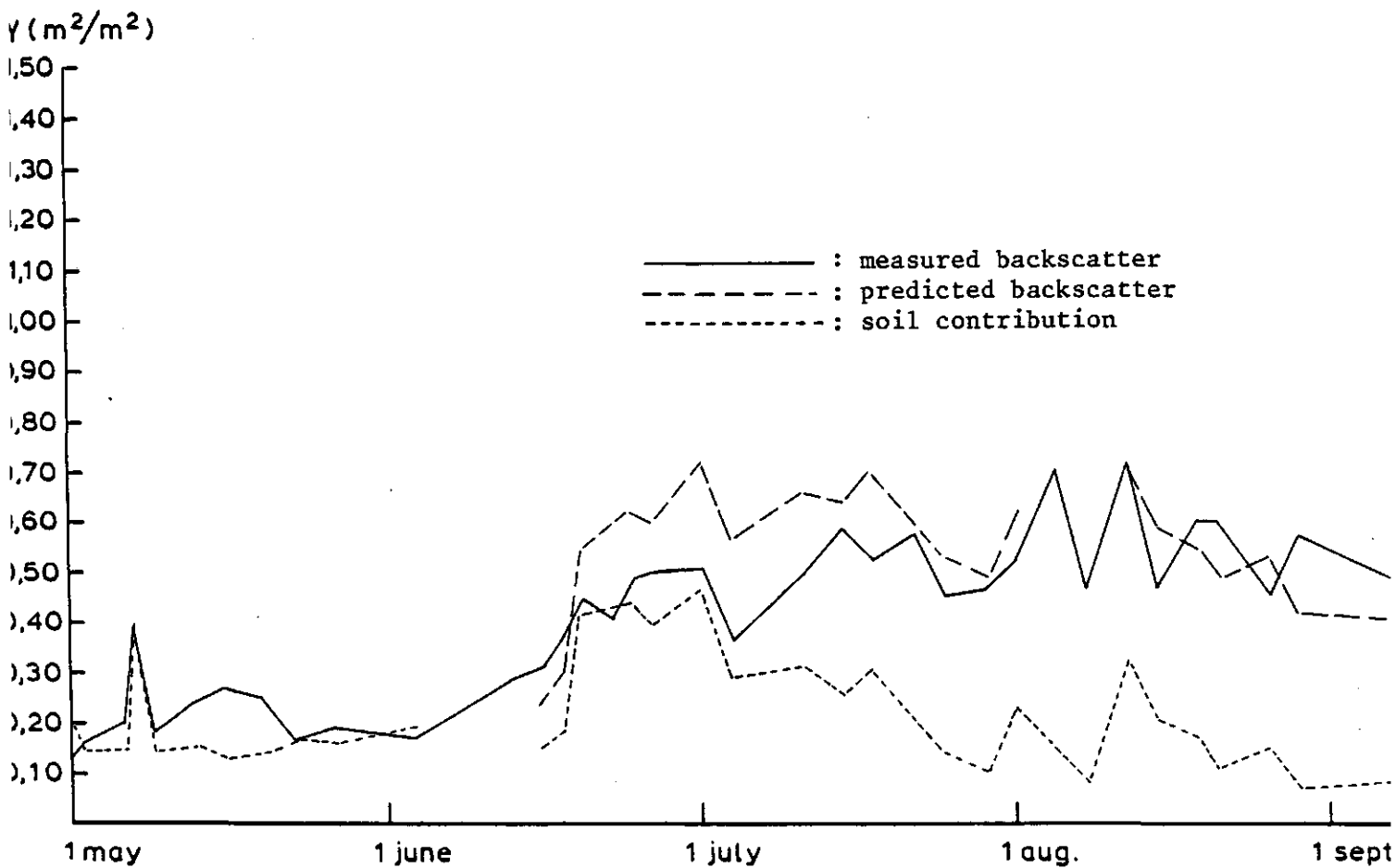


Figure 4.7b: Potatoes; observed and predicted radar backscatter VV40, 1980
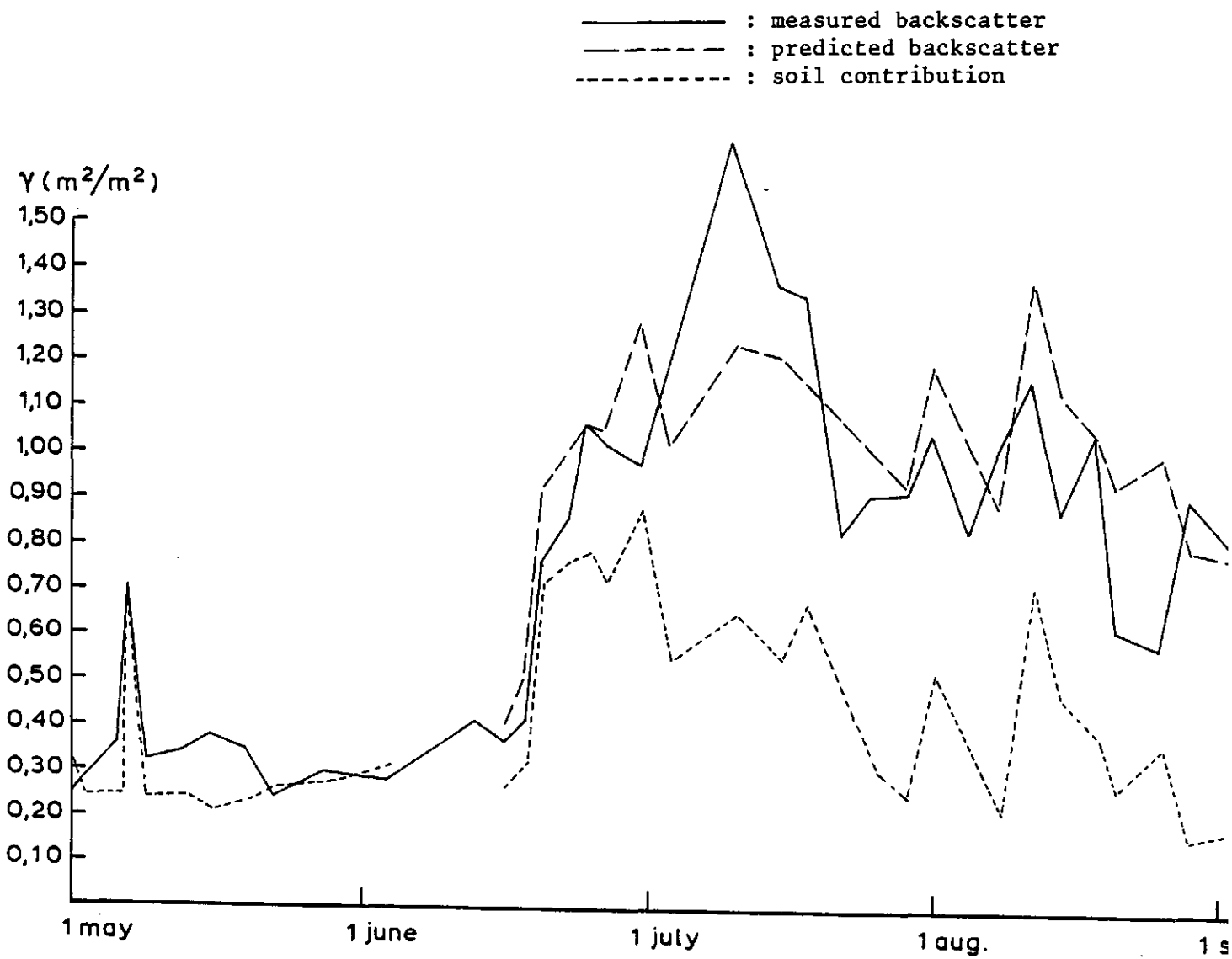
Figure 4.7c: Potatoes; observed and predicted radar backscatter VV80, 1980
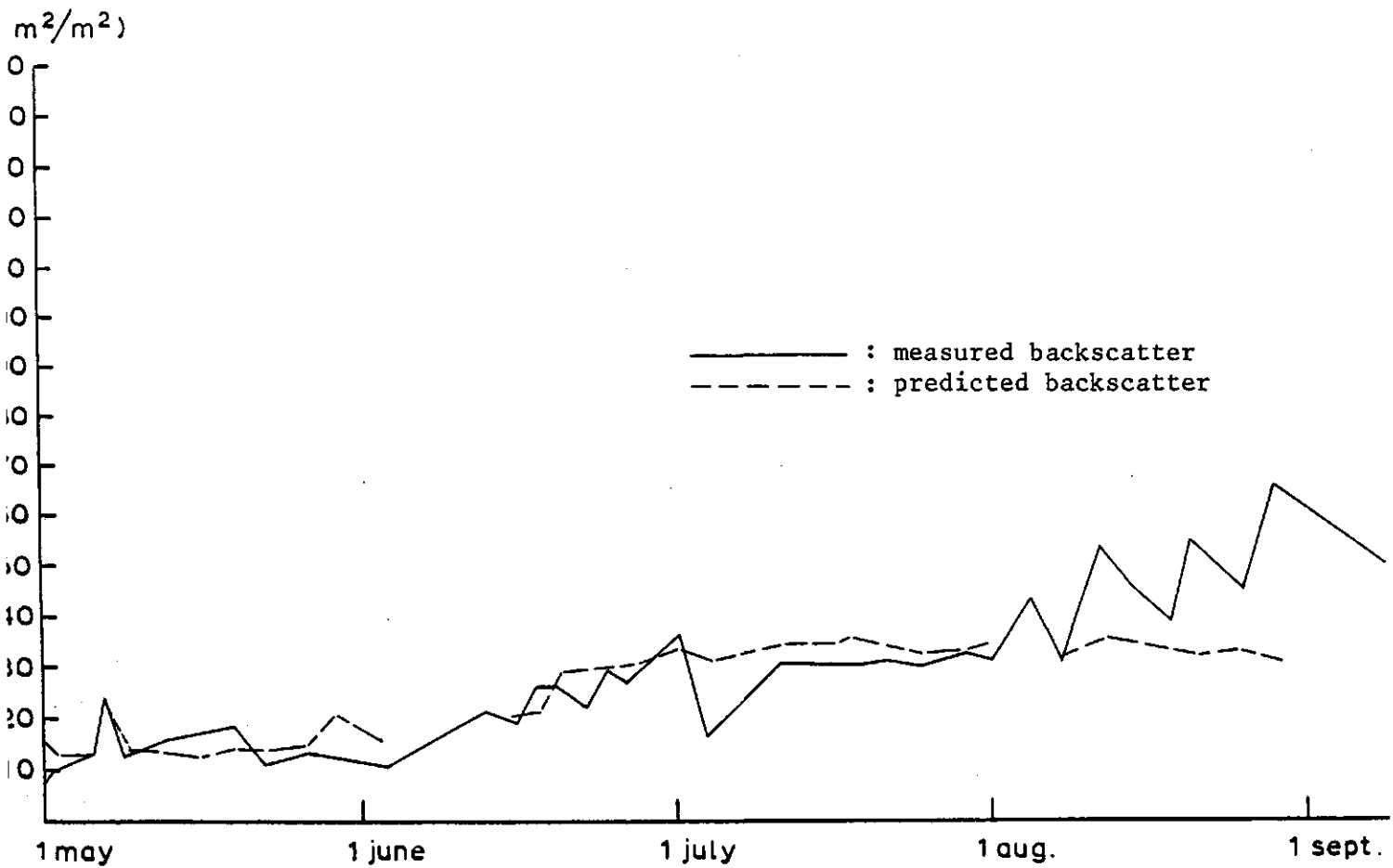
Figure 4.8a: Potatoes; observed and predicted radar backscatter VV20, 1980,
using separately determined soil parameters

1 may    1 june    1 july    1 aug.    1 sept.

: measured backscatter
: predicted backscatter

'(m²/m²)

,50
,40
,30
,20
,10
,00
,90
,80
,70
,60
,50
,40
,30
,20
,10

: measured backscatter
: predicted backscatter

1 may    1 june    1 july    1 aug.    1 sept.
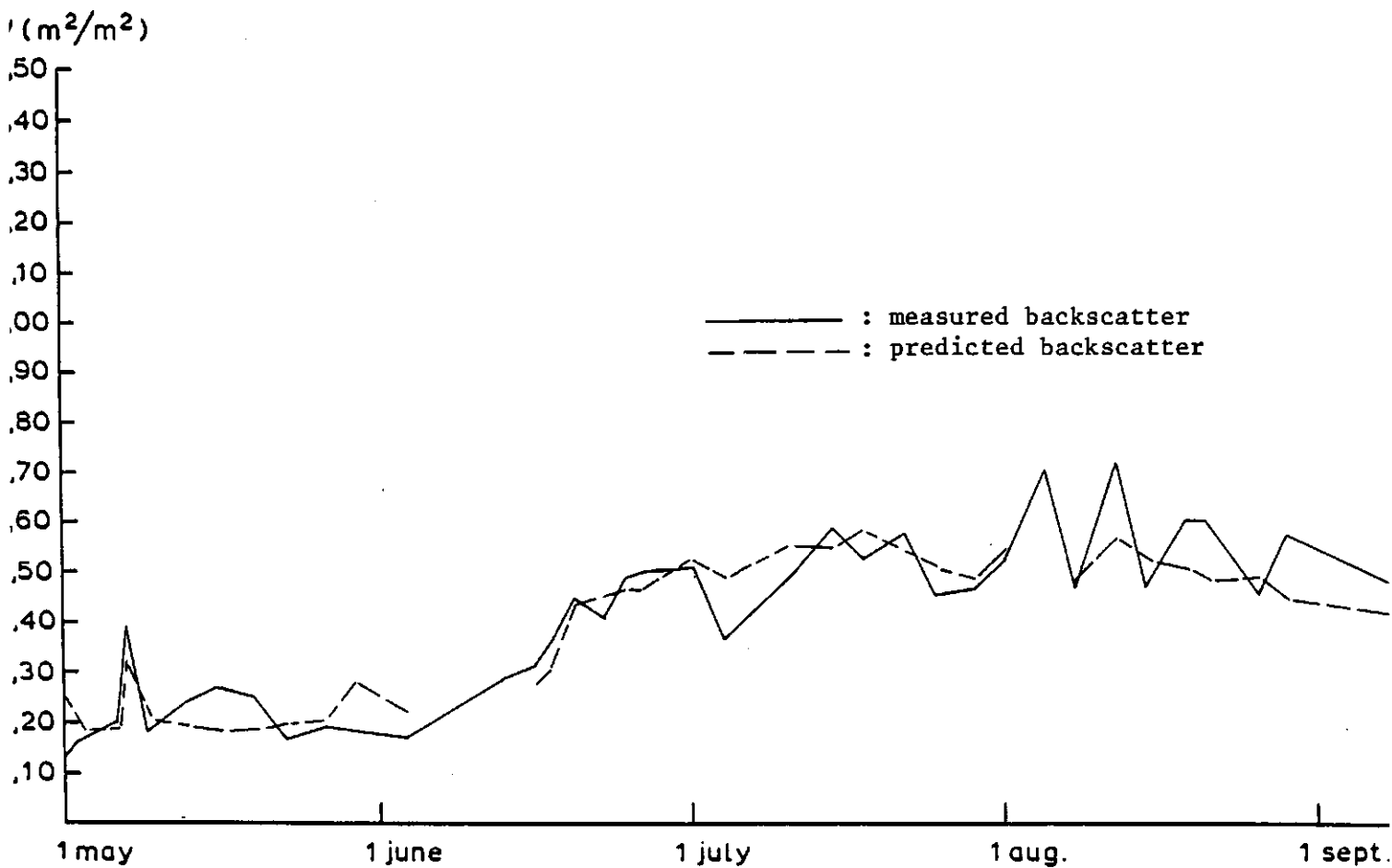
Figure 4.8b: Potatoes; observed and predicted radar backscatter VV40, 1980,
using separately determined soil parameters
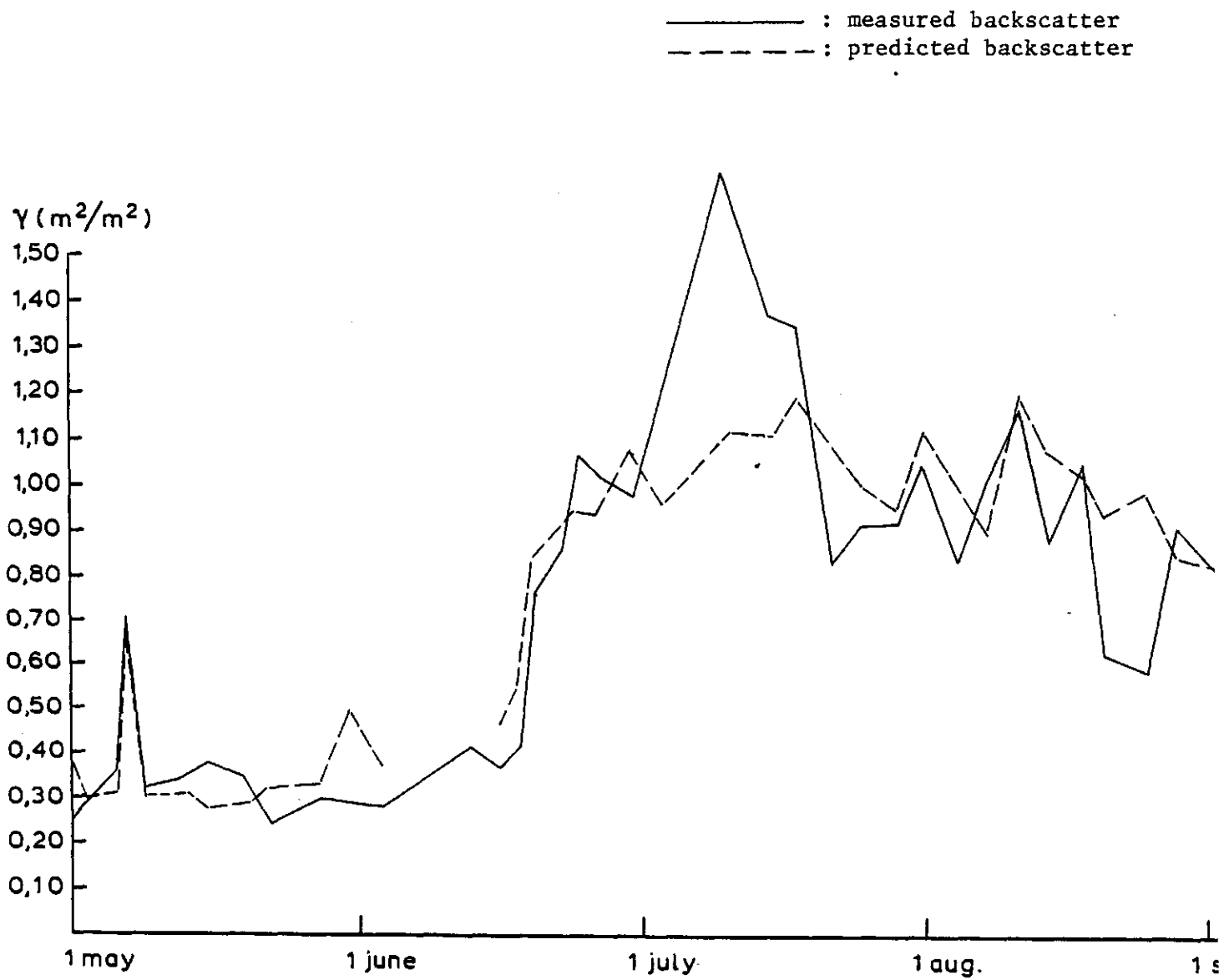
Figure 4.8c: Potatoes; observed and predicted radar backscatter VV80, 1980, using separately determined soil parameters
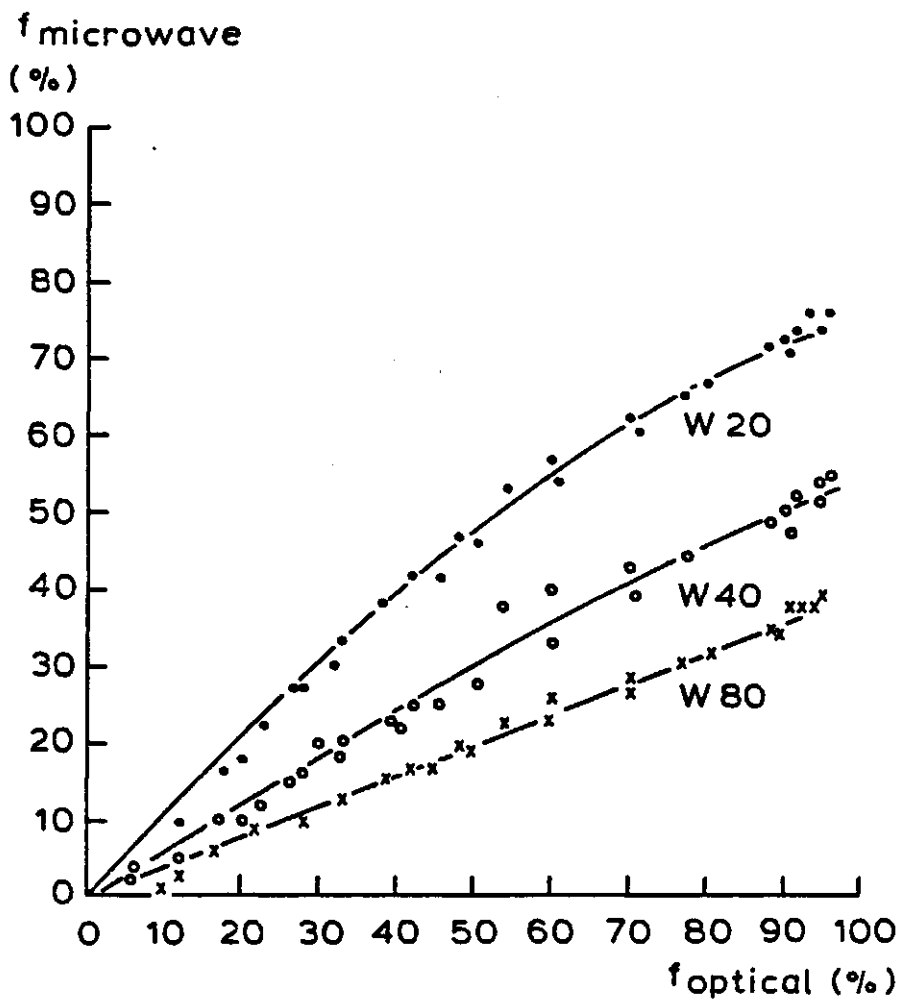
Figure 4.9: Potatoes; optical crop cover      versus microwave crop cover
          1979 and 1980 combined
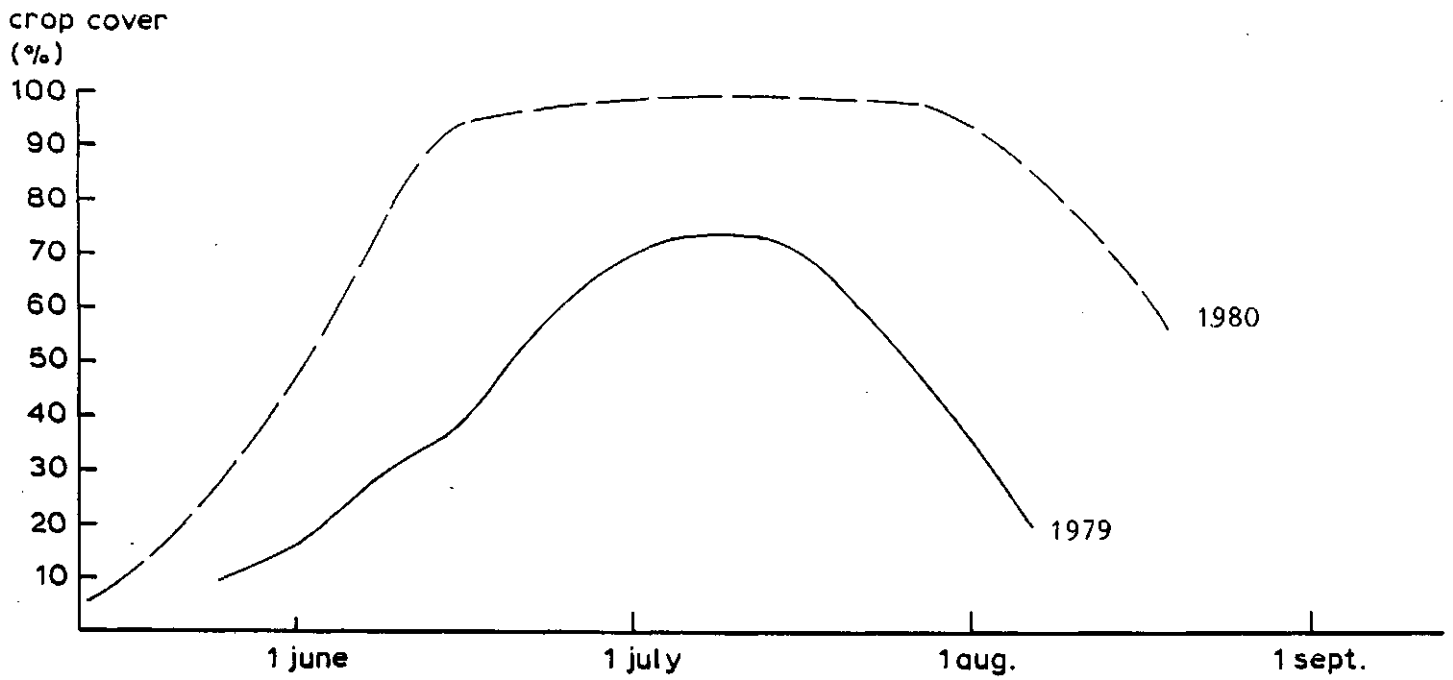
Figure 5.1: Peas; crop cover    during the growing season
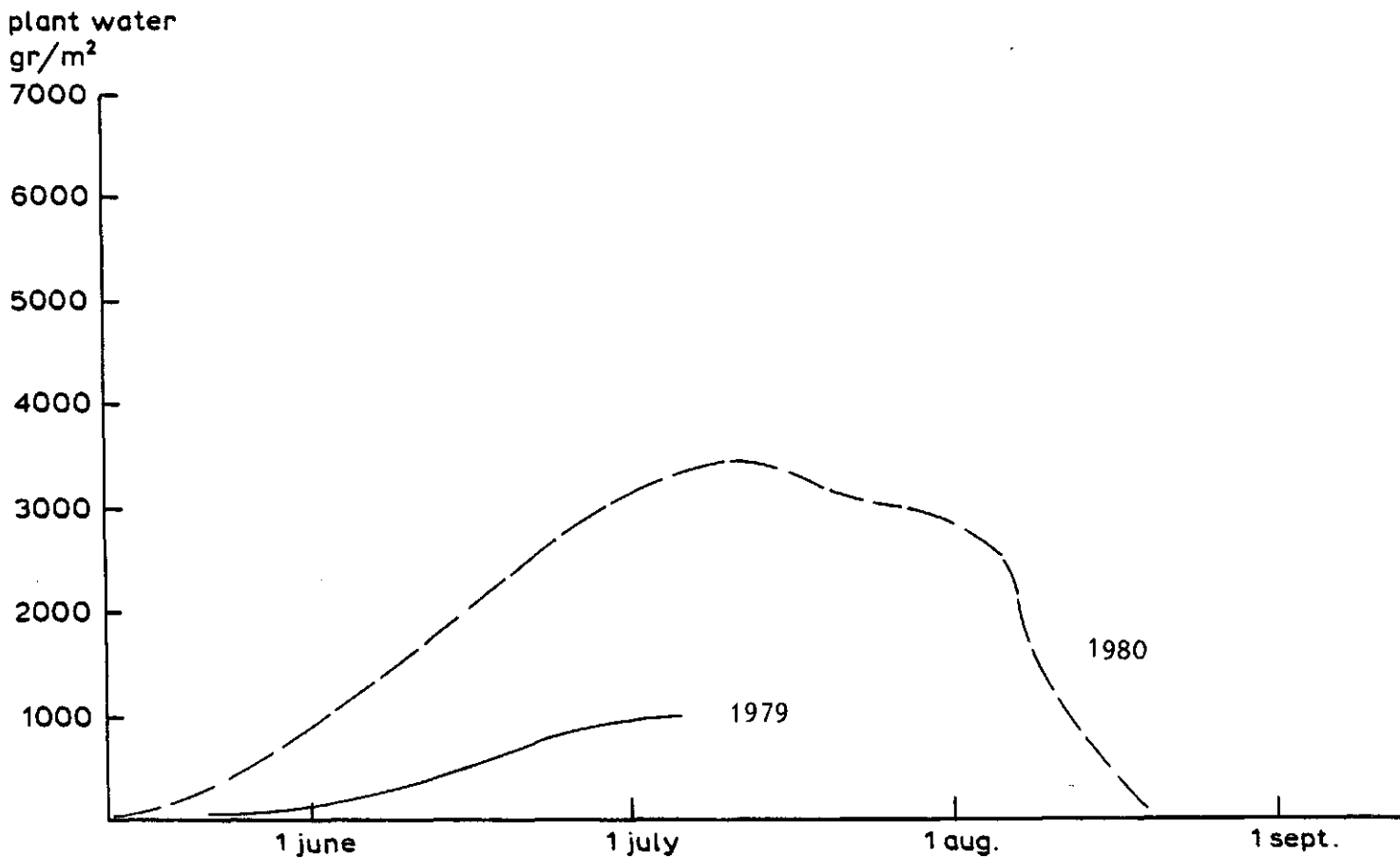


Figure 5.2: Peas; amount of above-ground plantwater during the growing season
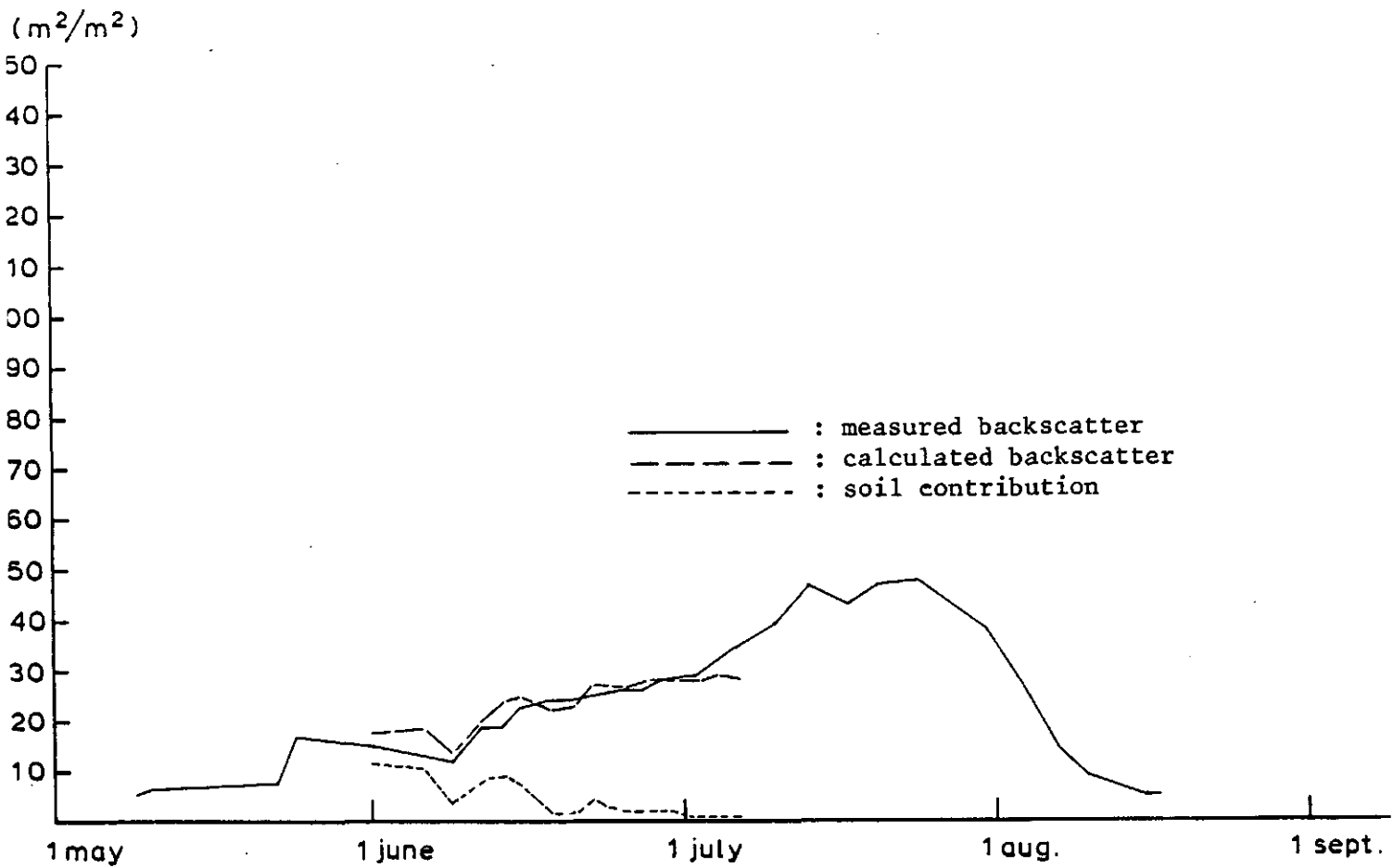
Figure 5.3a: Peas; observed and calculated radar backscatter VV20, 1979
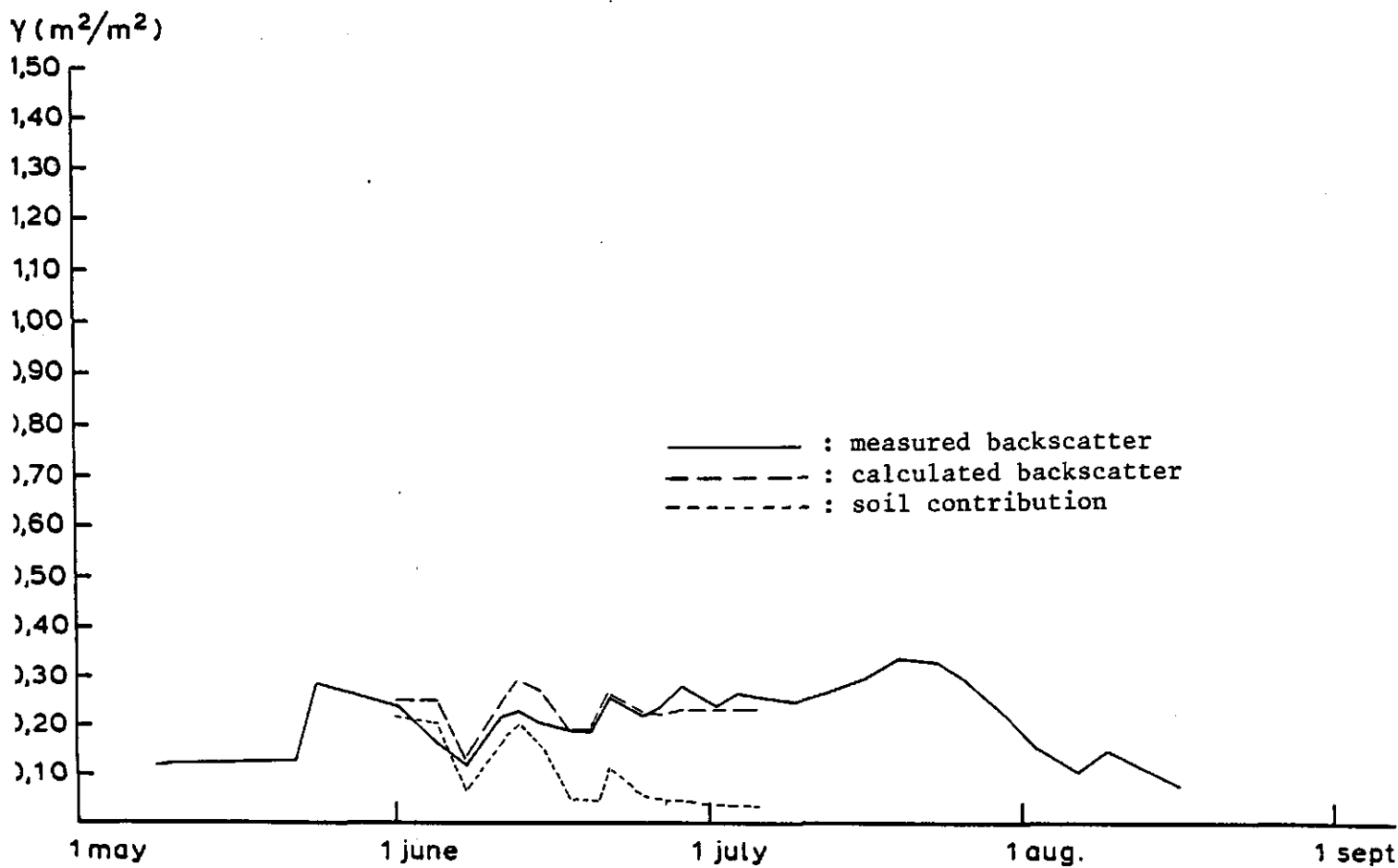


Figure 5.3b: Peas; observed and calculated radar backscatter VV40, 1979

Y (m²/m²)

3,50
3,40
3,30
3,20
3,10
3,00
2,90
2,80
2,70
2,60
2,50
2,40
2,30
2,20
2,10
2,00
2,90
1,80
1,70
1,60
1,50
1,40
1,30
1,20
1,10
1,00
0,90
0,80
0,70
0,60
0,50
0,40
0,30
0,20
0,10
0,00

———————— : measured backscatter
— — — — — : calculated backscatter

1 may          1 june          1 july          1 aug.          1 se|
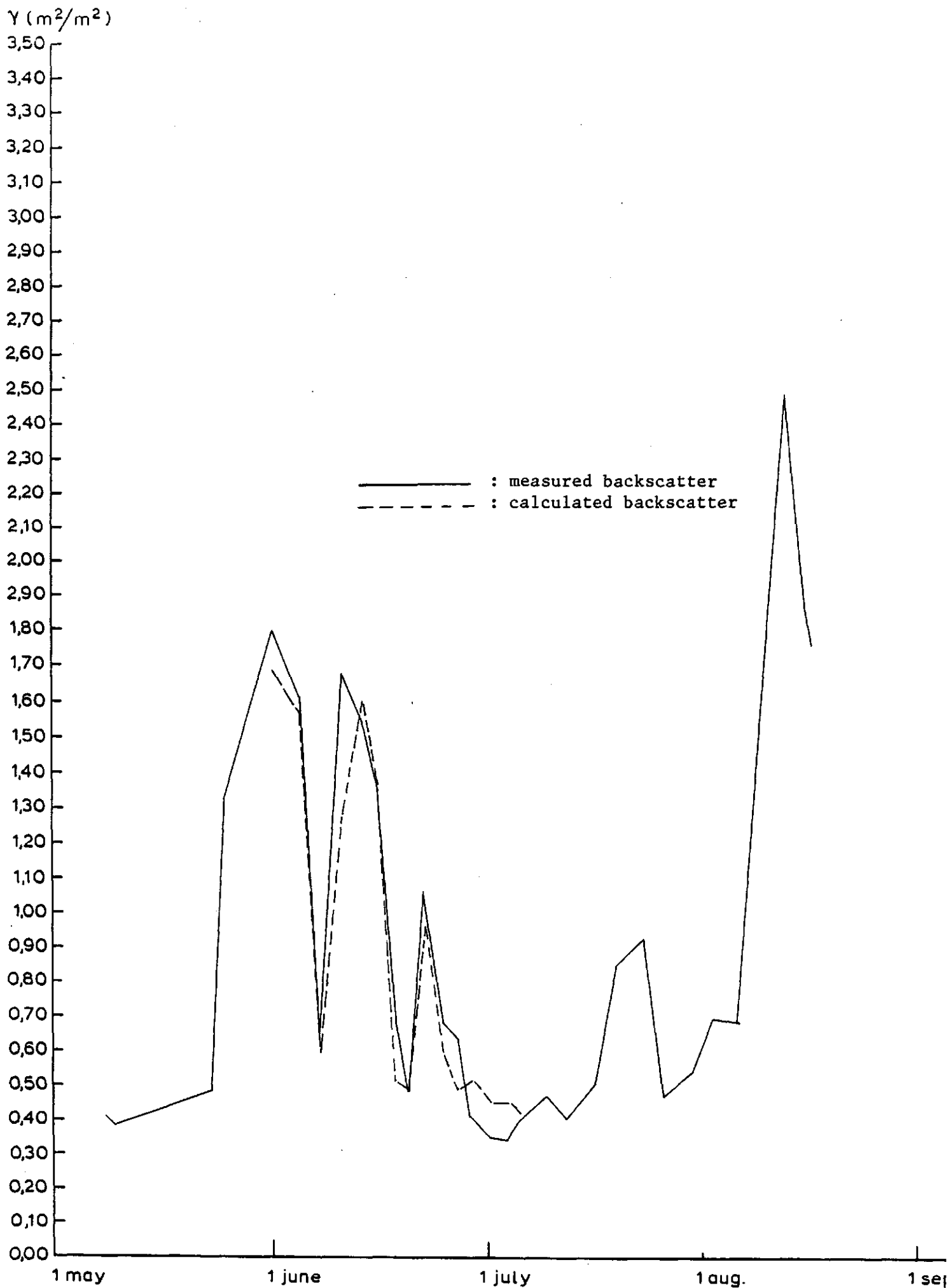
Figure 5.3c: Peas; observed and calculated radar backscatter VV80, 1979
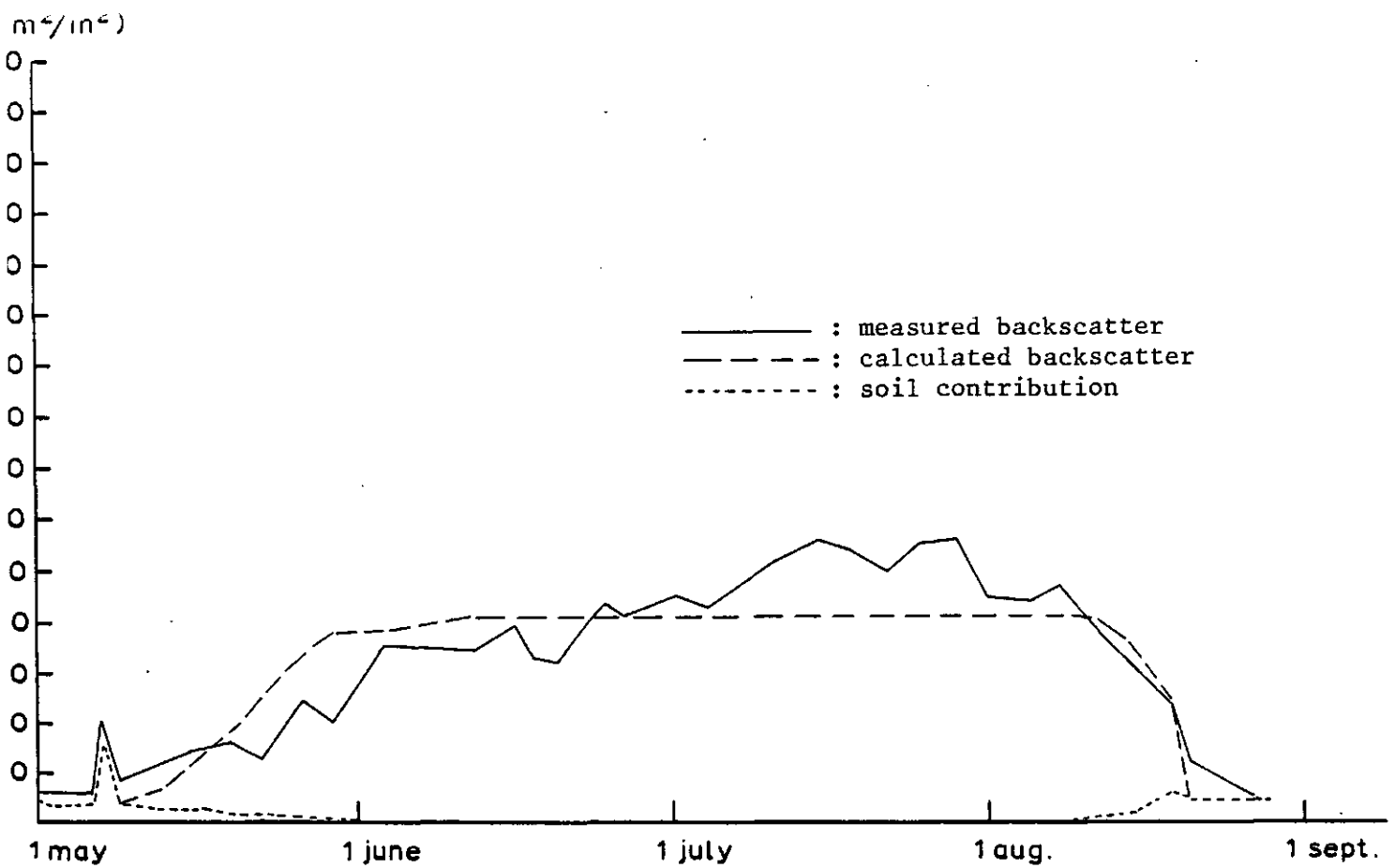
Figure 5.4a: Peas; observed and calculated radar backscatter VV20, 1980
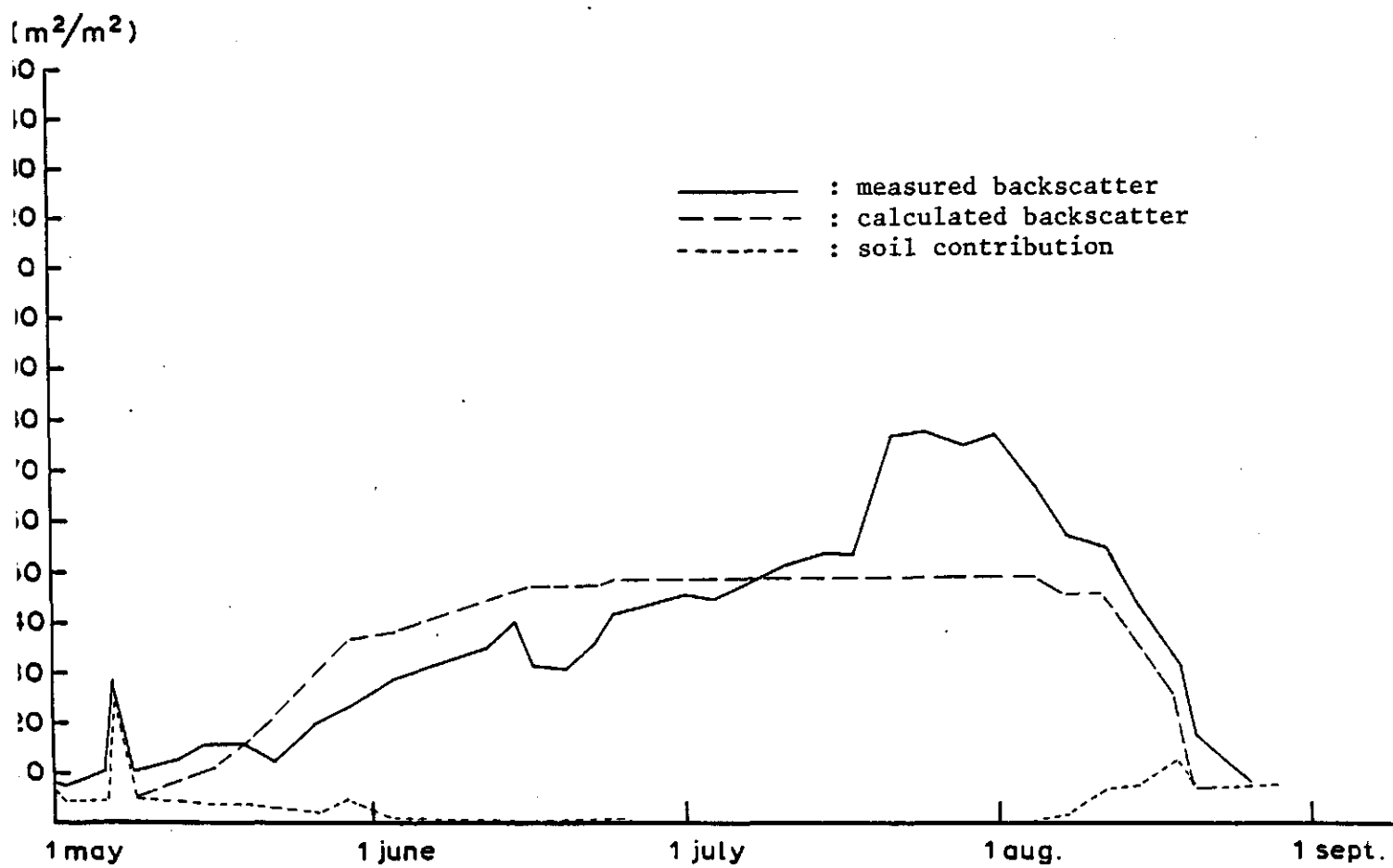


Figure 5.4b: Peas; observed and calculated radar backscatter
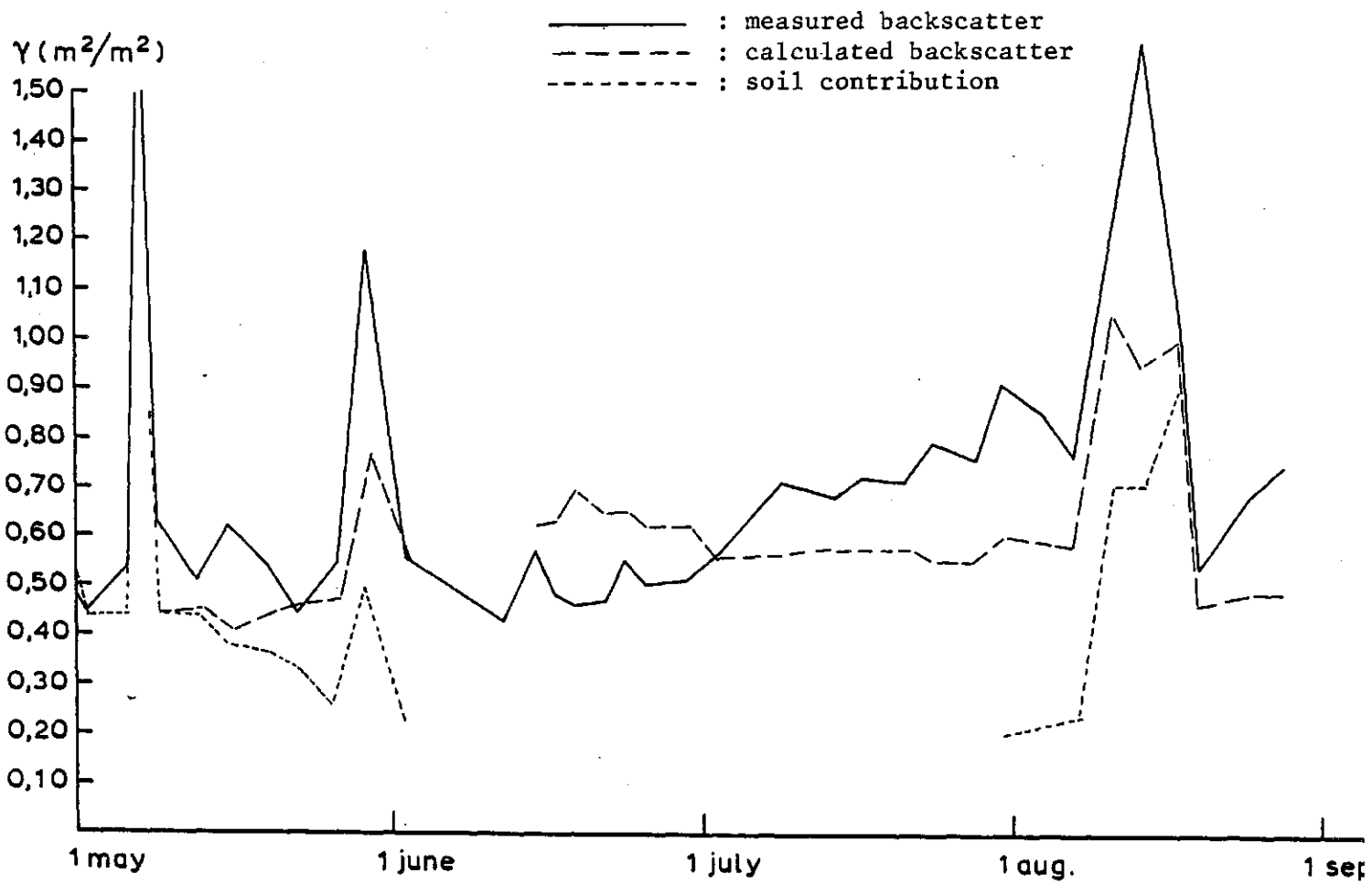
Figure 5.4c: Peas; observed and calculated radar backscatter VV80, 1980
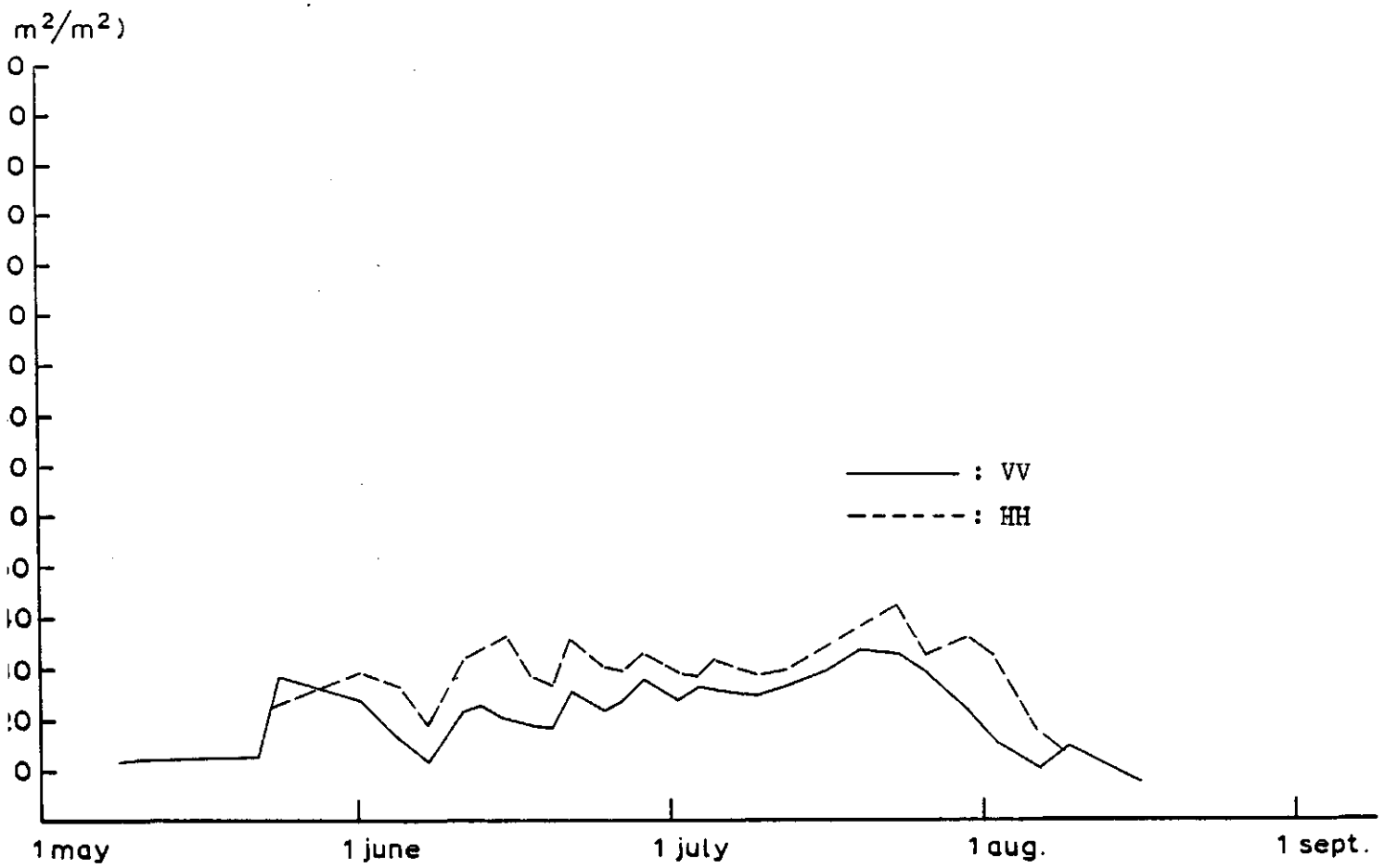
Figure 5.5a: Peas; radar backscatter in VV and in HH polarisation
40° grazing angle, 179
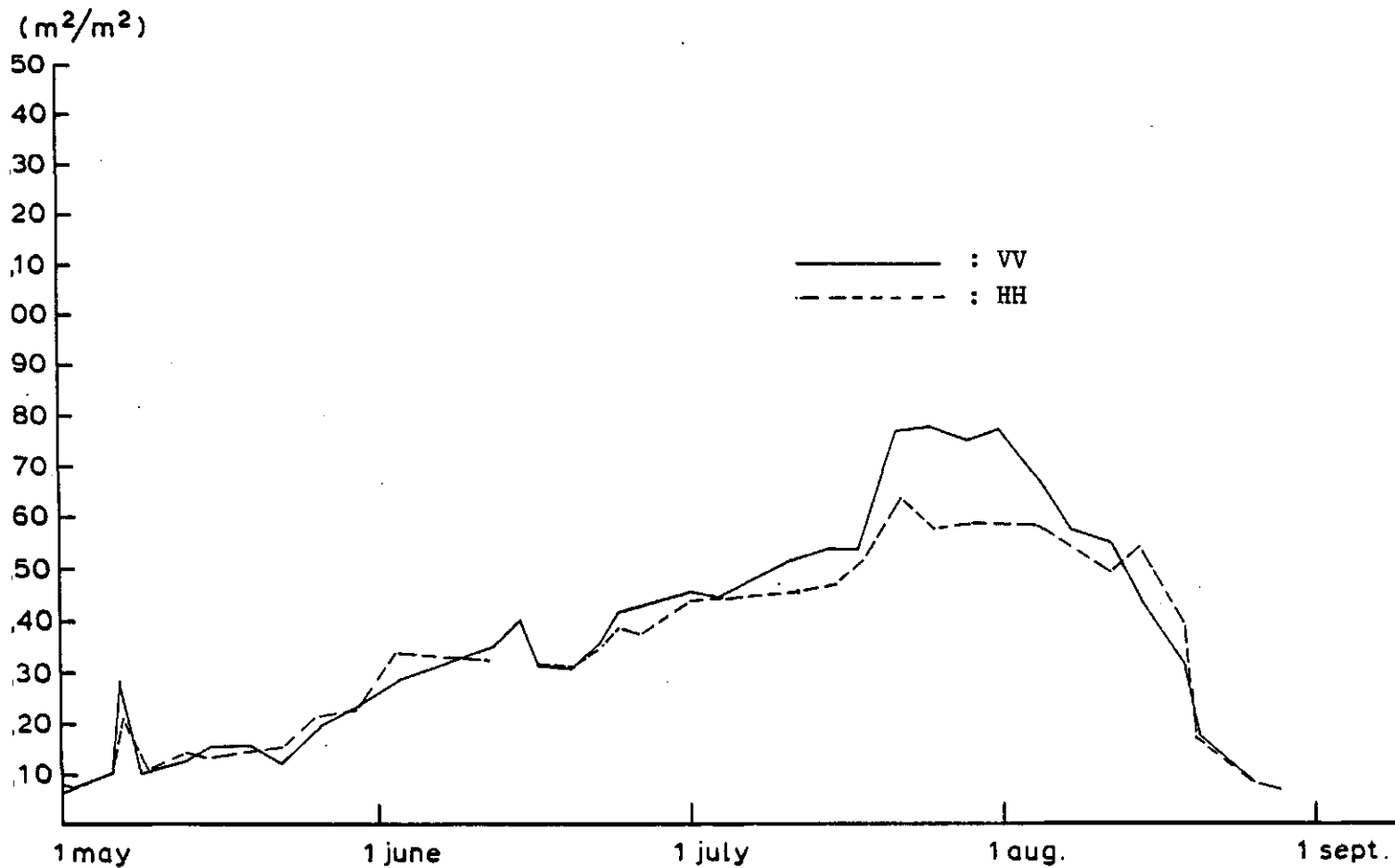


Figure 5.5b: Peas; radar backscatter in VV and in HH polarisation
40° grazing angle, 1980
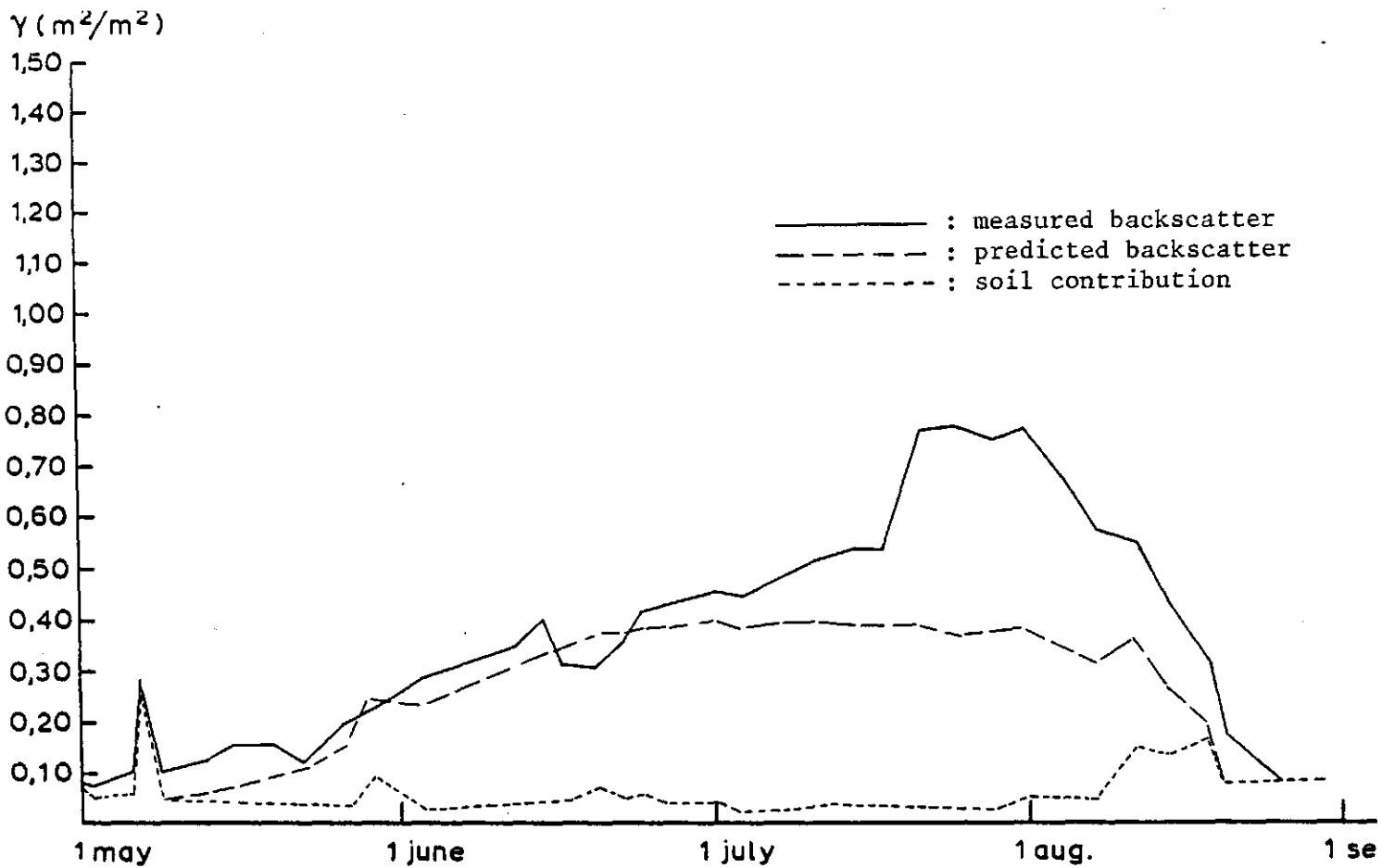
Figure 5.6a: Peas; observed and predicted radar backscatter VV20, 1980
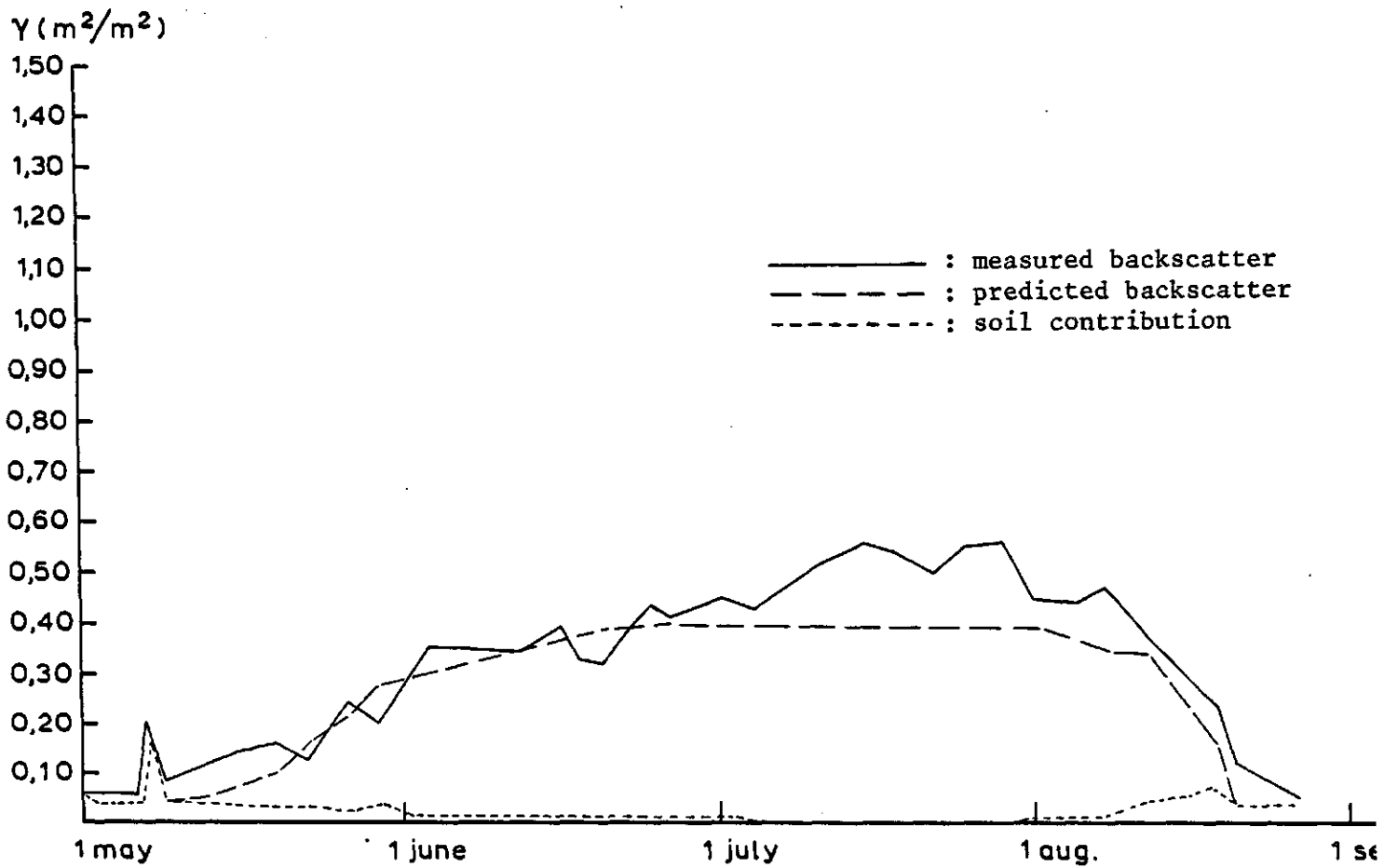


Figure 5.6b: Peas; observed and predicted radar backscatter VV40, 1980

Figure 5.6c: Peas; obsreved and predicted radar backscatter VV80, 1980
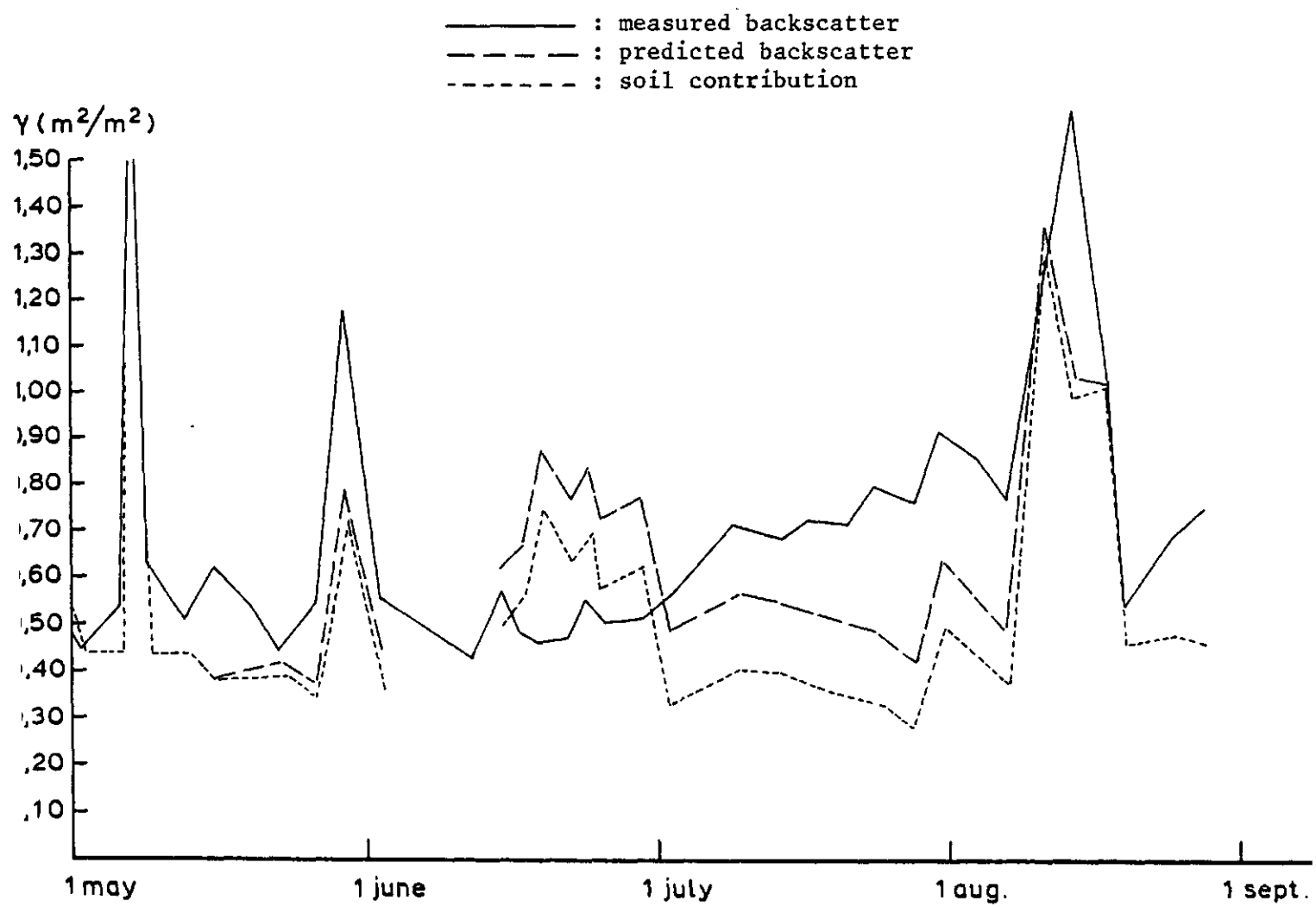
Figure 5.7b: Peas; optical crop cover    versus microwave
          crop cover    1980
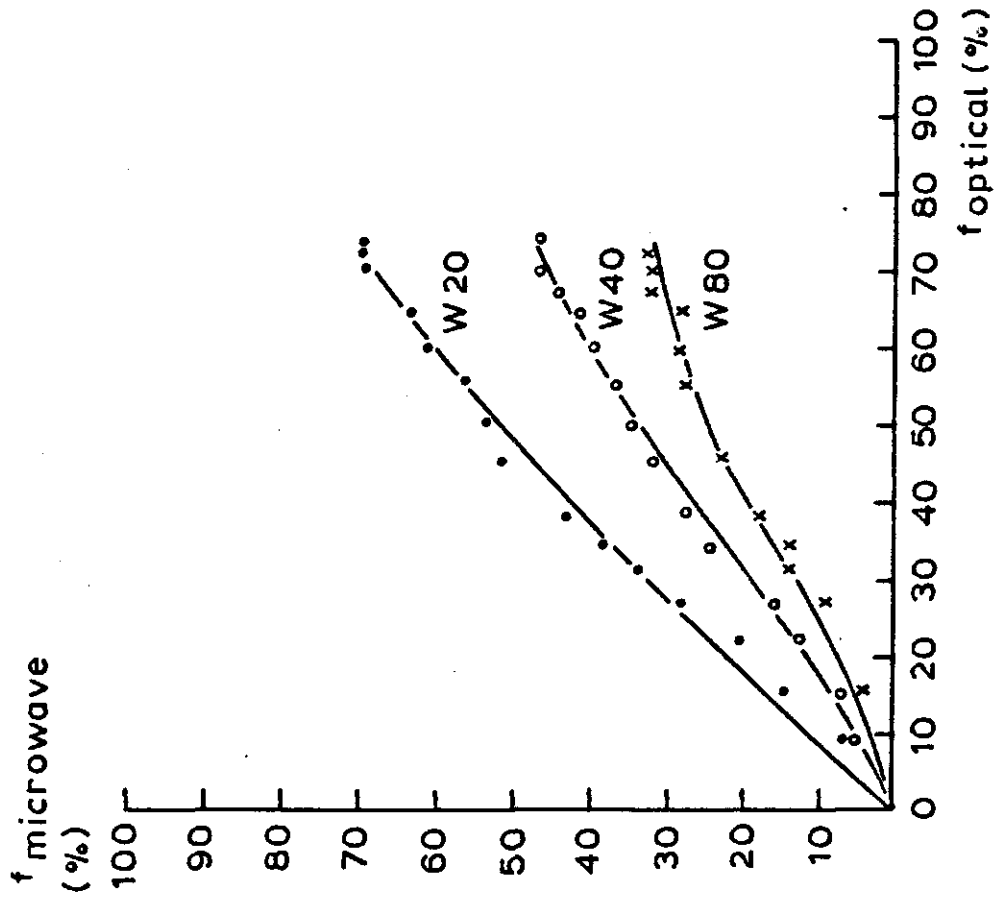
Figure 5.7a: Peas; optical crop cover    versus microwave
          crop cover    1979